

ENERGY STORES AND SWITCHES  
FOR RAIL-LAUNCHER SYSTEMS

Final Report

to

NASA/Lewis Research Center

Grant No. NAG-3-303

Reporting Period:

October 1, 1982  
through  
September 30, 1983

prepared by

Raymond C. Zowarka  
and  
Richard A. Marshall

William F. Weldon  
Principal Investigator

Publication No. RF41  
Center for Electromechanics  
The University of Texas at Austin  
Taylor Hall 227  
Austin, TX 78712

## TABLE OF CONTENTS

	<u>Page</u>
TABLE OF CONTENTS .....	1
LIST OF FIGURES .....	iii
LIST OF TABLES .....	v
INTRODUCTION .....	
TASK A. POWER SUPPLIES AND SWITCHES .....	2
Energy Stores .....	3
Capacitors .....	4
HPG-Inductor .....	6
Compensated Pulsed Alternator .....	8
Flux Compressors .....	11
Inverse Railgun Flux Compressor .....	13
Switches .....	13
Arcing Switch .....	13
Fuse Switch .....	16
Explosive or Rupturing Switch .....	17
Vacuum Switches .....	19
Explosive Switches .....	19
Semiconductor Switches (Corbino Disks) .....	20
TASK B. THE INVERSE RAILGUN FLUX COMPRESSOR FOR ESRL SYSTEMS .....	21
Introduction .....	21
The Concept .....	23
The Equations .....	26
The Form of the IRFC .....	28
A Specific Device .....	33
The Inductor .....	34
The Bore of the IRFC .....	35
The Gas Gun .....	35
The IRFC .....	36
IRFC Electrical Resistance .....	37
Inductance per Unit Length .....	37
Will it Take Off? .....	38
Initial Charging .....	38
Simulation .....	39
Inductance Check .....	40
The Device .....	41
TASK C. ARCING AND SHUTTLE SWITCHES .....	43



## TABLE OF CONTENTS - continued

	<u>Page</u>
TASK D. ALTERNATIVE SWITCH .....	49
TASK E. ROTARY SHUTTLE OPENING SWITCH EXPERIMENTATION .....	59
Testing of the RSOS Switch .....	64
SUGGESTIONS FOR FUTURE WORK .....	71
ACKNOWLEDGMENTS .....	73
REFERENCES .....	74
APPENDIX A - Energy Stores and Switches for Rail-Launcher Systems .....	78
APPENDIX B - Energy Considerations in Switching Current From an Inductive Store into a Railgun .....	87
APPENDIX C - Switching for an Earth-To-Space Rail Launcher .....	92
APPENDIX D - A Coaxial Radial Opening Switch for a Distributed-Energy-Store Rail Launcher .....	96
APPENDIX E - CEM-UT Technical Note .....	101

## LIST OF FIGURES

<u>Figure</u>		<u>Page</u>
1	Regions of usefulness for five types of energy-store railgun systems .....	4
2	Schematic representation of a compulsator .....	8
3	Cutaway view of CEM-UT prototype compensated pulsed alternator .....	9
4	Simple inductive transfer circuit .....	14
5	Single-stage switching .....	18
6	Staged switching .....	18
7	Conceptual inverse railgun/inductor ESRL system .....	23
8	Sliding metal armature in a conventional railgun .....	24
9	Sliding metal armature in an inverse railgun .....	25
10	Current, field, and force in an inverse railgun .....	25
11	Identification of variables in conventional analysis .....	27
12	Identification of variables in IRFC analysis .....	28
13	Simulation of end portion of IRFC as an inductor .....	29
14	Interconnections for asymmetric method for varying N along rails ...	30
15	Detail of rail layout for asymmetric method for varying N .....	31
16	Symmetric method for varying N along rails .....	32
17	Method for establishing preliminary current in IRFC .....	33
18	Conceptual IRFC device for ESRL .....	42
19	Original concept for ESRL rail construction .....	43
20a	Switch in the inductor-charging position .....	47
20b	Switch building commutation voltage .....	47
20c	Switch complete -- total current established in railgun .....	47

## LIST OF FIGURES - continued

<u>Figure</u>		<u>Page</u>
21	Opening switch configuration .....	50
22	Transfer switch configuration .....	51
23	Liquid metal experiment test fixture .....	52
24	Components of liquid metal test fixture .....	53
25	Components of solenoid-actuated valve .....	55
26	Velocity measurement of non-current-carrying liquid metal column .....	56
27	Cross-section through a Ga-In switch capsule .....	58
28	Design of laminated resistor .....	61
29	Masked resistor laminations .....	61
30	Telescoping air cylinder .....	62
31	Interlocking rings prior to assembly .....	62
32	Relation between shuttle and interlocking ring .....	63
33	Complete inventory of switch parts .....	63
34	Locations of damage to RSOS following testing .....	65
35a	Load current enlarged .....	66
35b	Voltage enlarged .....	66
35c	Voltage enlarged .....	67
36	Opening test at 50kA .....	69

## LIST OF TABLES

<u>Table No.</u>		<u>Page</u>
1	Earth-to-space rail launch requirements .....	2
2	Earth-to-space rail launch parameters .....	2
3	Required launcher timing .....	3
4	Maxwell High Energy Density Capacitors .....	5
5	Progression of energy density gains with additional technology required for each increase .....	7
6	Example compulsator parameters .....	10
7	Compulsator-driven rapid-fire gun test bed parameters .....	10
8	Compulsator-driven rapid-fire system energy balance .....	11
9	Rotary flux compressor parameters .....	12
10	Performance parameters under load .....	13
11	ESRL parameters used to calculate dissipated switching energy ..	15
12	Required 50-MJ gas gun piston/armature mass-velocity relationship .....	36
13	Required IRFC design parameters .....	36
14	Summary of high-current opening switch designs .....	46
15	Physical properties of liquid metals .....	54

## INTRODUCTION

This report summarizes research done at the Center for Electromechanics at The University of Texas at Austin (CEM-UT) under NASA/Lewis grant NAG-3-303. The work statement for this grant was to provide an overview of existing switch and power supply technology applicable to space launch. As part of the study, Richard Marshall was asked to look at a new candidate pulsed power supply for Earth-to-space rail launcher (ESRL) duty, the inverse railgun flux compressor. The final task was to design a set of switching experiments to study further the feasibility of Earth-to-space launch. The individual task studies provide the groundwork for identifying the switch technologically best suited for a space launcher.

## TASK A. POWER SUPPLIES AND SWITCHES

It is appropriate to begin this section with a review of ESRL requirements. In particular, the possibility of injecting payloads into Earth orbit will be the case under study. Table 1 presents the requirements as identified by Battelle Columbus Laboratories in an earlier study funded by NASA/Lewis under Contract NAS3-22882. [1]

Table 1. Earth-to-space rail launch requirements

<u>Parameter</u>	<u>Value</u>	<u>Units</u>
Projectile mass	6,500	kg
Projectile diameter	55	cm
Acceleration	2,500	G's
Escape velocity	10	km/s

---

From these requirements Marshall [2] calculated the ESRL design parameters (Table 2).

Table 2. Earth-to-space rail launch parameters

<u>Parameter</u>	<u>Value</u>	<u>Units</u>
Launcher length	2,039	m
Acceleration time	408	ms
Force	159	MN
Delivered energy density	159	MJ/m
Current	25.2	MA
Rail height	59.6	cm

---

A more detailed examination of Marshall's work was made under the present NASA/Lewis grant and is included as Appendix A. In that report, the launcher efficiencies were decreased because of flux trapping in the

inductive stores. It was felt that a more detailed look at machine parameters was required. For example, the generator buswork will influence the performance of the system. It was found that the rise time of the homopolar generator (HPG) current charging the inductor was faster than the dwell time of the payload in the launcher. The position of the projectile in the launcher would therefore have to be sensed in order to control the ESRL properly. The timing for energy store discharge and opening switch actuation are presented in Table 3.

Table 3. Required launcher timing

<u>Parameter</u>	<u>Value</u>	<u>Units</u>
Time to peak current (HPG charging inductor)	350	ms
Current transfer time from opening switch to launcher	4	$\mu$ s
Total time for which store is connected to launcher	400	$\mu$ s

An important calculated launcher performance parameter is the speed voltage associated with armature motion. For the launcher requirements under consideration, the maximum value of this parameter is 125 kV (Appendix A).

This list of parameters will provide a basis for the evaluation of state-of-the-art power supplies and switches presented in the next section.

## ENERGY STORES

Marshall has mapped the ranges of energy and velocity over which various types of railgun energy stores are useful (Fig. 1).

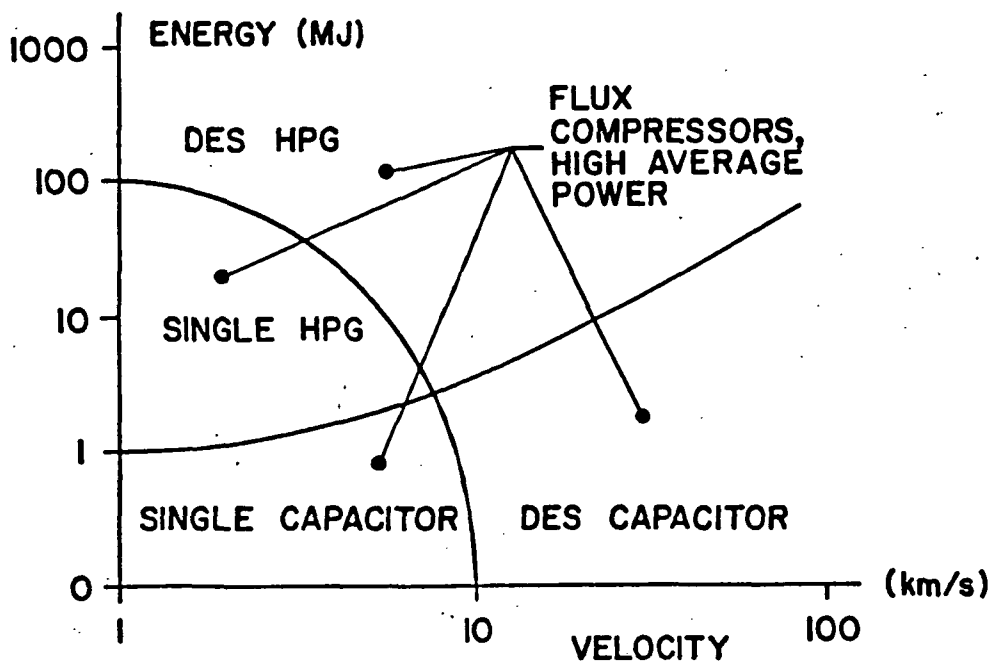


Fig. 1. Regions of usefulness for five types of energy-store railgun systems

The total energy requirement for the space launcher,

$$2,039 \text{ m} \times 159 \text{ MJ/m} = 32,000 \text{ MJ}, \quad (1)$$

and the required launch velocity, 10 km/s, single out the distributed-energy-store (DES) HPG and the flux compressor as launcher power supply candidates. Other power supplies will be reviewed because it is important to understand where present railgun technology stands and the large technological steps that will have to be taken to realize ESRL.

### Capacitors

Capacitors are candidates for hypervelocity work with low-mass projectiles. They are not candidates for Earth-to-space launch duty. They do represent a large fraction of the power supplies in use by the experimental railgun community today. A list of state-of-the-art devices marketed by Maxwell laboratories is presented in Table 4.



Table 4. Maxwell High Energy Density Capacitors

Model Number	Capacitance ( $\mu\text{F}$ )	Voltage (kV)	Energy (kJ)	Case Size (in.)	Voltage Reversal (%)	Design Life C/D Cycles	Peak Current (kA)	Bushing Style	Approximate Inductance (nH)
<u>Heavy Duty (High Voltage Reversal)</u>									
33838	120	10	6.0	8 x 14 x 24.3	80	> 100K	100	Low Profile	35
32184	6	60	10.8	11 x 14 x 27	60	> 10K	250	Scyllac	35
<u>Light Duty</u>									
33715	200	10	10	7-1/4 x 14 x 24.3	10	> 200K	100	Low Profile	35
32188	300	10	15	11 x 14 x 24.8	10	> 200K	100	L.P.	35
33593	50	20	10	7-1/4 x 14 x 24.3	10	> 200K	50	2 L.P.	60
33677	52	22	12.5	8-3/8 x 14 x 27	10	> 100K	65	2 L.P.	60
33830	300	10	15	7-1/4 x 14 x 24.3	10	> 50K	100	L.P.	35
33858	330	10	16.5	7-1/4 x 14 x 26.3	10	> 50K	100	L.P.	35
33859	82	20	15	7-1/4 x 14 x 26.8	10	> 50K	50	2 L.P.	60
32259	500	10	25	11 x 14 x 26.5	10	> 50K	100	Low Profile	35
32235	125	20	25	11 x 14 x 26.8	10	> 50K	50	1 Offset L.P.	50
32265	56	30	25	11 x 14 x 26.8	10	> 50K	35	1 O/S L.P.	80
32212	31.3	40	25	11 x 14 x 27	10	> 50K	25	1 O/S Upright	120
32266	20	50	25	11 x 14 x 27	10	> 50K	20	1 O/S U.R.	135
32225	11.1	60	20	11 x 14 x 27	10	> 65K	50	1 O/S U.R.	150

Source: Maxwell Laboratories Catalog

Low Profile Bushings are available up to 60 kV  
Capacitor designs at lower than 10 kV are also available

### HPG-Inductor

If the ESRL is to be driven with HPG-inductor power supplies, the configuration will necessarily consist of distributed energy stores, in which the power supplies are located along the launcher and are connected to deliver their energy as the payload passes the energy store-rail connection. In the case under consideration, each HPG would store 56 MJ and would transfer 40 MJ to the energy storage inductor at a charging current of 4 MA. To realize the 32,000 MJ of stored energy, there would need to be five energy stores per meter along the 2,039-m launcher, or 10,195 HPGs.

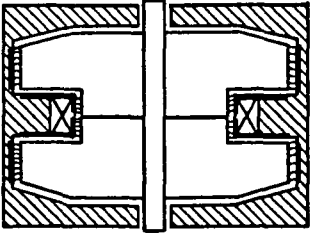
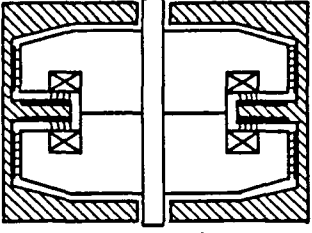
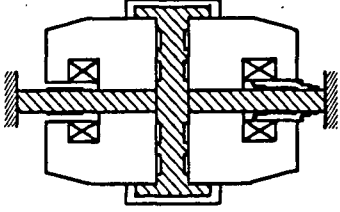
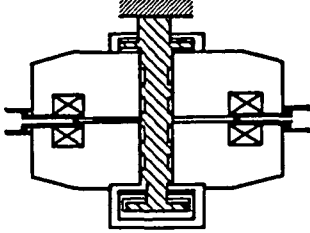
At the Australian National University in Canberra there is an operational 560-MJ HPG. Proposals have been written to charge that machine to 81 MJ and deliver 22 MJ to an energy storage inductor at 1.5 MA. [3] Actual experiments have been conducted in which the HPG stored 106 MJ and delivered 1.4 MJ to a storage inductor at 360 kA. [4] This HPG services several laboratories in a large facility, and long runs of buswork decrease system efficiency.

The Westinghouse HPG (EMACK) is a 17.5-MJ machine that has charged an energy storage inductor to 9.9 MJ at a charging current of 2.1 MA. This system has actually driven an electromagnetic launcher at a current greater than 1 MA. [5]

The final state-of-the-art HPG-inductor system is the CEM-UT 6.2-MJ compact HPG charging a 3-MJ, 5-turn coaxial cryogenic inductor at a charging current of 1 MA. Attention has been given to making the ESRL energy stores compact HPGs because compactness would be a design requirement for a launcher having the necessary linear energy density of 159 MJ/m.

Compactness of HPGs continues to be a goal of research at CEM-UT, as can be seen in Table 5. Compactness of the inductive stores, also an issue, is being improved by cryogenic cooling. A comparison between the volume energy density of the Maxwell Model 32184 capacitor in Table 4,  $0.016 \text{ MJ/m}^3$ , and that of the existing compact HPG,  $16.9 \text{ MJ/m}^3$ , further justifies the interest in the HPG-inductor power supply for ESRL duty.

Table 5. Progression of energy density gains with additional technology required for each increase

	ARRADCOM/DARPA COMPACT HPG	SINGLE-ROTOR HPG W/FACE BRUSHES AND SPINNING FIELD COIL	COUNTERROTATING- ROTOR HPG W/FACE BRUSHES AND STATIONARY SHAFT BEARINGS	COUNTERROTATING- ROTOR HPG W/FACE BRUSHES STATIONARY SHAFT BEARINGS AND ROTOR ACTUATION
				
VOLTAGE (V)	58	54.0	50	50
VOLUME * ENERGY DENSITY (MJ/m <sup>3</sup> )	16.9	26.5	45	60
REQUIRED TECHNOLOGY		FACE BRUSHES	STATIONARY SHAFT BEARINGS	ROTOR ACTUATION
GAIN IN ENERGY DENSITY (MJ/m <sup>3</sup> )		10	20	15

\* ALL ROTORS OPERATING AT 250m/s  
INCREASE IN ALLOWABLE OPERATING SPEED BENEFITS ALL DESIGNS EQUALLY.

### Compensated Pulsed Alternator

The compensated pulsed alternator, or compulsator, is shown schematically in Fig. 2. To a first approximation, the device can be modeled as a single-phase alternator having variable internal resistance and inductance. The output current wave shape depends upon both the load impedance and the internal configuration of the generator. Generally, the type of compensation (active or passive) is selected to best match the load characteristics at the desired pulse width.

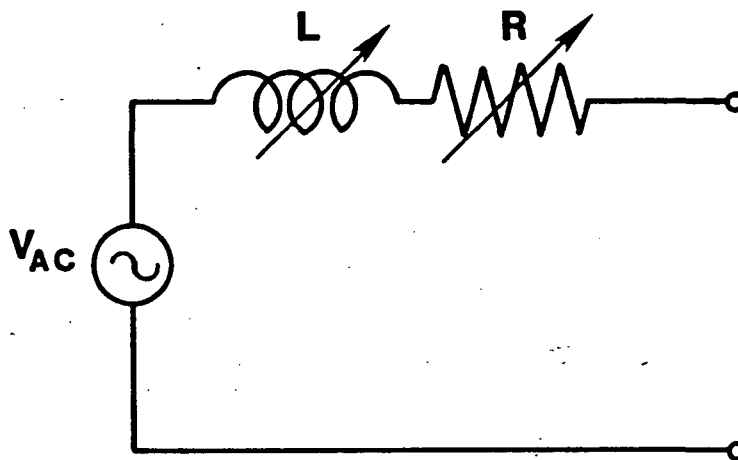


Fig. 2. Schematic representation of a compulsator

In 1979, a prototype pulsed generator was developed for driving xenon flashlamps for experiments funded by Lawrence Livermore National Laboratory (LLNL). The generator delivered 135 kJ in a single pulse to the flashlamp load at a peak power of 130 MW. [6] Peak current exceeded 30 kA at a pulse width of 1.3 ms (full width-half max). A cutaway view of the prototype generator is shown in Fig. 3.

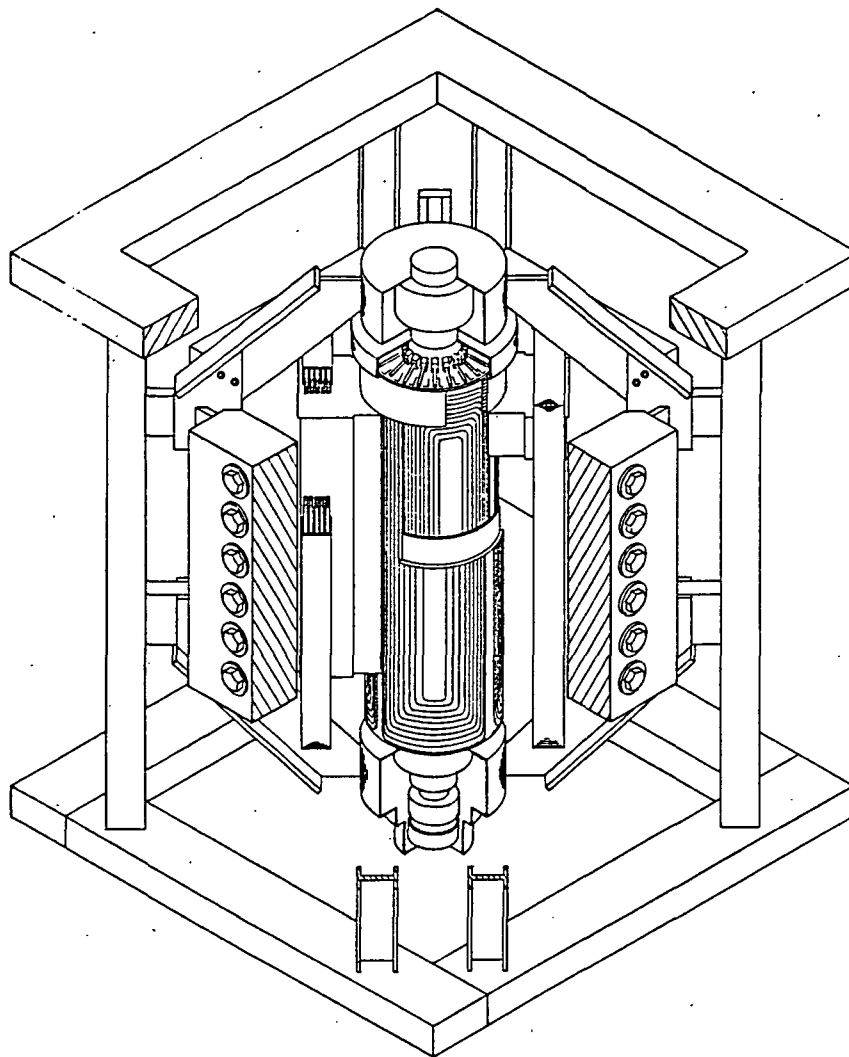


Fig. 3. Cutaway view of CEM-UT prototype compensated pulsed alternator

Currently, CEM-UT is under contract (Contract No. DAAK10-83-R-0099) to the U.S. Army Armament Munitions, and Chemical Command (AMCCOM) to produce a conceptual design for a rapid-fire electromagnetic launcher (EML).

Design parameters for two EML compulsators are presented in Table 6. Table 7 gives the rapid-fire gun test bed parameters. Table 8 shows that the compulsator must store much more energy than it delivers so that the pulse width can be kept short.

Table 6. Example compulsator parameters

<u>Parameter</u>	<u>Case I</u>	<u>Case II</u>	<u>Units</u>
Number of poles	8	8	
Number of conductors per pole	2	1	
Rotor speed	3,520	3,520	rpm
Laminated rotor diameter	0.813	0.813	m
Total rotor diameter	0.847	0.847	m
Lamination tip speed	150	150	m/s
Laminated rotor $\lambda/D$ ratio	2.0	2.0	-
Overall rotor length	2.66	2.66	m
Rotor inertia	714	714	kg·m <sup>2</sup>
Inertial energy stored	48.6	48.6	MJ
Effective inductance	8.0	2.0	$\mu$ H
Total Resistance	1.7	0.43	m $\Omega$
Open-circuit voltage	6.0	2.65	kV
Average magnetic flux density (applied field)	1.53	1.35	T

Table 7. Compulsator-driven rapid-fire gun test bed parameters

<u>Parameter</u>	<u>Nominal Value</u>	<u>Units</u>
Projectile mass	0.08	kg
Projectile velocity	2.0	km/s
Projectile kinetic energy	160	kJ
Repetition rate	60	pps
Pulses/burst	10	-
Barrel length	3.0	m
Peak current	730	kA
Acceleration time	3.0	ms

Application of the compulsator to the ESRL would require either development of machines capable of operation at 125 kV or design of special pulse transformers to couple the compulsators to the launcher. Also, a method for disconnecting the compulsators from the launcher on a current zero would have to be developed. An inherent advantage of the compulsator, however, is that if it is designed to drive against the speed voltage of the launcher, no opening switch is required.

Table 8. Compulsator-driven rapid-fire system energy balance

<u>Parameter</u>	<u>Case I</u>	<u>Case II</u>	<u>Units</u>
Initial energy stored	48,640	48,640	kJ
Remaining rotor kinetic energy	47,280	47,570	kJ
Final speed/initial speed	98.6	99.3	%
Change in inertial energy	1.36	1.07	MJ

During the past five years, under sponsorship of LLNL and the Naval Surface Weapons Center (NSWC), [6] CEM-UT has developed an engineering basis for the design of larger machines that are capable of delivering up to 10 MJ at peak power levels exceeding 10 GW. The effort to date has included

- development of computer codes for generator design, impedance calculation, and nonlinear transient circuit simulation
- compulsator proof-of-principle experiments at 130 MW
- demonstration of inductance variation >40:1 for a small-scale active rotary flux compressor with fully laminated steel rotor and stator construction, and
- development of vacuum-pressure-impregnated air-gap armature and compensating windings.

#### Flux Compressors

Small explosive strip-type flux compressors have been used in conjunction with railguns to accelerate small masses to hypervelocity. [7] Typical operating parameters are 1.2 MA at a 600- $\mu$ s pulse duration. Typical energies stored in the compressor excitation capacitor bank are 360 kJ. The devices are not reusable and would therefore not be candidates for the ESRL. They do demonstrate the applicability of flux compression for producing large currents at short pulse widths, however.

CEM-UT has also been active in the development of rotary flux compressors. This class of machine is used with a start-up capacitor bank similar to the explosive strip-type flux compressors. After the current is injected into the winding, inertial energy is converted into electromagnetic energy by flux compression. As a result, more energy is

delivered to the load than was stored in the start-up bank. The cross-section of this machine resembles the compensated pulsed alternator shown in Fig. 3. Table 9 gives typical parameters for a rotary flux compressor capable of delivering a 10-MJ, 670- $\mu$ s pulse. [8] An example of the performance parameters of this machine under load is included in Table 10. The operating voltage for this device is 20 kV, which is far less than the 125-kV launcher operation. This machine, which is similar to the compensated pulsed alternator, would require a pulse transformer to interface properly with the launcher.

Table 9. Rotary flux compressor parameters

<u>Parameters</u>	<u>Value</u>	<u>Units</u>
Number of poles	8	
Number of conductors per pole	3	
Rotor speed	2,680	rpm
Laminated rotor diameter	1.067	m
Lamination tip speed	150	m/s
Laminated rotor $\lambda/D$ ratio	1.64	
Overall $\lambda/D$ ratio	2.25	
Shaft length	3.0	m
Shaft diameter	0.52	m
Outer winding diameter	1.090	m
Mechanical clearance	0.32	cm
Rotor inertia	2,120	kg·m <sup>2</sup>
Total rotor mass	15,650	kg
Inner stator diameter	1.096	m
Outer stator lamination diameter	1.532	m
Stator stack length	1.750	m
Stator mass (laminations and winding)	11,800	kg
Maximum stator length	2.10	m
Total stator length	2.58	m
Total stator mass with housing	20,500	kg
Total mass	36,000	kg



Table 10. Performance parameters under load

<u>Parameters</u>	<u>Value</u>	<u>Units</u>
Peak current	754	kA
Peak terminal voltage	17.8	kV
Peak output power	13.4	GW
Peak torque	61.9	MN·m
Peak mechanical power	16.6	GW
Initial speed	2,680	rpm
Final speed	2,500	rpm
Polar moment of inertia	2,120	kg·m <sup>2</sup>
Inertial energy stored	84	MJ

### Inverse Railgun Flux Compressor

The final type of flux compressor of interest is the inverse railgun flux compressor. This device is conceptual at this point and is discussed in detail in the section of this report dealing with Task B.

## SWITCHES

### Arcing Switch

Comparison of the foregoing characteristics of the various possible power supplies shows that the HPG-inductor system is presently the most promising candidate for ESRL. This section will therefore begin with a discussion of suitable switches for this system.

It is important to understand the physical requirements for such a switch. A simplified schematic diagram of the operation is shown in Fig. 4.

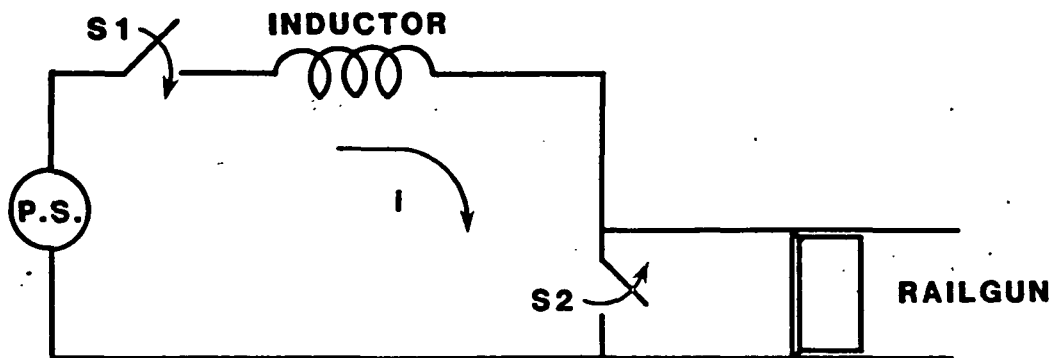


Fig. 4. Simple inductive transfer circuit

A power supply, in this case the HPG, charges the energy storage inductor through switch S1. At peak stored energy, which is also at peak current in this case, switch S2 opens and develops sufficient voltage to transfer current into the armature, which may consist of an arc, a solid armature or a combination of both.

The physical requirements for the ESRL switch during charging are that it carry a sinusoidal current that peaks at 4 MA in 350 ms. The  $\int i^2 dt$  implied by this requirement is  $1.48 \times 10^{12} \text{ A}^2 \cdot \text{s}$ , or in more familiar switch parlance, the  $\int i dt$  must be  $6.5 \times 10^5$  coulombs. The candidate switch types for this duty are electronic switches (semiconductors), gaseous or metal vapor switches (ignitrons), or mechanical switches (galvanic contacts). High-power silicon controlled rectifiers advertise a rating of a 1/2-cycle surge current of 35 kA, or  $5 \times 10^6 \text{ A}^2 \cdot \text{s}$ . The General Electric SCR applications manual for ignitrons used in capacitor discharge service advertise a model GL-8205 device with a coulomb rating of 1,500. It can be seen that large numbers of either of these types of devices would have to be paralleled to realize the required duty cycle.

Close attention to topology would be required to distribute the inductance such that the transient charging current is shared equally among the hundreds of devices. This is not a workable alternative, and galvanic contacts are therefore required. Galvanic contacts have an interface resistance, so  $\int i^2 dt$  is a better indication of heating considerations than coulomb rating in sizing devices.

Independent testing at CEM-UT has established a butt contact rating for copper-to-copper joints. A 6.5-cm<sup>2</sup> (1-in.<sup>2</sup>) joint loaded with a force of 8.9 kN (2,000 lbf) successfully carried 100 kA before spot welding of the contacts occurred. The  $\int i^2 dt$  of the current wave form for this testing was  $5 \times 10^9$  A<sup>2</sup>·s. The area required for the butt contact in the ESRL switch is therefore 1,900 cm<sup>2</sup> (296 in.<sup>2</sup>), or a square 43 cm (17 in.) on a side.

Thus far, only the charging duty for the switch has been addressed. The opening duty requires consideration of the principles by which energy can be transferred from the inductor to the railgun via the opening switch. These are presented in Appendix B, which is a paper by Woodson and Weldon of CEM-UT, entitled "Energy Considerations in Switching Current from an Inductive Store into a Railgun". This paper not only covers the theory involved in the transfer, but also presents numerical examples typical of operational HPG-inductor powered railguns. If the analytical technique presented in this paper is applied to the first stages of the ESRL, the energy accepted by the switching element is 3.56 MJ per stage.

The assumed parameters that led to this energy are taken from Appendix A and are presented in Table 11.

Table 11. ESRL parameters used to calculate dissipated switching energy

<u>Parameter</u>	<u>Value</u>	<u>Units</u>
L <sub>1</sub>	6	μH
I <sub>j</sub>	4	MA
W <sub>j</sub>	41	MJ
L <sub>2j</sub>	0.5	μH
L <sub>2i</sub>	0.5	μH/m
M	6,500	kg
X <sub>f</sub>	0.4	m

The material eroded from the contacts during a switch opening will be

$$18 \text{ mm}^3/\text{kJ} \times 3,560 \text{ kJ} = 64,000 \text{ mm}^3 (3.91 \text{ in.}^3)$$

Because of this large material loss during each opening cycle, an arcing switch can be dismissed for ESRL duty. The mating surfaces of the contacts would become so scarred during the first opening cycle that a second inductor charging sequence could not occur.

### Fuse Switch

To alleviate this problem, a replaceable element (a fuse) is placed in parallel with the butt contacts. This element is sized to accept the commutation of full charging current from the butt-contact switch. Shortly after peak current is established in the fuse, it ruptures electrothermally and produces voltage to transfer current to the railgun. With this arrangement the fuse element can be tightly coupled inductively to the butt-contact switch, and the energy absorbed by the contacts decreases substantially. Assuming that 10 percent of the butt joint area consists of available contact spots and that one is willing to accept pitting 0.005 mm (0.002 in.) deep, the energy that can be absorbed by the contact is 52.8 kJ. The expression for the absorbed energy is

$$W_{so} = \frac{L_{2i}}{L_1} W_i \quad , \quad (2)$$

where

- $W_{so}$  = energy absorbed by switch, J,
- $L_{2i}$  = inductance between butt contacts and fuse, H,
- $L_1$  = inductance of the energy storage inductor, H,
- $W_i$  = initial stored energy, J.

The required inductance between butt contact and fuse is then 0.008  $\mu$ H.

General Dynamics Corporation has designed a 41-MPa (6,000-psi) pulsed pressure butt-contact switch rated at 750 kA and with  $\int i^2 dt$  of  $4.5 \times 10^{10}$  A<sup>2</sup>·s. This device was built and tested at 300 kA peak current and an  $\int i^2 dt$  of  $1.57 \times 10^{10}$  A<sup>2</sup>·s. It opened 0.25 mm (0.1 in.) in 1 ms. This opening time will be typical of mechanical systems. [3,9]

### Explosive or Rupturing Switch

The explosive or rupturing switch is from a family of switches that has received much experimental attention. [10-12] The butt contact is replaced by a solid conductor that is ruptured at the appropriate time by means of chemical or electromagnetic energy. This type of device is useful for pulse compression because of its very short actuation time.

Rupturing switches have been designed for use with an HPG-inductor system. Actual testing has been done only for devices with an  $\int i^2 dt$  capacity of  $1.35 \times 10^7 \text{ A}^2 \cdot \text{s}$ , however, five orders of magnitude below the ESRL requirement. It is believed that a rupturing switch can be sized to handle the ESRL charging duty. This type of switch device has received the most attention from the French, who believe that the explosive energy or magnetic command energy must be equal to the energy being transferred into the launcher from the inductive store. [11] The single-shot duty and the large quantity of explosives required eliminate this technology as a self-sufficient switch for ESRL.

Up to the present time, nothing has been said about the switching requirements of a DES ESRL. Rail erosion may be a formidable problem in plasma-driven launchers.

Nothing but the simplest design is acceptable for a rail system 2,039 m long that has to be reclaimed between shots and replaced only after a number of shots. One such design is parallel continuous rails. The switching scheme shown in Fig. 4 now becomes more complicated. The shorting contacts, S2, cannot be connected to the rails while the power supply is charging the inductor. This would present a set of shorted rails in front of the arc armature that would shunt current out of the arc. Also, an individual DES power supply cannot remain connected to the launcher once its energy is depleted. Otherwise, subsequent stores would lose energy recharging this supply. The switching scheme now becomes that shown in Fig. 5. In position A, the energy storage inductor is charged.

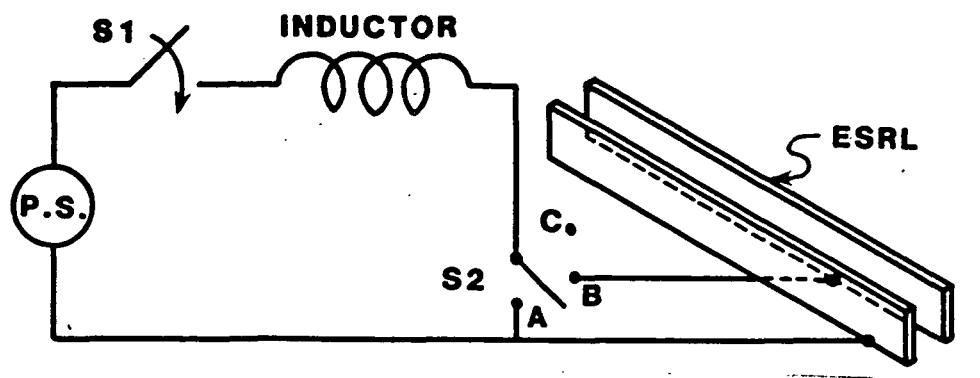


Fig. 5. Single-stage switching

In position B, the inductor is switched into the rails. Position C disconnects the depleted store from the launcher. The voltage to be applied to the launcher, which is the voltage developed between points B and A, must be greater than the ESRL voltage, which is the sum of the rail drop, the armature drop, and the back voltage or speed voltage of the armature. Another requirement is that the connection to B must not be made until the arc armature has passed the point where the energy store connects to the launcher rails. Simulations of the DES configuration show degradation of performance if this requirement is not met. It has already been shown that the large galvanic contact switch alone cannot perform this duty, but this same switch is capable of transferring current to an inductively close-coupled parallel path. This second path is shown in Fig. 6.

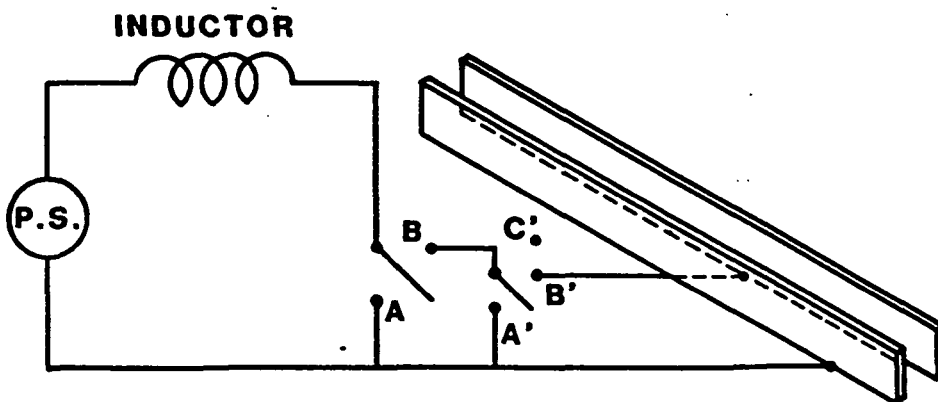


Fig. 6. Staged switching

The advantage of staged switching is that under the assumption that the galvanic contact switch can transfer current in from 5 to 10 ms, the coulomb rating of the second path is between 20,000 and 40,000 coulombs, or  $\int i^2 dt$  is between 8 and  $16 \times 10^{10} \text{ A}^2 \cdot \text{s}$ . This will allow a manageable number of devices with lower energy ratings to be considered as candidate opening switches for the second path. These switches are faster-interrupting and therefore develop more voltage than a slower-acting switch. This is a fundamental requirement if voltages on the order of 125 kV are to be developed to drive the back voltage of the arc armature near the end of the ESRL. Candidate switches for second- or possibly third-path duty are:

#### Vacuum Switches

Arrays of vacuum switches can be considered. One such state-of-the-art device is described by Honig [13] as follows:

Vacuum switches are characterized by their capability to conduct large current in a diffuse mode at low arc voltages and yet recover rapidly to high voltages after a current zero. Under a research contract with EPRI, General Electric Co. investigated and developed the rod array triggered vacuum gap (RATVG) switch for high-voltage, high-fault-current ac breaker applications. During tests at GE, the G1 RATVG switch successfully interrupted a current of 150 kA peak (after conduction for 1/2 cycle at 60 Hz) and sustained a recovery voltage of 135 kV. [14 -- this report] An earlier experimental model carried an ac half cycle of 240 kA peak with an arc voltage of less than 70 V while showing no evidence of electrode melting even though the total charge transferred was over 1400 C. [15 -- this report] These current levels were actually test facility limited and the ultimate current limit of RATVGs is still unknown.

#### Explosive Switches

This staging concept has been widely used in the explosive switch community. Conte, et al., [16] describe the procedure and make an interesting prediction:

In tests using a 60- $\mu$ H inductor storing 90 kJ, a 6 section explosive switch and a 40 cm long by 1.5 in. wide by 1 mil thick aluminum fuse, generated a 30 kA, 120 kV pulse. Of the 90 kJ stored, approximately 9 kJ was required to vaporize the fuse while only 320 J was dissipated in the explosive switch arc. Comparable efficiencies can be expected for systems handling energies at the megajoule level.

### Semiconductor Switches (Corbino Disks)

Another possible third-stage switching device is the Corbino disk. As the transfers from path to path became more rapid, the  $\int i^2 dt$  requirement decreases, and semiconductors might well be viable technology. Inall [17] describes this device:

A new type of circuit interrupter is described based on the increase in resistance that occurs when a magnetic field is applied to a material with a strong Hall effect in the configuration known as Corbino's disc. Measurements on discs of indium antimonide showed an increase in resistance of about two orders of magnitude in a time of five microseconds. Larger resistance ratios should be possible by optimizing the properties of the material...

It is important to note that it will not be necessary to use the switches of the type employed at the front end of the launcher all the way to the exit end. Nothing has yet been said about the mechanism that takes the switch from B' to C' in Fig. 6. At the end of the launcher, where the voltages are very large, a triggered spark gap might provide the B' connection to the launcher. Upon a current zero the arc will go out and will naturally disconnect the discharged energy store.

This section has given a brief overview of the switching problem for ESRL. Some candidate state-of-the-art switches have been presented that show promise for the realization of ESRL.



## TASK B. THE INVERSE RAILGUN FLUX COMPRESSOR FOR ESRL SYSTEMS

by  
Richard A. Marshall

### INTRODUCTION

It is worthwhile to examine the use of the inverse railgun flux compressor (IRFC) as an energy source for ESRL systems because of the possible gains that might be achievable. The prime candidate at present for energy stores is the homopolar generator/inductor (HPG/I) combination, and it could be that in the long run this will remain the favorite. Of necessity the HPG/I is the yardstick by which alternative systems must be judged.

The HPG/I has many factors in its favor. It has been used to power three railguns, the Australian University (ANU) railgun at Canberra, the railgun at Picatinny Arsenal, and the General Dynamics railgun tested at The University of Texas at Austin. [9,18-20] As well, there is now a large body of literature on homopolar generators. [21-34] Their design, construction and operation are well understood.

There are two aspects of the HPG/I combination in which improvement may well be possible. The first concerns the relatively low voltage available. Because the ESRL will require such large energies, it is imperative that the cost of the energy stores be kept as low as possible. This means that only iron-core HPGs with normal excitation are likely to be acceptable. Higher voltages are possible with higher excitation fields such as might be provided by the use of superconductors. This is likely to be too costly, however, unless some elegant way can be found to integrate the HPG with a superconducting inductor. It is probable that HPGs of the compact (all-iron-rotating) type [35] will be the main contender because of their relatively low cost.

The low voltage produced means that the resistance of the inductor is embarrassingly low for reasonable energy transfer efficiencies. It then

becomes almost necessary to use cryogenic inductors using liquid nitrogen-cooled aluminum. Because flux compressors are fast acting (i.e., produce higher voltages), the effective resistance of the inductive storage element of the system can be much higher, and can therefore have lower mass, bulk, and cost.

It is sometimes said that the voltage produced by HPGs can be made as high as desired by increasing the number of flux-cutting conductors. In fact, this is not possible in practice without reducing the current that can be obtained because of the space required for current collection brushes. A further difficulty is that useful flux cutters must be placed in the excitation air gap, which increases the excitation required. The Canberra HPG was designed to use four voltage-generating conductors to obtain high voltage. Because the conductors (the rotors) are steel, increased excitation was not required, but the use of multi-pass conductors in general poses considerable problems.

Another possibility is to use an air-core HPG with its inductive energy store combined as has been done at NRL, [36] but it is not probable that any cost reduction would result from this approach.

The second aspect in which improvement may be possible, concerns the manner in which the IRFC can be integrated into the system. As indicated in Fig. 7, if HPG energy stores are used, then a power plant is required to produce the energy required to bring the HPGs up to speed. With the IRFC driven by a heat engine of the single-shot diesel type, for example, a major power plant is not required. Note that this argument does not hold if the source of energy for the launcher is nuclear rather than oil.

Assuming for the moment that successful IRFCs can in fact be built, there will of course be many other practical considerations to weigh before their use could be recommended, such as how they should be "corked," excited, switched, and the volume they occupy.

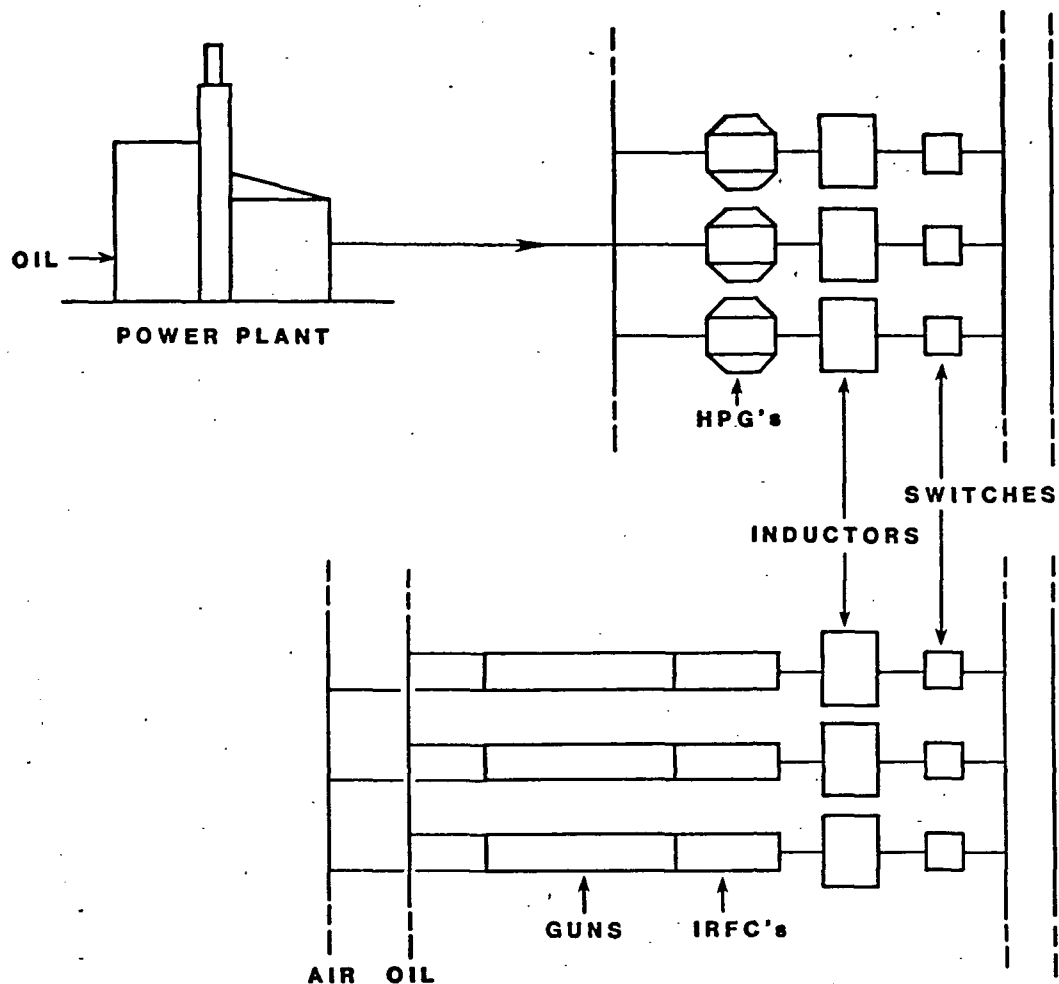


Fig. 7. Conceptual inverse railgun/inductor ESRL system

### THE CONCEPT

The fact that flux compressors can be used to power railguns has been demonstrated by the railgun work at LLNL and Los Alamos National Laboratory, [37-39] using strip-type explosively driven compressors. Flux compressors of this type have two disadvantages. They are one-shot devices, and their inductance change available is relatively small, thus making their ratios of excitation energy to delivered energy large.

The concepts involved in the IRFC overcome both of these difficulties. The work at ANU [40,41] showed how metal-on-metal sliding contacts can

be made to work at high speeds and high current densities in a railgun (see Fig. 8) with minimal damage to the rails. There is thus every reason to believe that a multi-shot inverse device could be built to compress flux, rather than to expand flux as in the normal railgun. Furthermore, there is no obvious upper limit to the flux compression ratio that can be achieved, particularly if one considers the multi-rail IRFC that is discussed below.

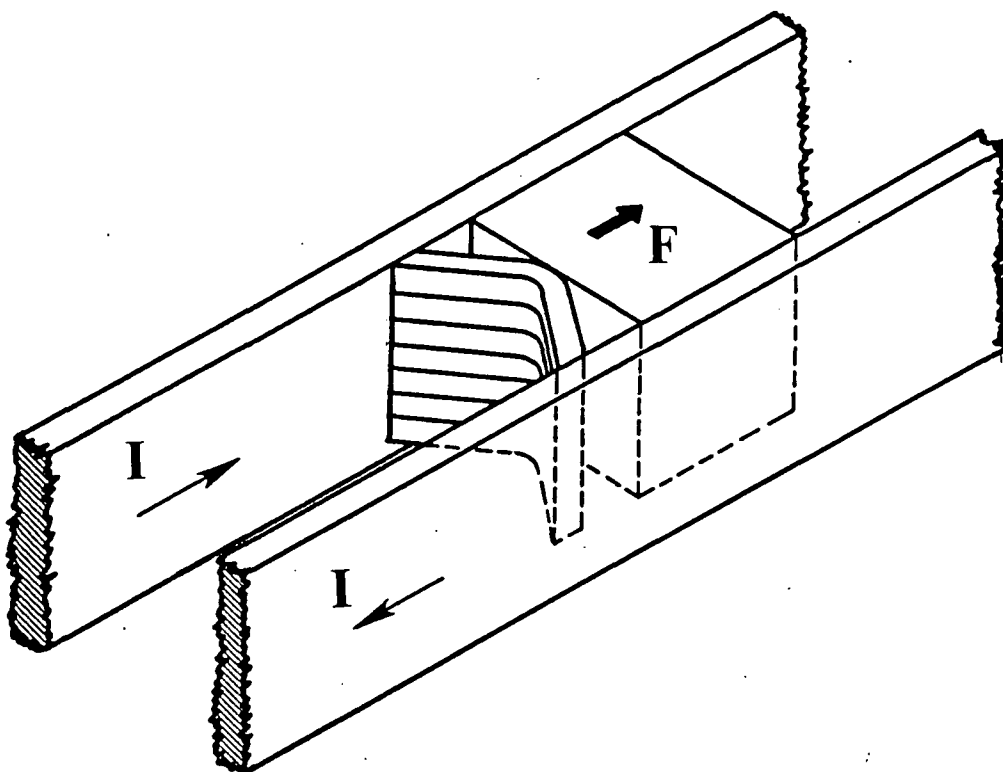


Fig. 8. Sliding metal armature in a conventional railgun

The principles involved are indicated in Figs. 9 and 10. The IRFC is simply a railgun forced to run in reverse, and the electrical loop, consisting of the armature rails and bridge, is forced to diminish, thus causing the magnetic energy in the loop to increase.

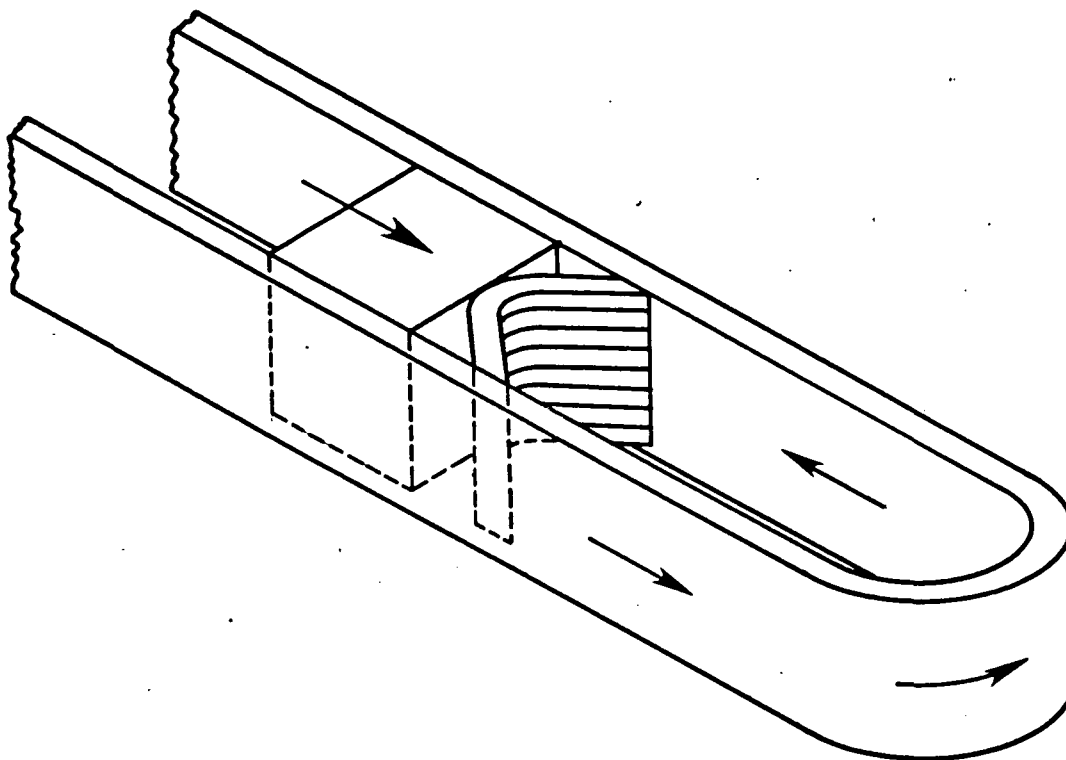


Fig. 9. Sliding metal armature in an inverse railgun

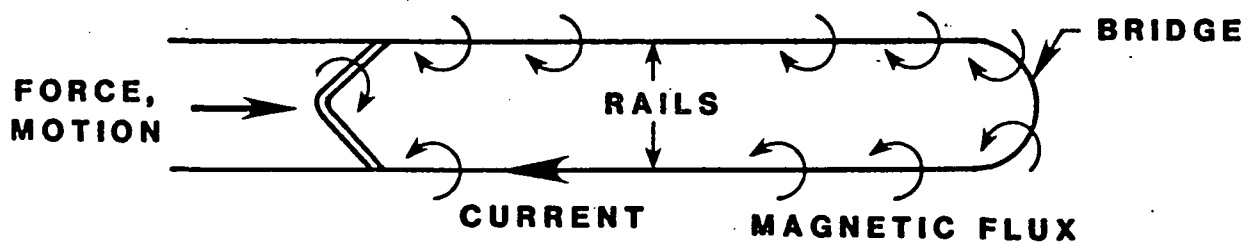


Fig. 10. Current, field, and force in an inverse railgun

## THE EQUATIONS

For an inductor of inductance  $L$  having variable geometry [42] and zero resistance carrying a current  $I$ , the magnetic flux,  $\phi$ , is constant, i.e.,

$$LI = \phi = \text{constant} \quad (3)$$

The energy,  $W$ , in the inductor is given by

$$W = 0.5 LI^2 \quad (4)$$

Substituting from (3) into (4) gives

$$W = 0.5 \phi I = 0.5 \phi^2 / L \quad (5)$$

or

$$\frac{W_1}{W_0} = \frac{I_1}{I_0} = \frac{L_0}{L_1} \quad (6)$$

where  $W_0$ ,  $I_0$ ,  $L_0$  are the initial values of energy, current, and inductance for the inductor and  $W_1$ ,  $I_1$ , and  $L_1$  are for the changed geometry.

Thus, if a hundred-fold increase in the energy of the inductor is required, then its initial inductance must be a hundred times greater than its final value, and the initial current a hundred times smaller.

The derivations of the equations for the railgun and the inverse railgun begin in a similar manner. The voltage,  $E$ , generated in a circuit in which flux is varying with time,  $t$ , is

$$E = \frac{d\phi}{dt} = \frac{d(LI)}{dt} \quad (7)$$

The voltage  $E$  required for the railgun in Fig. 11 is then given by

$$E = \frac{d(LI)}{dt} + IR \quad (8)$$

$$= L\dot{I} + I\dot{L} + IR \quad (9)$$

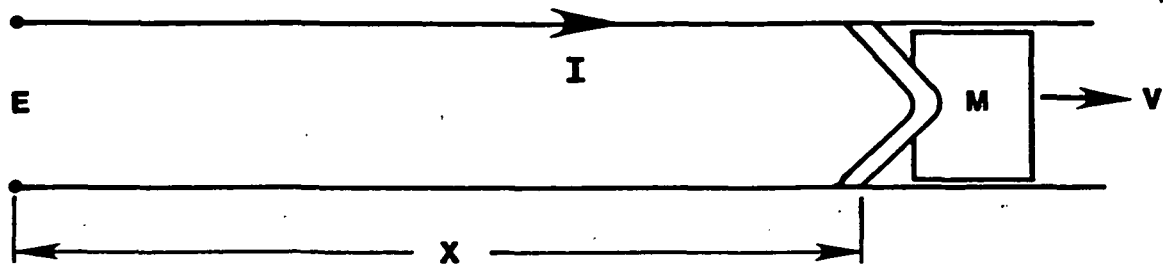


Fig. 11. Identification of variables in conventional analysis

where  $R$  is the combined resistance of the rails and the armature. Substituting  $L'$  for the inductance per unit railgun length and  $R'$  for unit resistance gives

$$E = L'x\dot{I} + IvL' + IR'x + IR_{\text{other}} \quad (10)$$

where  $R_{\text{other}}$  is any other resistance, such as that of the armature, and  $x$  is linear distance along the railgun.

The rate of change of current is then given by

$$\dot{I} = (E - I(L'v + R'x + R_{\text{other}}))/L'x \quad (11)$$

Equation (11) is the standard starting point for the numerical simulation of the simple railgun.

For the simple IRFC as shown in Fig. 12,  $E$  of Eq. (11) is zero, giving

$$\dot{I} = - I(L'v + R'x + R_{\text{other}})/L'x \quad (12)$$

This is the starting point for the simulation of the IRFC, noting that  $v$  is negative.

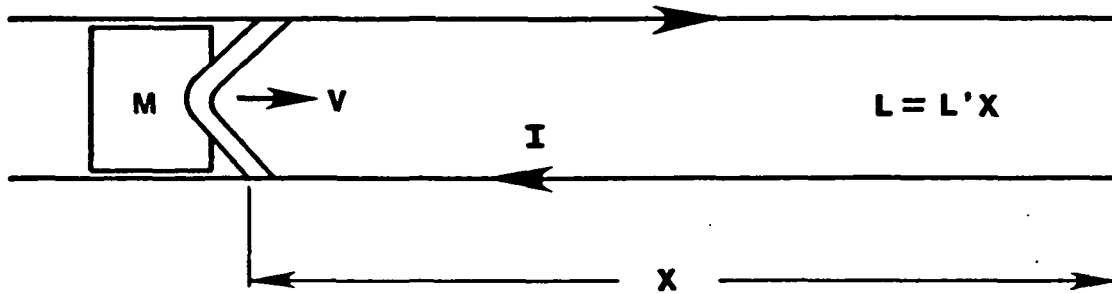


Fig. 12. Identification of variables in IRFC analysis

It is interesting to note that in order for  $I$  to be positive, that is for current amplification to occur rather than decay, the following conditions must be met:

$$|L'v| > R'x + R_{\text{other}} \quad (13)$$

A similar expression can be obtained for the condition that must be met for a self-excited HPG generator to self-excite.

In general, because it is the "end point" that is known, i.e., the current and energy in the flux compressor at the end of its compression stroke, it is better to perform simulations in reverse and to add the dissipative terms being included rather than subtracting them.

#### The Form of the IRFC

The inductor portion of the IRFC, the "end point," may best be considered as a single-layer solenoid with its diameter equal to its height as shown in Fig. 13. It consists of the armature in its rest position and the rails wrapping around the end. The reason for the square geometry is so that it will match a square-bore inverse railgun. It is not profitable to consider anything other than a square bore at this stage. The physical size of this inductor will be determined by the energy it is to contain when charged, and the number of turns will be determined by the current required when charged. Other factors that must be considered are the limit of current per unit rail height, the stress in the inductor, and the rail and inductor resistances.



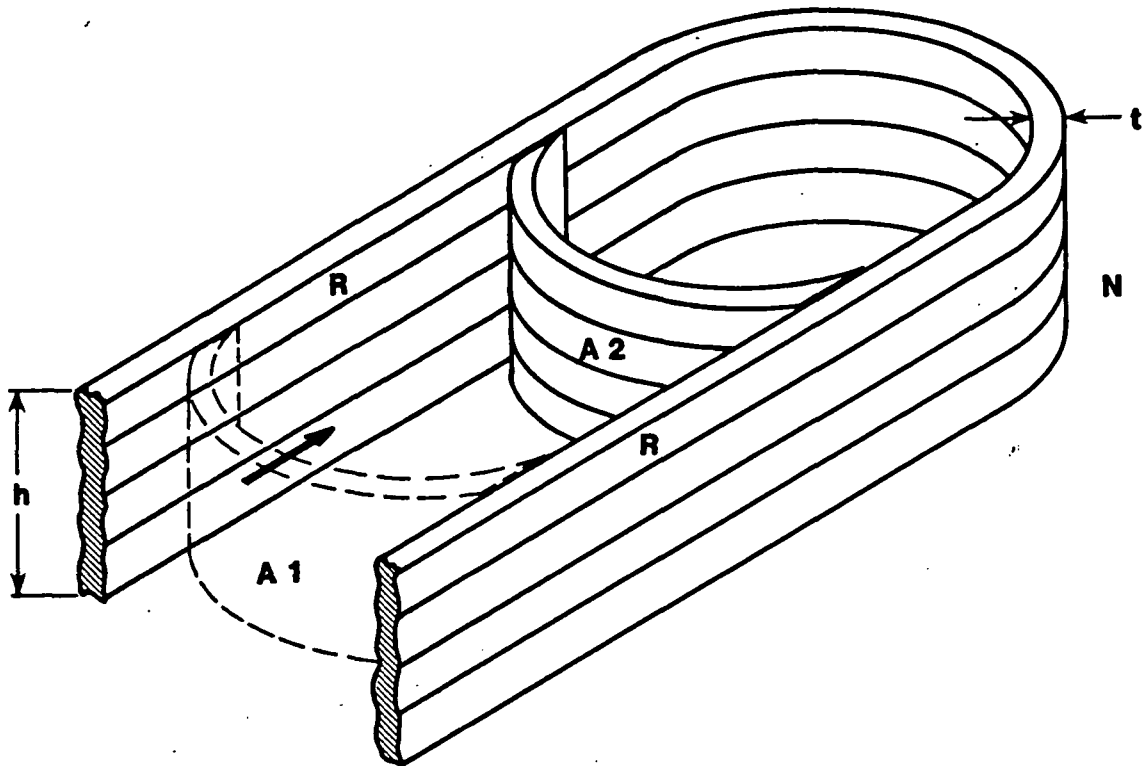


Fig. 13. Simulation of end portion of IRFC as an inductor

The next point to be considered is the required inductance change. As shown above, if a charging energy of one percent of the final energy is required, then the inductance of the IRFC must be 100 times higher at the beginning of the compression than at the end. It may well be desirable to have an inductance change of ten times higher still. This would make for an impractically long device if  $N$ , the number of rails per side, is kept constant, so  $N$  must be varied along the compressor. The logical way to do this as the compression proceeds is to reduce  $N$  progressively, so that the current per unit rail height,  $NI/h$ , is kept below some limiting value.

There are two ways in which  $N$  can be varied along the compressor. It can be varied in factors of two at a time as shown in Figs. 14 and 15. The number of armature bars equals the largest (initial) value of  $N$ . As the transition from  $N$  to  $N/2$  occurs, the number of armature bars connected in series is halved, each new pair being then connected in parallel. Thus, the current in each armature bar falls to half its pre-

vious value as the switching occurs, then returns to its full value as the next switching position is approached.

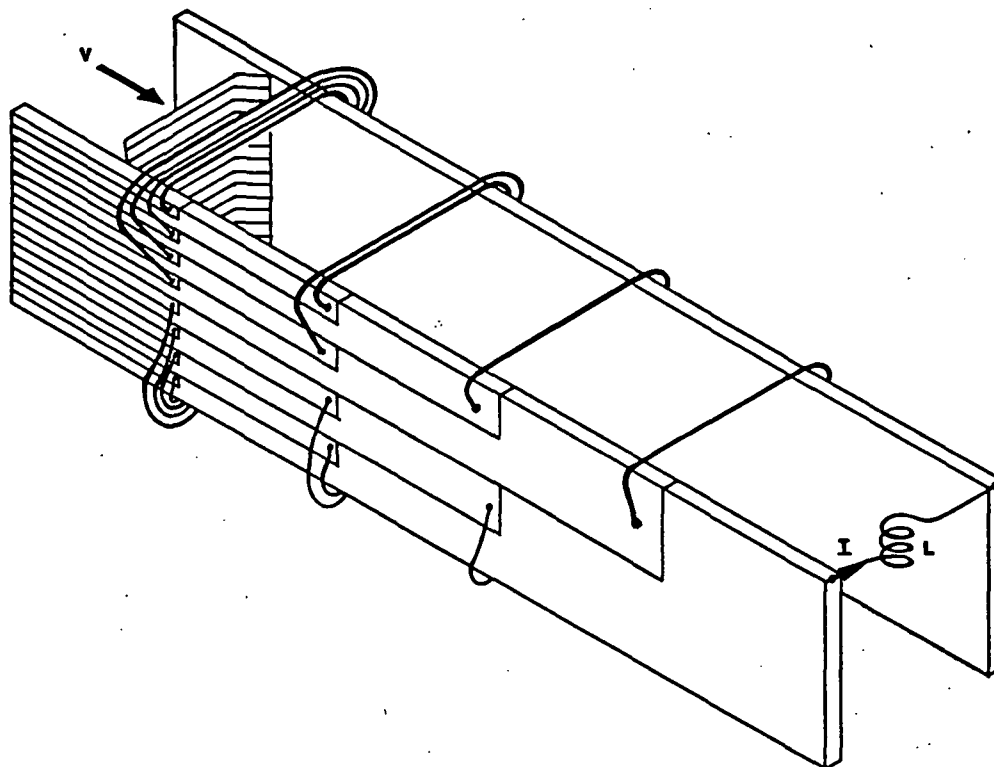


Fig. 14. Interconnections for asymmetric method for varying N along rails

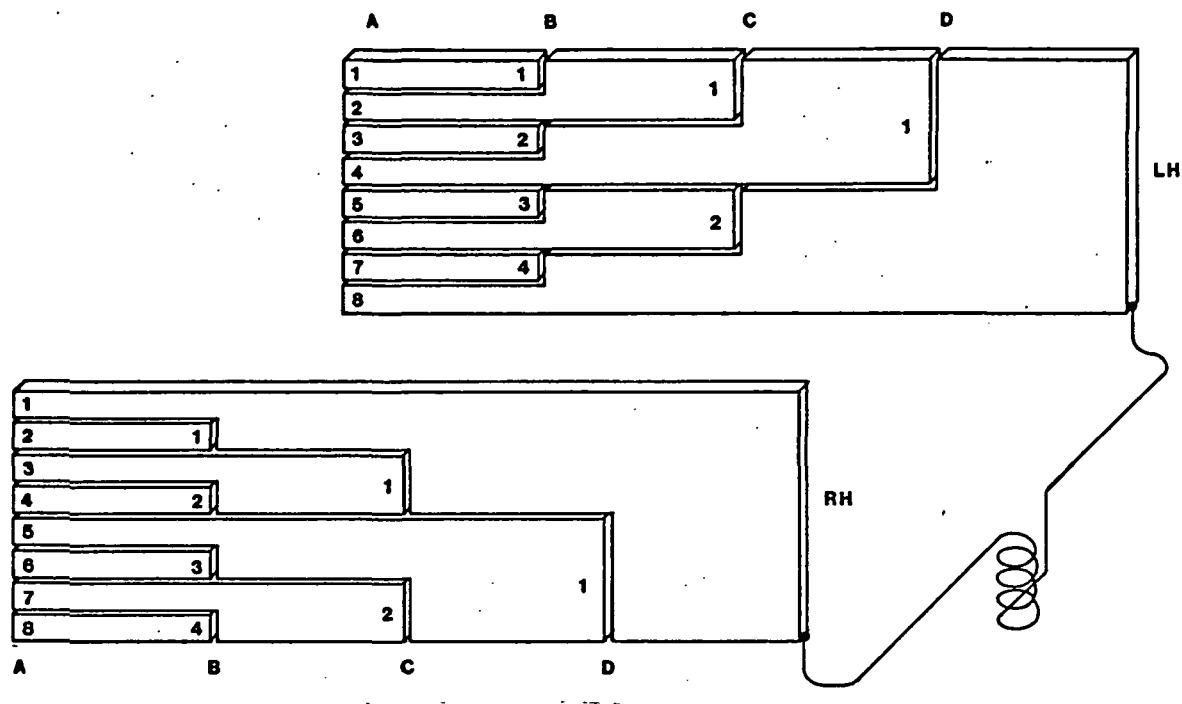


Fig. 15. Detail of rail layout for asymmetric method for varying N

There may well be a problem with inductance as the switching occurs. Inductive energy associated with the current in the armature bars will try to keep the current flowing. It may be desirable to use an angled (scarfed) transition in the rails at the switching point so that the current is not required to switch instantly. These "ramps" could be made of resistive material to absorb the energy. It may also be desirable to carry the armature bars from one rail to the other near the top and bottom of the launcher bore, rather than straight across, to reduce the inductance.

The other way to reduce N along the rails is to decrease it by two at each switching point as indicated in Fig. 16. In this way, the current in each armature bar can be kept more nearly constant, and the inductive problems will be much less. The crossover bars from rail to rail occur naturally at the edge that is both mechanically and inductively desirable. The cost of this is that many more switchings are required. Until some appropriate experiments have been conducted, it will not be known whether the switching is simple or difficult, but it looks as if there would be no particular problems.

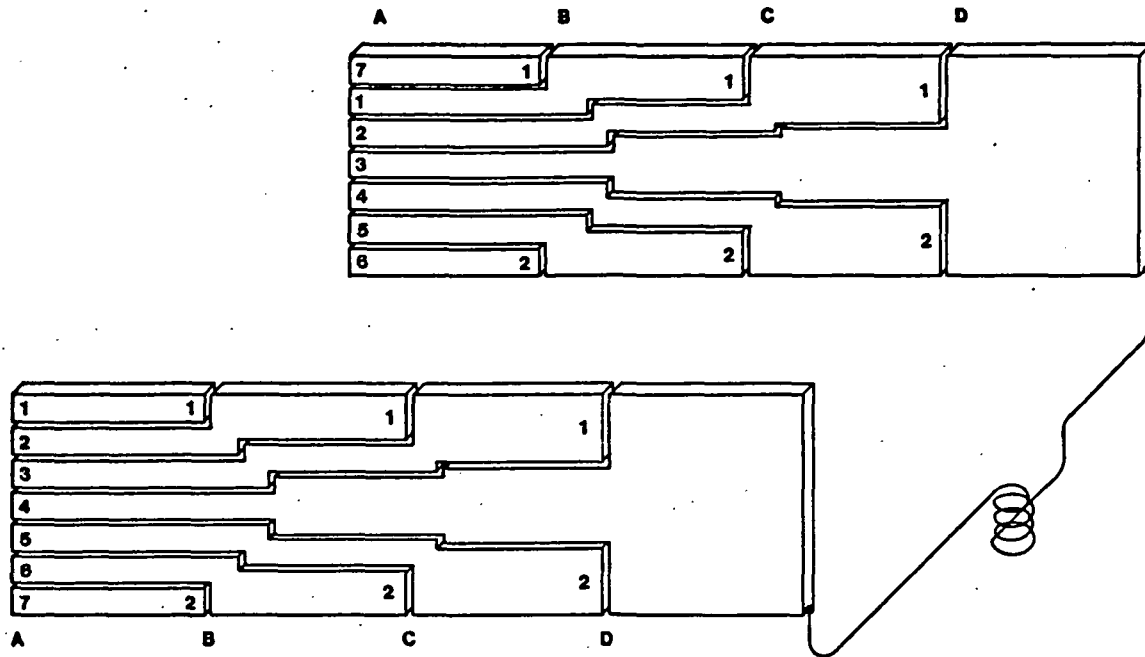


Fig. 16. Symmetric method for varying N along rails

The preliminary current can be established in the IRFC as indicated in Fig. 17. A capacitor is connected to the main rail loop and to a floating length of rail as shown. The circuit is closed as the armature enters the compressor, and the current rises, driven by the capacitor. rises. The length of the floating rail is chosen such that the capacitor is discharged when the armature has traveled its full length. The armature then crosses over the junction, and the charging part of the cycle is complete. It may be desirable to have more than one capacitor (two are shown in Fig. 17). This effectively puts capacitors in series and decreases the charging time. If capacitor voltage is too low, then the length of the charging rail (B to C) can become excessive.

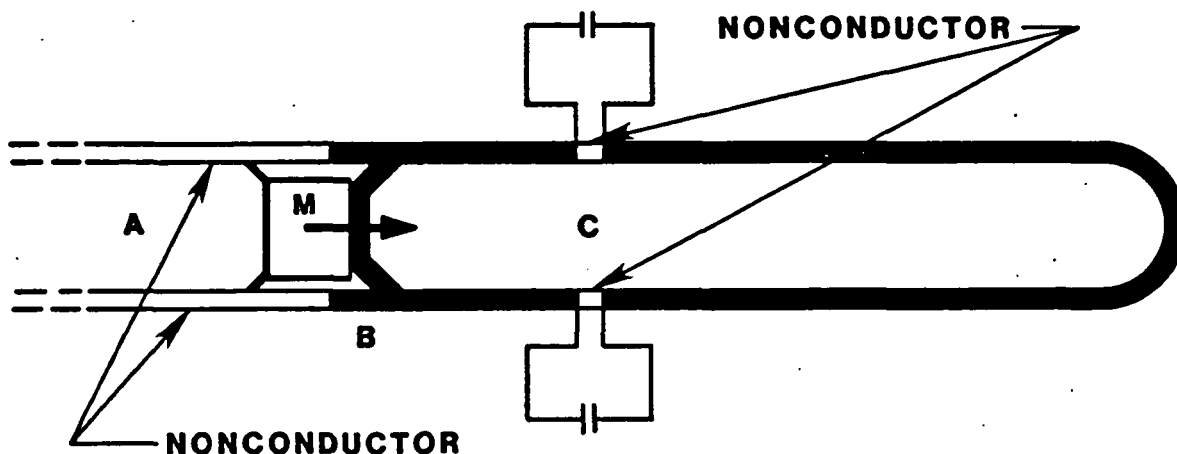


Fig. 17. Method for establishing preliminary current in IRFC

The final major component to be considered is the prime mover, the gas gun, that provides the energy in the first place. The form it is likely to take is a piston-and-cylinder arrangement in which the back face of the piston is acted on by high-pressure gas, and the front of the piston is the IRFC armature.

One way the gas gun might be constructed is in a manner similar to a diesel engine. With the piston latched back into its starting position (cocked), air is pumped into the firing chamber to the desired pressure. Fuel is then injected and burned in the firing chamber, the piston being released at the appropriate point in the cycle. The hot gas then accelerates the piston to the required velocity.

Another possible approach would be to charge the firing chamber initially with a combustible mixture, as is done in a conventional gasoline engine. Some suitable baffling may be required, also.

#### A SPECIFIC DEVICE

We now examine what an IRFC energy store device may look like, taking the ESRL Case number 1B set forth in Ref. [1].

### The Inductor

Each store consists of an inductor that is capable of being charged to 48 MJ with a current of 4 MA, and the means of producing this charge.

The bore of the device tends to be set by the inductor, and the inductor size in turn is set by the energy it is required to store. Regarding the inductor as a pressure vessel with an allowable internal pressure of 35 MPa (5,080 psi), an idea of its size is obtained as follows:

$$\begin{aligned}
 \text{Energy} &= \text{Pressure} \times \text{Volume} && (14) \\
 \text{Volume} &= \text{Energy/Pressure} \\
 &= 48 \text{ MJ}/35 \text{ MPa} \\
 &= 1.37 \text{ m}^3
 \end{aligned}$$

The inductor can be considered as approximate cube, thus giving its linear dimensions as  $\sqrt[3]{1.37} = 1.1 \text{ m}$  (44 in.). Coil radius,  $a = 1.1/2 = 0.55 \text{ m}$  (22 in.).

The inductance required for the inductor is  $6 \mu\text{H}$  ( $= 2 \times \text{Energy}/I^2$ ). The inductance of a single-layer solenoid having its diameter equal to its height is given by

$$L = 0.2 \pi^2 a N^2 \times 0.688 \quad (15)$$

where

$a$  = radius of the solenoid, meters,  
 $N$  = number of turns.

For  $a = 0.55$ , the required value for  $N$  is 2.8. Taking  $N$  as an integral number,  $N = 2$ , then  $2a$  is required to be 2.2 m, which is double the size determined above using the energy and pressure values given.

### The Bore of the IRFC

For the purposes of this study, it will be assumed that the IRFC has a bore of 1.1 x 1.1 m (43 x 43 in.) and that the number of rails per side will be two at the completion of the flux compression. The inductor's inductance can be adjusted by the addition of a partial third turn.

The allowable current in railgun sliding contacts is conservatively 100 kA/half-inch height (ANU railgun), i.e., 7.8 MA/meter of rail height. The rail current density in the case chosen above is 4 MA x 2 rails per side/1.1 m = 7.3 MA/m, which is comfortably within the limit.

### The Gas Gun

To get the energy into the IRFC, a gun of some sort is required to give energy to the armature. From an energy point of view the most direct way of doing this will be to use a thermodynamic or gas gun that would be like a one-stroke free piston diesel engine. The piston/armature would be latched back in its "cocked" position, compressed air would be introduced behind the piston, and when fired, fuel would be injected and burned in the air. At the appropriate point of the cycle, the piston would be unlatched and allowed to accelerate towards the IRFC.

For convenience, it will be assumed that all the energy delivered by the gas gun appears as kinetic energy of the piston/armature before flux compression begins. In practice, some overlap of the processes would be desirable, both to reduce the overall length of the device and to reduce the maximum velocity of the piston/armature by a slight amount. About 50 MJ of kinetic energy will be required.

Table 12 gives corresponding values of velocity and mass for this energy.

Table 12. Required 50-MJ gas gun piston/armature mass-velocity relationship

V, m/s	300	400	500	600	700
M, kg	1,111	625	400	278	204

---

Assuming that an effective average pressure of 17.5 MPa (2,540 psi, 35 MPa/2) is a reasonable gas gun pressure, then the average force on the piston is  $17.5 \times 1.1 \times 1.1 = 21.2$  MN. The gun length is then  $\text{Energy/Force} = 50/21.2 = 2.36$  m (93 in.).

#### The IRFC

In order to keep the charging energy small, an inductance change of 1,000 times is assumed, giving values in Table 13.

Table 13. Required IRFC design parameters

<u>Parameters</u>	<u>Value</u>	<u>Units</u>
Initial inductance	6,000	$\mu\text{H}$
Initial current	4,000	A
Initial energy	48	kJ

---

Aiming at an IRFC length of around 2 meters, and noting that the inductance of a railgun with N rails in parallel is  $0.5 N^2$  ( $\mu\text{H}/\text{m}$ ), to get an inductance of 6,000  $\mu\text{H}$  requires an average value of N of around 80.

Assuming an initial value for N of 100, the total current in one rail, when charging is complete, is  $100 \times 4,000 \text{ A} = 0.4 \text{ MA}$ .

The current-carrying capacity of a rail based on the sliding contact limit given above is  $7.8 \text{ MA}/1.1 = 8.5 \text{ MA}$ . This is a 20-fold increase in current, requiring a 20-fold reduction inductance, i.e. from 6,000 to 300  $\mu\text{H}$ . The IRFC length required to effect this reduction is about 1.1/2 meters, leaving about half a meter to reduce N from 100 to 2.



If  $N$  is reduced by 2 per step (one top and one bottom), 48 steps are required, or about 1 step per cm.

The width of each part of the rail in the first 1.1/2 m of the IRFC is 1.1 m/100, or around 1 cm.

Thus, a change of 1 step per cm will be acceptable for the first few (approximately half of) the steps, but some overlapping of crossover conductors will be required towards the end of flux compression. The last step requires conductors with the current-carrying capacity of 26 cm width of rail. Crossover bars having around 5 x 5-cm (14 x 14-in.) section, or even smaller, may be acceptable.

#### IRFC Electrical Resistance

Consider first the rails. The length of rail per meter length of IRFC is 200 m for  $N = 100$ . Assuming a rail cross-section of 1 x 1 cm, and that copper has a resistivity,  $\rho$ , of  $3 \mu\Omega\text{-cm}$ , then  $R'$  is given by

$$R' = \frac{\rho l}{A} = 3 \times 20,000/1 = 0.06 \Omega/\text{m} \quad (16)$$

There are fixed resistances consisting of the armature conductors and the reducing part of the flux compressor with the inductor. To be conservative, take the total of this to be equal to two armatures, i.e., a rail length of 200 m, giving

$$R_{\text{fixed}} = 0.06 \Omega$$

There are also the contact voltage drops associated with the sliding contact between armature ends and rails. Assuming a 3/4-V drop (the melting voltage of copper on copper) at each of these (200 in all), the total resistance is

$$R_{\text{contact}} = 150/I \Omega$$

#### Inductance per Unit Length

As stated above, the inductance per unit length,  $L'$ , for a multi-railgun is proportional to  $N^2$ . Thus, for the 100-turn part of the IRFC,

$$L' = 0.005 \text{ H/m} .$$

### Will it Take Off?

Equation 13 above gives the condition that must be met for take-off to occur, namely

$$| L' v | > \text{total resistance}$$

i.e., 
$$> R' x + R_{\text{fixed}} + R_{\text{other}} .$$

Using the values derived above,

$$0.005 v > 0.06 \times 2 + 0.06 + 150/I .$$

For the initial current of 4,000 A assumed,

$$v > 43.5 \text{ (m/s)} .$$

Thus, for initial armature velocities in the hundreds of meters per second range, the current will rise immediately rather than decay.

### Initial Charging

To give the IRFC its initial charge of 4,000 A within a distance of 0.5 m (say, with an armature velocity of 500 m/s) requires a charging time of 1 ms, giving a rate of rise of current of 4 MA/s.

An indication of the voltage necessary to meet this requirement may be obtained by using Eq. 10.

$$E = L' \times I + I (v L' + \text{total resistance}) .$$

Substituting the values given above gives

$$\begin{aligned} E &= 0.006 \times 2 \times 4 \times 10^6 + (500 \times 0.005 + 0.18 + 150/I) \\ &= 40,000 + I (2.68) + 150 . \end{aligned}$$

To be conservative, taking  $I = 4,000$  gives

$$E \cong 50 \text{ kV.}$$

Since a charging energy of 48 kJ is required, five 10-kJ capacitor cans, each charged to 10 kV, will be adequate. They would be connected as indicated in Fig. 17.

As a check on the above, if the flux compressor inductance is regarded as fixed and the resistance is neglected, then the classic expression for energy transfer time from a capacitor to an inductor

$$t = \pi W_0 / (V_0 I_{\text{peak}}) \quad (17)$$

can be used, to give

$$\begin{aligned} V_0 &= \pi W_0 / (t I_{\text{peak}}) \\ &= \pi \times 48,000 / (0.001 \times 4,000) \\ &= 37,700 \text{ V} , \end{aligned}$$

which is consistent with the 50 kV obtained above.

### Simulation

Simulation of the first 1.5 m or so of compression using the equations

$$\dot{I} = -(I (L'v + R'x + R_{\text{fixed}}) + 150) / L'x$$

$$I = I + \dot{I} \, d\Delta t$$

$$a = L' I^2 / 2m$$

$$v = v + a \, \Delta t$$

$$x = x + v \, \Delta t$$

yields the following results:

1. For the case in which the initial armature velocity is 700 m/s, the loss in energy as the current is "compressed" from 4 kA to 80 kA is

168 kJ. This is small compared with the 50 MJ of kinetic energy (k.e.) in the armature/piston originally plus the 48 kJ of charging energy. The k.e. at the 80-kA compression is still 49.21 MJ, and the inductive energy is 670 kJ, indicating that this stage of compression is more a current-amplifying stage than one of energy-compression. The inductive energy (at 0.067 MJ) is still low enough that the possibility arises of reducing the number of turns by a factor of two at this stage. Compression takes a total of around 5 ms.) One cannot lose what one does not have, so even if the inductive losses involved in this change were a substantial fraction of the inductive energy present, the losses would still be a small part of the total energy in the system. The prime consideration would be that losses should cause a minimum of contact damage or other untoward effects.

2. For the case with the slow (300-m/s), heavy (1,111-kg) piston/armature, the losses are the same, 168 kJ. The difference is that for the current compression to 80 kA, the k.e. is a little larger (49.25 MJ), and the inductive energy is a little smaller (0.63 MJ). Thus, the choice of piston/armature mass and velocity can be made on practical engineering and economic grounds, rather than being dictated by efficiency considerations.

A more subtle effect than the small loss of efficiency in the two cases simulated is that during the current amplification by a factor of 20, the inductance reduces by a factor of 30 (32 for Case 2), so to reach the required end point of some desired current in an inductor of some desired inductance, the original (uncompressed) inductance will have to be something like 50 percent higher than the required energy and current ratios indicate. This poses no particular problem.

#### Inductance Check

Because the geometries given above for the IRFC are quite fat compared with their lengths, the inductances chosen based on long geometries are in fact a factor of 1.6 too low.

The complete inductance [43] for a rectangular coil 1.5 m long with 1 m for each of its other dimensions is 0.012 H for  $N = 100$ , compared with the value of  $0.005 \times 1.5$  H used above.

Repeating the calculation for a coil 1 m long, an inductance of 0.0083 H is obtained. Thus the inductance change is 0.0037 H for a half-meter change in length, giving a value for  $L'$  of 0.0074 H/m, about 50 percent higher than the value assumed.

These increases come very close to providing the higher inductance ratios required, as discussed above.

### The Device

The complete device would look something like Fig. 18. The bursting pressures that the device is required to withstand are an average of around 17 MPa (1,500 psi) in the gas gun and around 3.5 MPa (5,000 psi) in the inductor and the latter end of the IRFC. If steel is used to hold this pressure, some 4,500 kg (five tons) of it will be required. If copper is used for the conductor, around 450 kg (half a ton) will be required for the rails and also for the inductor. The armature and cross-over could require a further 225 kg (a quarter ton) total. Adding 50 percent for such necessities, plus 500 kg (a half ton) for the piston (taking a middle value for its mass) gives a 9,000-kg total weight for the device, or around ten tons.

A further drawback is that the IRFC produces an external magnetic field that may be undesirable. In principle, a coaxial IRFC can be devised, but it would probably require the use of a constant number of rails, rather than a reducing number as assumed above. The reason is that the carrying of cross-over conductors from a center rail assembly to an outer one in such a way that the armature can pass by is a formidable problem. It may be possible to gang coaxial IRFCs, having diminishing inductances, together in some way. This would introduce a new set of problems, however.

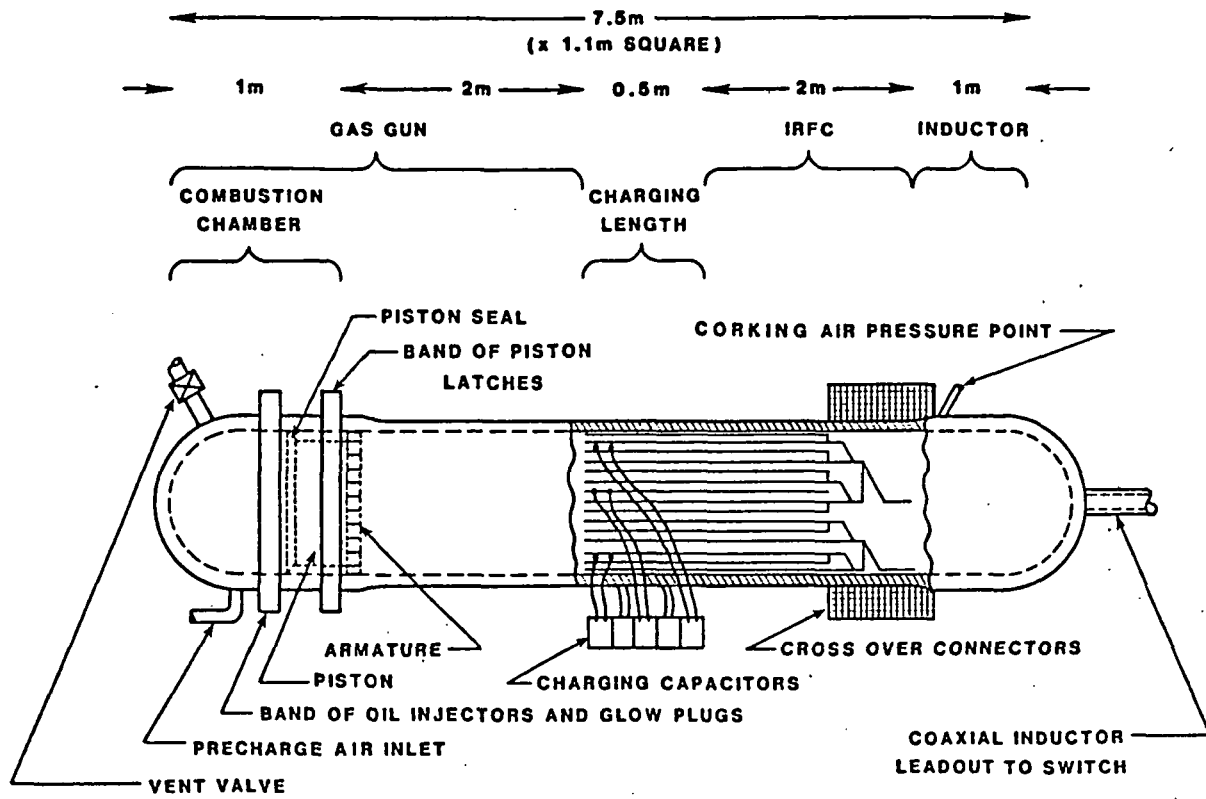


Fig. 18. Conceptual IRFC device for ESRL

### TASK C. ARCING AND SHUTTLE SWITCHES

The objective of Task C was originally to pursue the concept for self-synchronous ESRL switching that Marshall proposed in his report "Earth-to-Space Rail-Launcher System". [2] As the concept was first understood, the rail body would be a composite structure made up of individually-insulated chevron conductors as shown in Fig. 19. This same pattern would be repeated for the upper rail, and the two would be clamped together with insulating spacers to form a square-bore launcher. One HPG/inductor energy store would supply current to a single chevron on each side of the bore.

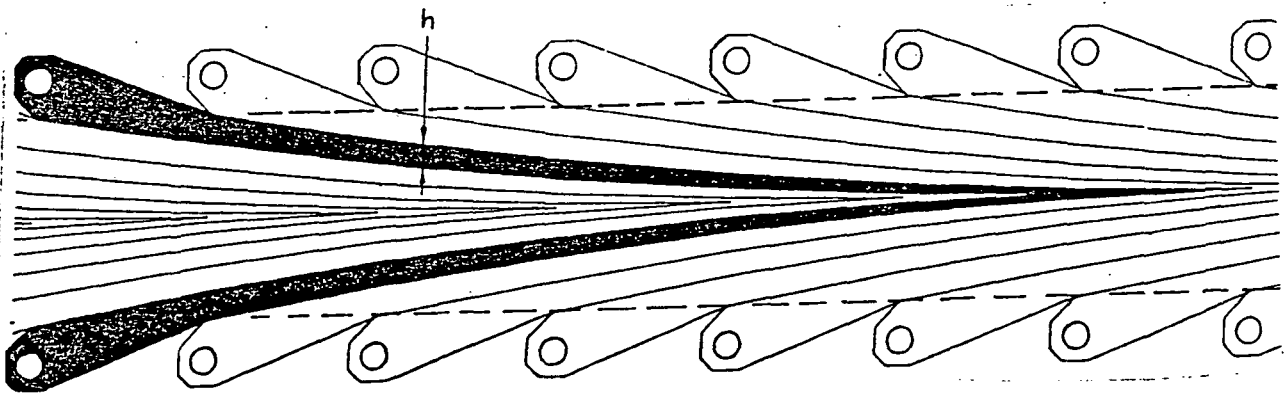


Fig. 19. Original concept for ESRL rail construction

A butt contact would short the top and bottom left-side shaded rail as well as the right-side shaded rail. Before the main arc passes down the launcher, the butt contacts would be opened, and the field from the main arc would accelerate the new arcs into the main body of plasma. As the arc moves down the gun and the newly connected store delivers its energy, the rails would gradually taper and shut off the current, thus disconnecting the discharged store.

The concept as just stated sounds logical, but as with any concept, it must continue to make sense as new questions of system operation arise.

The first such question involves timing. The launch time for the payload is 408 ms (Table 2). The time for the HPG to charge an inductive energy store is 350 ms (Appendix A). It can be seen that an HPG near the end of the launcher cannot be discharged until the payload has been in flight for 58 ms. Payload velocity and position will still have to be sensed in order to control the launch. The next function is to open the butt contacts. These contacts are not the 1,900-cm<sup>2</sup> (296-in.<sup>2</sup>) contacts identified in Task A, but are more likely either second- or third-stage contacts. Once these contacts are pulled open, the characteristic anode arc drop of 50 V transmitting 4 MA requires a power dissipation of 200 MW at the anode spot. For a point of reference, assume that the final-stage butt contacts are the switch that General Dynamics has built and tested. Further assume that the contacts need to move 0.013 mm (0.005 in.) to clear surface asperities, so that an arc is actually formed and no galvanic contact remains. Then the arc duration time on the butt contact is

$$0.005 \text{ in.} \times 1 \text{ ms} / 0.1 \text{ in.} = 50 \times 10^{-6} \text{ s} \quad , \quad (18)$$

or that 10 kJ are absorbed by the contact. The equivalent of 180 mm<sup>3</sup> (0.01 in.<sup>3</sup>) of copper is eroded.

At this point it is clear that the scheme is not self-synchronous. Both the velocity and the position of the arc must be measured accurately to know when to command the butt contacts to open. If the switch is open for any longer than 50  $\mu$ s before the main arc passes, severe erosion occurs, and the device is not reusable. A second- or third-stage switch capable of developing more voltage than the butt contact would be a better option.

After this discovery, the goal of Task C was changed. It was felt that work needed to be done on the heavy galvanic first-stage switch, which must be efficient, rep-rateable, and, if possible, self-synchronous. The only point on the launcher where this mechanical switch could be used by itself would be the first stage, where the payload is moving slowly and the armature on the payload is behaving as a flying fuse and providing some galvanic sliding contact with the rail system. Beyond



this point, the galvanic switch can be used only as a first-stage device to handle the charging  $\int i^2 dt$  requirement.

A study was then undertaken to evaluate the performance of existing opening switches. From this study a paper was written and presented at the 4th IEEE International Pulsed Power Conference. A copy of the paper is included as Appendix C, and its contents are summarized in Table 14. It can be seen that the explosive switches are not efficient, even at low currents. The butt contact switch tested by Inall showed good efficiency, but the efficiency did not scale to higher currents, as seen in the General Dynamics switch. The Marshall switch was the most promising. Gora, in discussion following the paper presentation, stated that while under contract to AMCCOM, Westinghouse had used a similar switch design on EMACK, [20] and that similar efficiencies were observed at 1.6 MA.

A good technological base had been identified, and it made good sense to continue fabrication of a segment of the coaxial shuttle switch design presented in the paper.

The rotary shuttle opening switch (RSOS) first reported in the paper that appears in Appendix C, is electromagnetically coaxial with radial mechanical actuation. It is best described with a simple one-dimensional representation Fig. 20. In Fig. 20a, the switch is shown in the charging position. A low-mass sliding contact provides the path through which the HPG charges the energy storage inductor. At peak current, the shuttle moves to path A, as shown in Fig. 20b. In a full-scale device, this actuation force will be provided by magnetic pressure. Path A is resistive and is tightly coupled inductively to the original charging path. As the shuttle contacts move onto path A, a voltage is developed. Shortly after peak voltage occurs, the trailing contacts on the shuttle connect the switch into the rail launcher (Fig. 20b). The developed voltage commutates current into the rails, and the fundamental (inductive-to-inductive transfer) switching energy is absorbed by the fixed resistance. The contacts on the back of the shuttle continue to be accelerated by electromagnetic force, and the resistance path is removed from the circuit by a two-part independent motion inside the shuttle (Fig. 20c).

Table 14. Summary of high-current opening switch designs

<u>Experiment</u>	<u>Actuation Scheme</u>	<u>Rep-rateable?</u>	<u>Test Current (kA)</u>	<u>Time to Peak Current</u>	<u>Efficiency (%)</u>
ANU - Inall	High-pressure N <sub>2</sub> gas - nondestructive	yes	70	600 ms	83.5
University of Paris - Rioux, et al.	Electromagnetic force - destructive	no	28	40 $\mu$ s	-
NRL - Vitkovitsky, et al.	Explosives - destructive	no	55	900 $\mu$ s	30
ANU - Marshall	Electromagnetic force - nondestructive	yes	320	600 ms	62
University of Texas/ General Dynamics	High-pressure N <sub>2</sub> gas in combination with dielectric fluid - nondestructive	yes	285	250 ms	30

---

Source: Appendix C

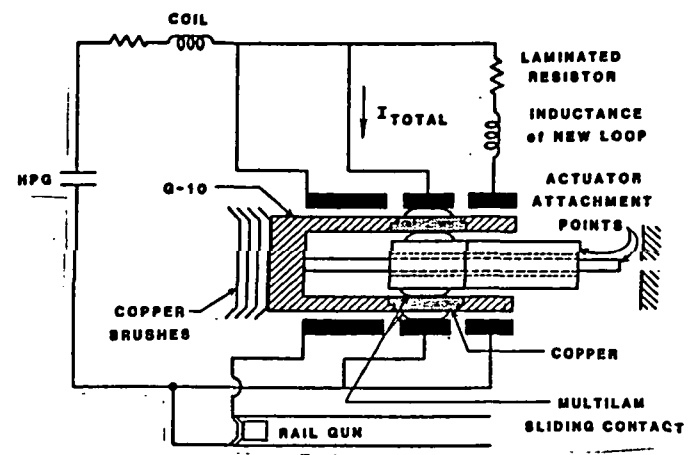


Fig. 20a. Switch in the inductor-charging position

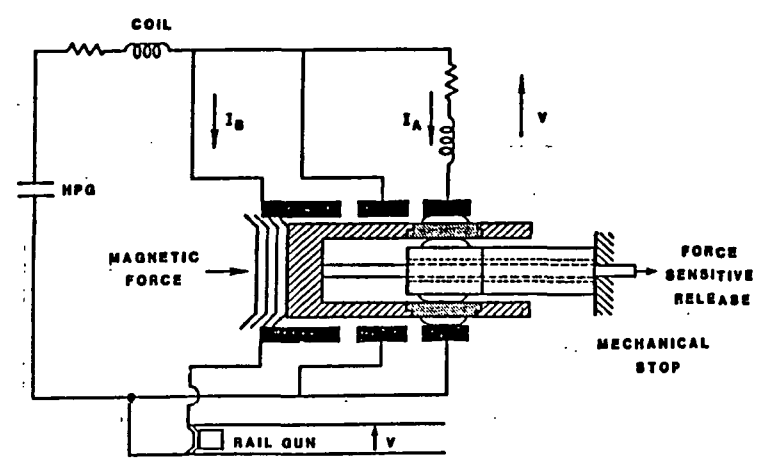


Fig. 20b. Switch building commutation voltage

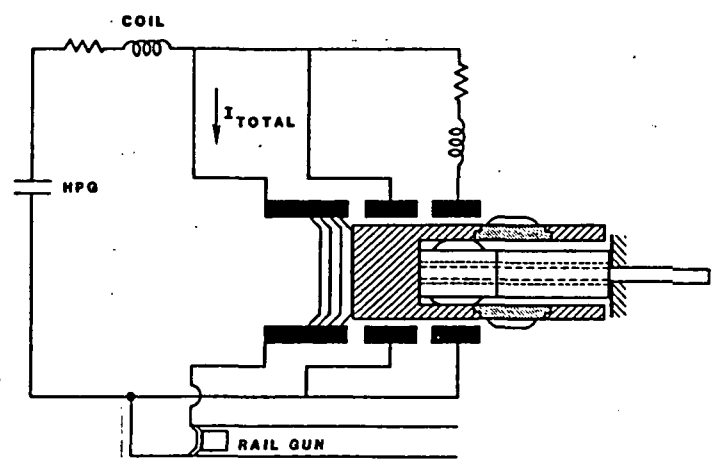


Fig. 20c. Switching complete -- total current established in railgun

Fig. 20. Action of DES circuit switch

In the first energy store position, the resistor in the opening switch can have a low value. A low voltage is developed as the switch actuates at peak current. The decay of inductive energy is slow in the low-resistance path. When the payload is injected into the launcher, continuity is established in the rails, and voltage previously developed across the switch commutates current into the sliding contact armature. As current rises in the rails, the low resistance inside the switch is removed by the electromagnetic force (Fig. 20c). The switching action is synchronous in that only the current rise time in the inductor, a repeatable interval, was required. For the actuation of subsequent stages, both armature position and velocity will have to be sensed. The RSOS, when used with later stores, will handle the inductor charging  $\int i^2 dt$  duty and will provide an efficient means of transferring current to a fast second-stage switch.

#### TASK D. ALTERNATIVE SWITCH

Task D was included to study an alternative switch as a fallback option to the arc switch.

The alternative switch is an attempt to address the opening-switch requirements of high current capacity, fast operation, variable resistance profile, cooling, and maintenance. [44] The only moving components are fluids (liquid metal, dielectric oil, and gases), thus reducing fatigue and wear problems.

In its simplest "opening switch" configuration (Fig. 21), the concept consists of a pair of coaxial electrodes mounted in an insulating plate and enclosed in a pressure tank. Various sections of the enclosure are filled with liquid metal, dielectric oil, and high-pressure inert gas such as nitrogen. In some cases, it may be attractive to replace the dielectric oil and inert gas with a high-pressure gas such as sulfur hexafluoride ( $\text{SF}_6$ ), which is commonly used for extinguishing electric arcs.

In the closed position (left-hand side of Fig. 21) the liquid metal bridges the gap between the coaxial electrodes, conducting current between them. The magnetic (Lorentz) force tending to eject the liquid metal from between the electrodes is balanced by the high-pressure gas in the outer cavity between the outer electrode and tank. The device can function as an over-current protection device by allowing the increased magnetic force due to excess current to overcome the pressure in the outer cavity and eject the liquid metal from the area between the electrodes. In this case, the pressure initially set in the outer cavity determines the current rating of the device, and it could be pre-set or even remotely or dynamically controlled. The device can also be made to function as a switch by manipulating the gas pressures in the inner and outer cavities. An attractive feature is that the components required to control the cavity pressures are external to the switch.

They can easily be made redundant and can be serviced while the device is in operation.

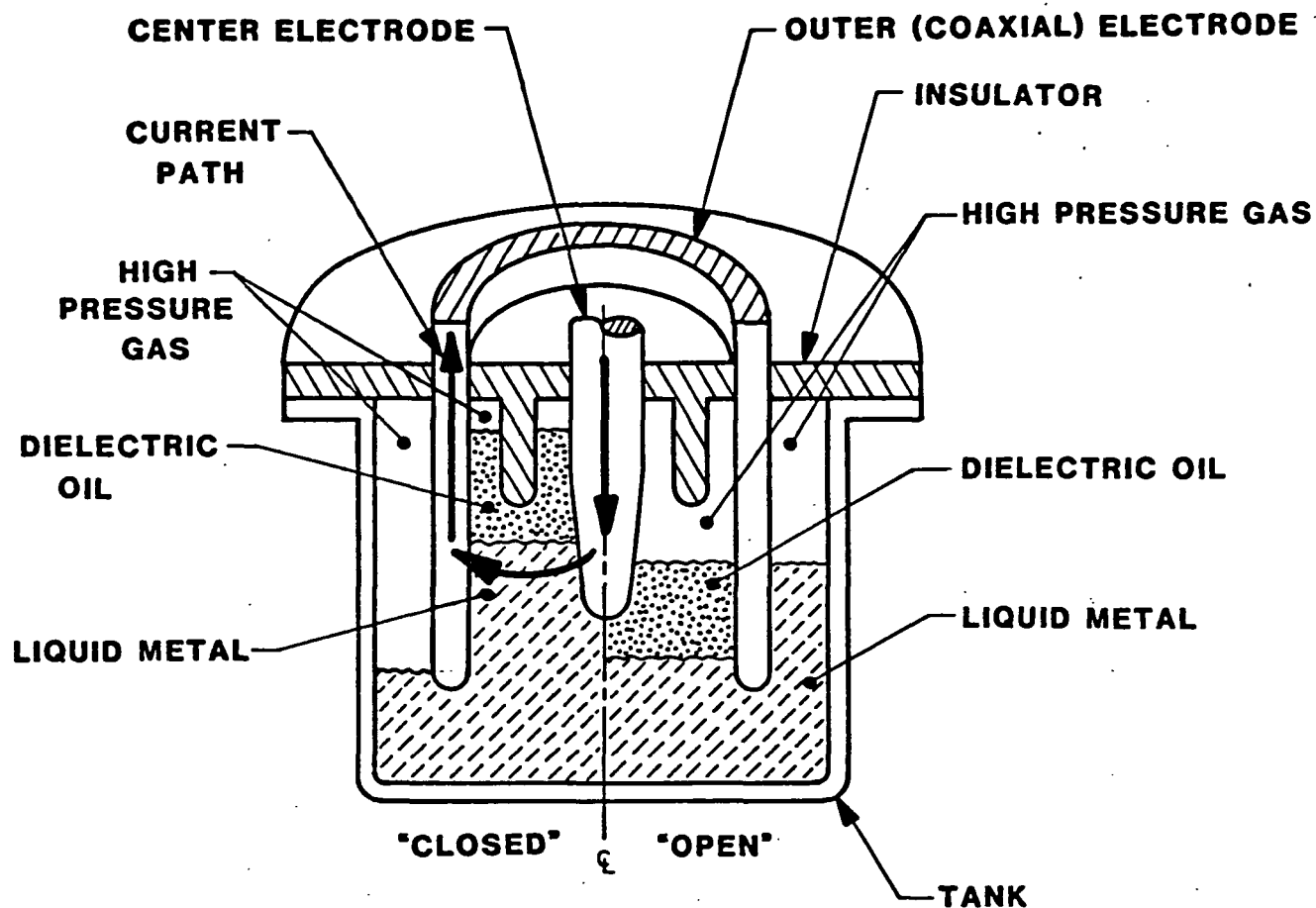


Fig. 21. Opening switch configuration

As the liquid metal is forced out of the area between the coaxial electrodes, either by magnetic field or high-pressure gas, dielectric oil or SF<sub>6</sub> is forced into the gap between the liquid metal and the inner electrode, helping to cool and extinguish the arc. Furthermore, the center electrode can be tapered so that its resistance increases as the liquid metal is forced out, assisting in the transfer of current out of the switch.

The liquid metal chosen for use in the switch can be one of a wide variety of materials, depending upon the specific duty of the switch. Although they are quite active chemically, low-melting-point metals such

as sodium-potassium eutectic (NaK), which have been used to carry electrical current in other applications, may be useful in some cases. In the railgun application, in which substantial current flows for relatively long periods, joule heating may be used to liquify metals with somewhat higher melting points. Alloys commonly used as solders appear attractive, since they are much less active and are less toxic than NaK, and their excellent metal surface wetting properties insure good electrical contact and offers a self-healing effect for arc-damaged electrodes (Fig. 22), the device becomes the transfer switch described in Fig. 5.

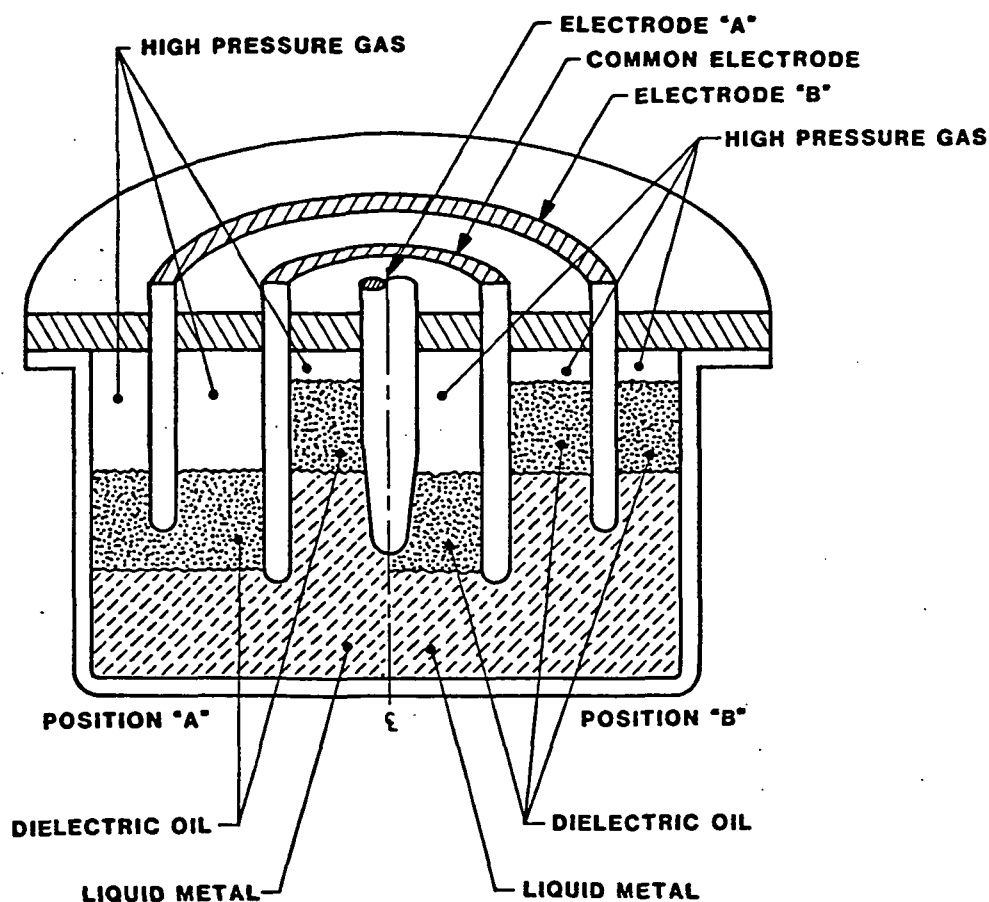
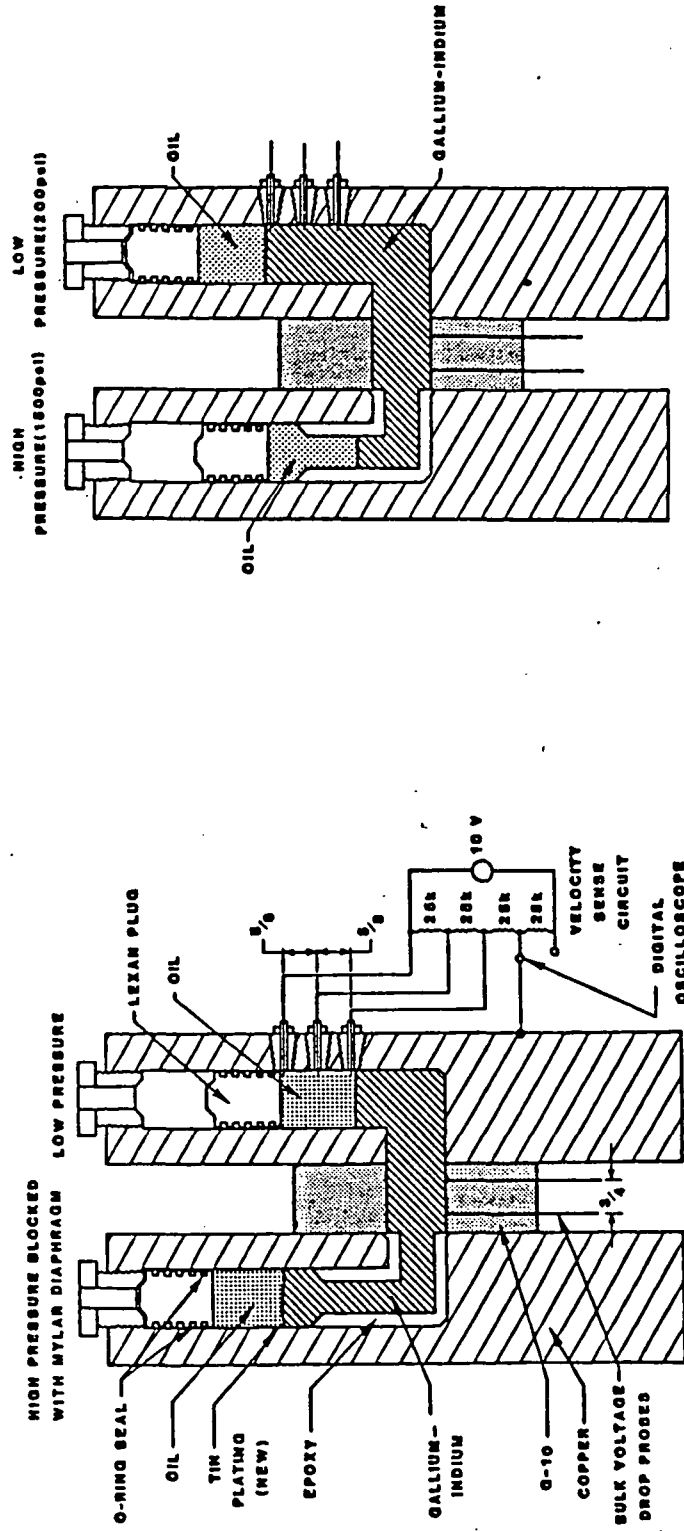


Fig. 22. Transfer switch configuration

In this case, operation is similar to operation of the simple opening switch in Fig. 4, except that as the liquid metal is ejected from the innermost coaxial cavity it rises in the outer cavity, contacting the



Experiment Actuated

Liquid Metal Experiment in Initial State

Fig. 23. Liquid metal experiment test fixture



outer B electrode and closing the second circuit. By changing the relative heights of the A and B electrodes and the volumes of their respective cavities, the timing of the opening and closing of the contacts can be varied. Thus, the B circuit can be closed before, during, or after the breaking of the A circuit. Again, by varying the cross-sections of the A and B electrodes, relatively complex resistance variations can be achieved in the two circuits.

To test this concept, the experimental fixture shown schematically in Fig. 23 was built (Fig. 24) and tested. The physical properties

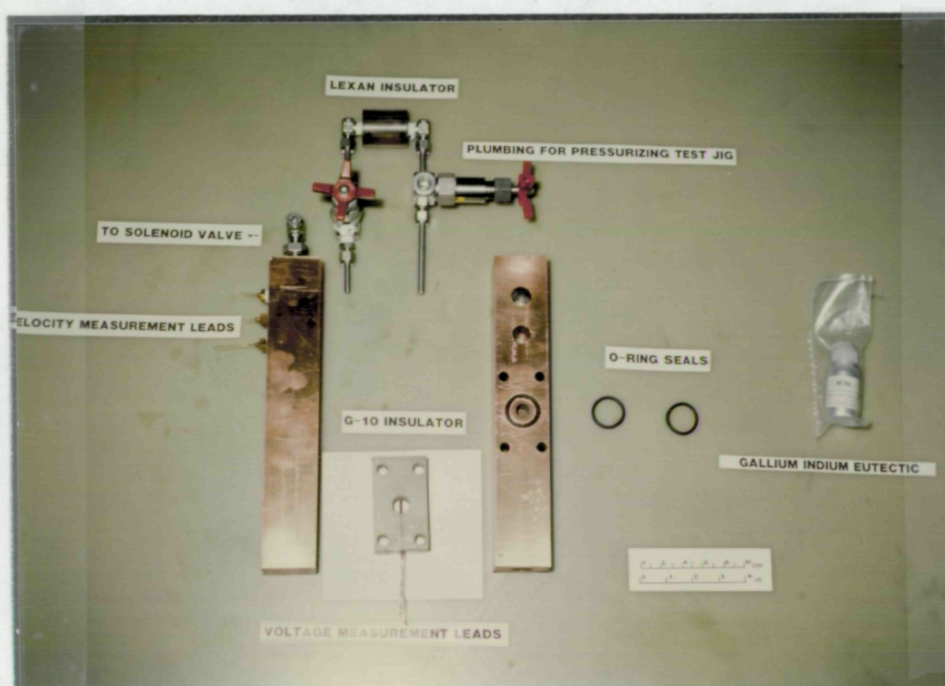


Fig. 24. Components of liquid metal test fixture

required for the liquid conductor are low resistivity for current-carrying capability and low density for fast actuation. As can be seen from Table 15, liquid Na is the best candidate metal for switch duty. The fixture was designed for operation with sodium, but as safety reports and handling requirements for Na were considered further, Ga-In eutectic was substituted as the test metal. The fixture was designed to measure several key physical parameters, as well as the influence of electromagnetic effects.



Table 15. Physical properties of liquid metals

<u>Metal</u>	<u>Electrical Resistivity (<math>\mu\Omega</math>-cm)</u>	<u>Density (kg/m<sup>3</sup>)</u>
Na	9.65	928
Ga-In	29.4	6,355
Hg	125	13,570
Cd	6.83	8,664

From these measured quantities, a full-scale device could be designed. The electromagnetic effects would be identified by first actuating the device with no current flowing and then repeating the test with current passing through the switch. By recording the velocity for the two tests, the severity of electromagnetic interaction could be identified. The physical parameters measured would be the static and dynamic interface drop from liquid metal to the metal fixture. This would be accomplished by measuring the drop from one of the bulk voltage drop probes to the metal fixture (Fig. 23). The voltage drop in the bulk liquid metal column is measured using the bulk voltage drop probes. Having this information, a basis for designing a larger switch could be established. A valve was constructed to apply the high pressure to the liquid column with negligible pressure drop at high flow rates. This valve consists of a high-pressure cavity sealed with a Mylar diaphragm. Inside the cavity is a solenoid, the plunger of which is a sharp spike. The electrical leads to the solenoid are routed into the pressure cavity by means of a pressure feedthrough. On command, the solenoid is actuated, and the spike ruptures the Mylar, providing a large discharge orifice. The resulting pressure pulse is routed into the left arm of the switch (Fig. 23).



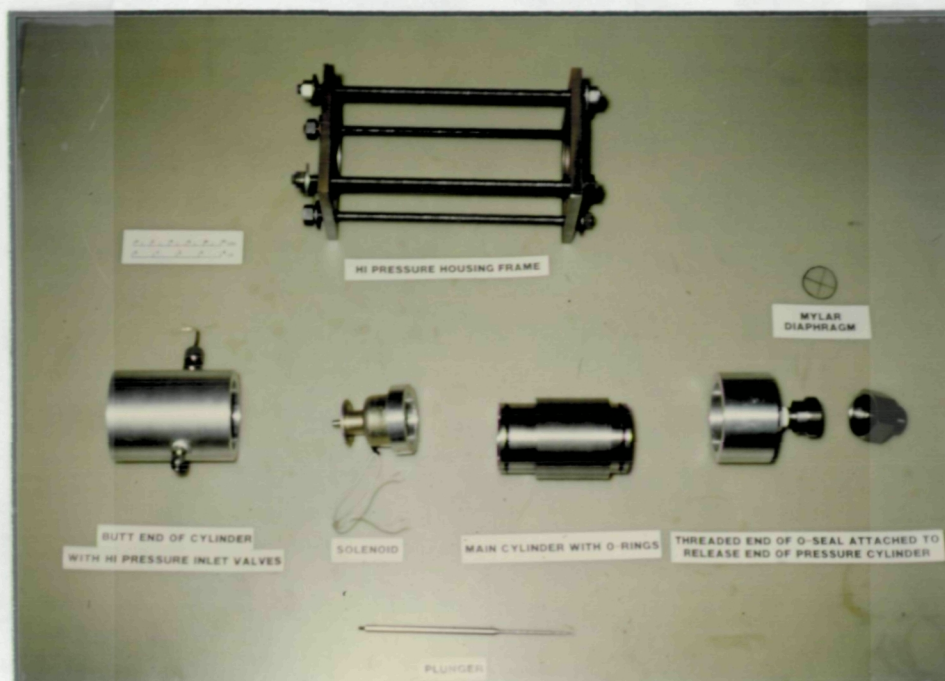


Fig. 25. Components of solenoid-actuated valve

The results of the non-current-carrying switch actuation are shown in Fig. 26. The liquid metal column moved 1.6 mm (5/8 in.) in 1.25 ms. It can be seen that this is a very fast-acting mechanical switch. It is not fast enough to perform ESRL duty as a single-stage device, but it demonstrates excellent speed, suggesting the possibility of reducing  $\int i^2 dt$  requirements on second-stage devices.

In the next series of tests, attempts were made to pass dc current through the liquid metal switch. A 3-kA dc SCR-fired power supply was used for this test. The low-pressure side of the test fixture was pressurized to 1.4 MPa (200 psi) and current was ramped up. At 1.5 kA, the switch arced open, and subsequent attempts to pass current through the fixture failed. The fixture was disassembled, and the oil was found to be heavily carbonized. The liquid metal was no longer wetting the copper surfaces. What appears to have happened is that during the mechanical tests the oil displaced the liquid metal and coated the copper surface.



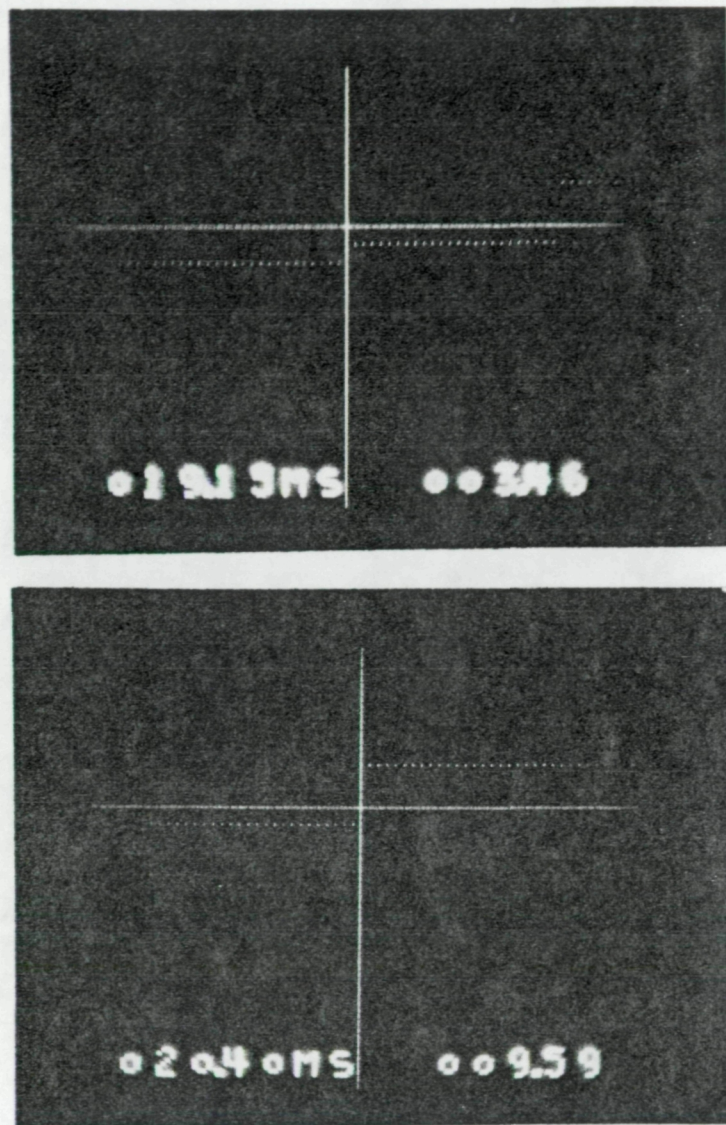


Fig. 26. Velocity measurement of non-current-carrying liquid metal column. In the top trace the cursor shows the liquid metal passing the first probe at 19.15 ms. The bottom trace shows that the column has moved 5/8 in. in 1.25 ms (20.40 ms - 19.15 ms).



At this point, one of the authors (RCZ) contacted Howard Stevens at the David Taylor Naval Ship Research & Development Center, [45] who has experience in running a NaK loop and years ago had limited experience with Ga-In. He stated that when a small amount of oil leaks from their pumps into the NaK, the oil exhibits a greater affinity for metal surfaces than does the NaK, and that it tends to insulate the conductors. He suggested that Frank Orcella at Westinghouse be contacted, who has operated a small HPG that had Ga-In liquid metal brushes. Orcella recommended plating the copper surface with Ga-In. [46] It was his feeling that the Ga-In would rewet itself after an initial actuation despite the presence of oil.

To date, this has been the extent of the liquid metal testing at CEM-UT. More tests need to be run with a plated fixture.

During a literature search that preceded the fixture design, an interesting paper was located, entitled "Liquid-metal Switching of Ultra-high Direct currents." [47] The liquid metal switch described in this paper was tested at 50 kA on an HPG having a circuit inductance of 9  $\mu$ H. The switch cross-section is shown in Fig. 27. The maximum voltage that could be produced by this device was approximately 30 V. This voltage is too small for direct use for ESRL, but it would provide a good first-stage switch capable of healing its contacts by reformation of the liquid metal pool, a key design advantage of this switch was that the bottom contact of the switch is movable.

The bottom contact comes into hard galvanic contact with the upper fixed electrode. This greatly enhances the  $\int i^2 dt$  capacity of the device. The switch will be slower, because a solid mass as well as the liquid metal will have to be accelerated by the driving force. Even the slower actuation would be acceptable in a first-stage switch that has already proven rep-rateability, however.



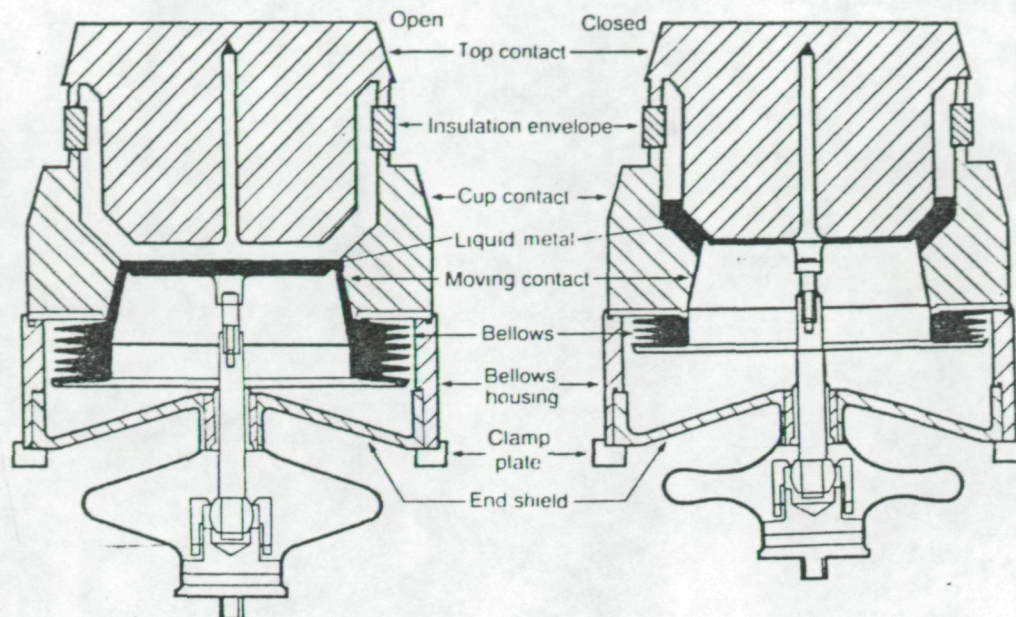


Fig. 27. Cross-section through a Ga-In switch capsule  
(after Walkden, et al., Ref. [46])



## TASK E. ROTARY SHUTTLE OPENING SWITCH EXPERIMENTATION

The rotary shuttle opening switch was selected as the experimental switch design to pursue. This decision was made because it used principles that had shown good efficiency in the Marshall shuttle switch, [4] and this efficiency was known to have scaled to currents approaching ESRL levels in the switch used by Westinghouse on their EMACK facility. [20]

A paper that presents the design considerations, calculation of performance, fabrication, and initial test results for the RSOS is included as Appendix D. This paper gives a concise overview of the switch. Therefore, in this section of the final report, only some of the details and general conclusions from the experiments will be presented.

At one point, it was generally believed that the proposed Marshall switch was completely self-synchronous. All of the butt contacts were pulled open, and the main arc swept by and pulled arcs into the launcher. Now it is seen that  $50 \mu\text{s} +$  (time for the pressure to build up in the actuator that opens the butt contacts) before the arc passes, the command has to be given to open the contacts. If the timing misses on the high side, the contacts are closed when the arc passes and the plasma decays. If the timing misses on the low side, the contacts open early and suffer increased erosion. If the timing is within 5- or 10- $\mu\text{s}$  accuracy, an arc 0.13 mm (0.005 in.) long has to be accelerated from 0 to 10 km/s over a distance of 1 m and must grow to 59.6 cm (23 in.) in length. The process is not self-synchronous. A trigger signal resulting from accurate velocity and position data must control the launch timing, and new technology (arc pick-up and coalescence) has to be explored. The later technology is really not required, however. The DES railgun at CEM-UT uses capacitors connected to continuous copper rails distributed along the launcher. As the arc passes, it is fed additional energy because the voltage on the capacitor most recently connected to the rails is greater than the sum of the IR drop of the



rail plus the plasma arc voltage plus the speed back-voltage of the arc. Current naturally flows from high potential to low potential to low potential through the arc. The same procedure is being used with interrupted inductive stores at the megavolt level by other investigators. [48] A voltage is developed with staged switches until a final spark gap is triggered, and the developed voltage commutates current into the load. Techniques for the control and timing of the launcher are being developed on the DES railgun at CEM-UT and are functioning well at 3-km/s armature velocities. No fundamental limit is seen beyond which this same scheme could not control a DES railgun for ESRL.

switch capable of transferring energy rapidly and efficiently to subsequent switch stages. The RSOS design was adopted for reasons already presented. Three difficult technical issues were addressed during design and construction of the experimental switch. The first issue was the design of a compact resistive element that could be close-coupled to the charging path. The resistor design is shown in Fig. 28. The insulation thickness is 0.13 mm (0.005 in.). The tab that provides the interconnection between laminations is 0.15 mm (0.006 in.) wide and was fabricated by chemical milling of stock silicon-iron motor laminations. The masking used in the production as shown in Fig. 29.

The next challenge was the production of a mechanical actuator for the low-current testing that would model the electromagnetic actuation expected at higher currents. The telescoping air cylinder shown in Fig. 30 was designed for this duty.

The final issue was the selection of a fabrication technique that would hold the close tolerances required for proper operation of the Multi-Lam contact band. The solution to this problem was the coaxial geometry realized by the fabrication of interlocking rings as shown in Fig. 31.

Other figures of interest are the shuttle positioned on an interlocking ring (Fig. 32) and the complete inventory of switch parts (Fig. 33).



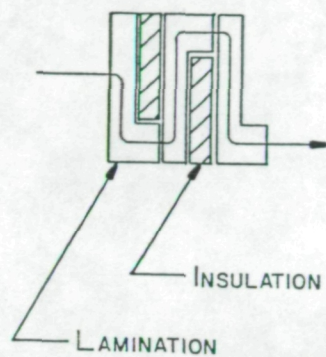
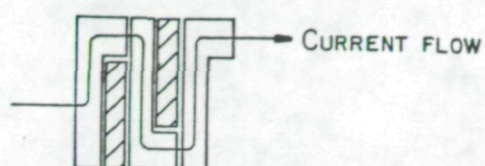


Fig. 28. Design of laminated resistor



Fig. 29. Masked resistor laminations



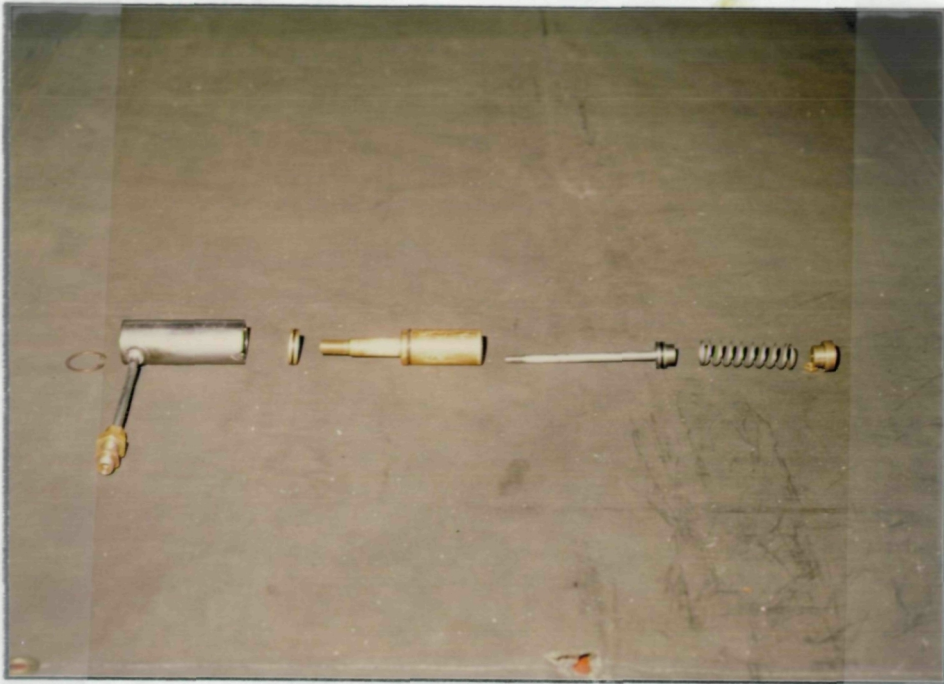


Fig. 30. Telescoping air cylinder

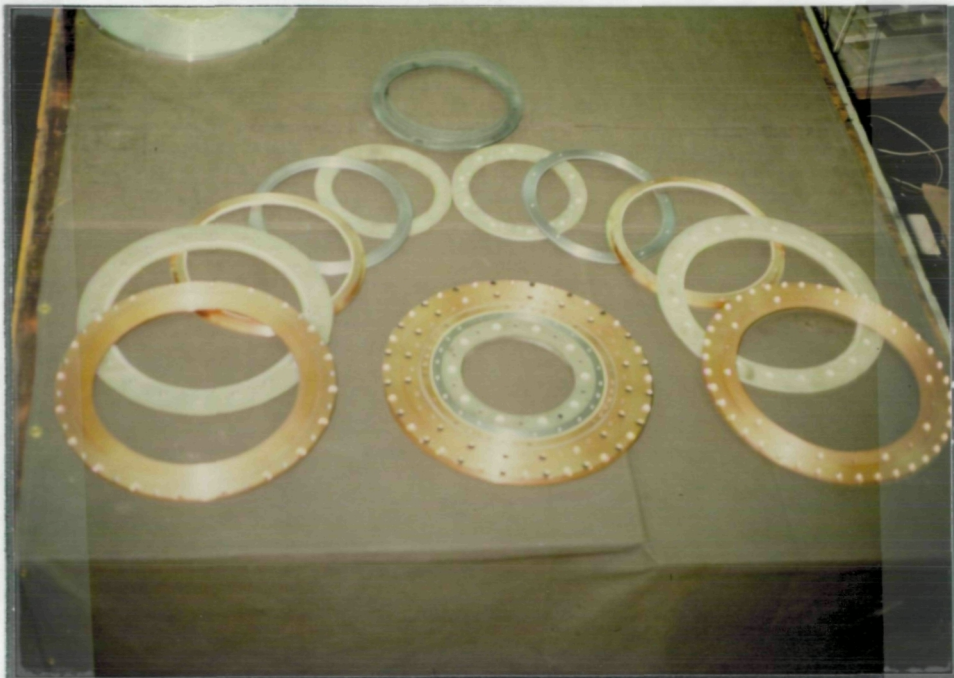


Fig. 31. Interlocking rings prior to assembly



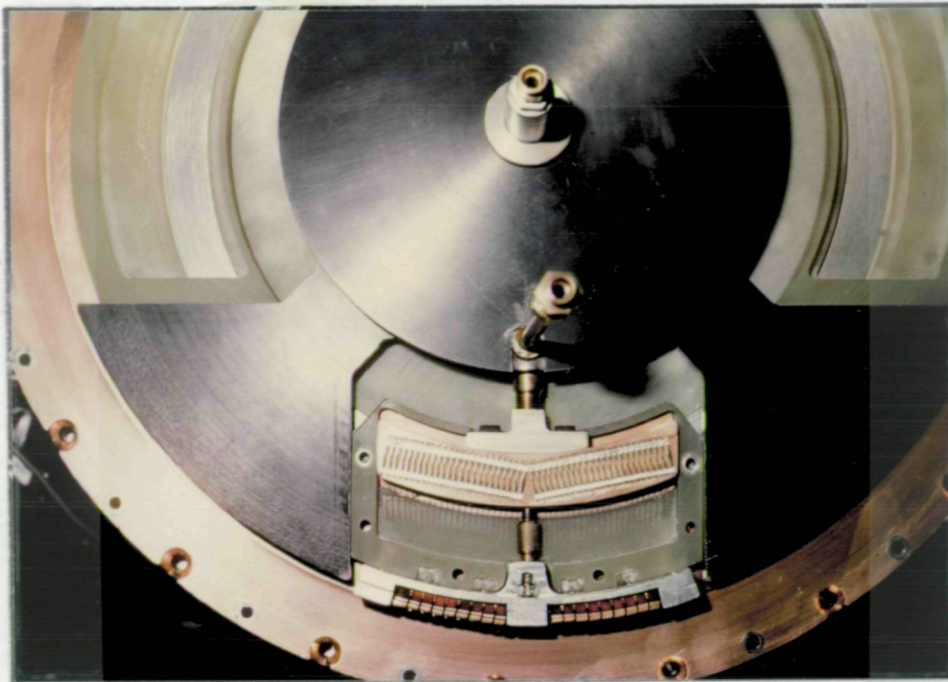


Fig. 32. Relation between shuttle and interlocking ring

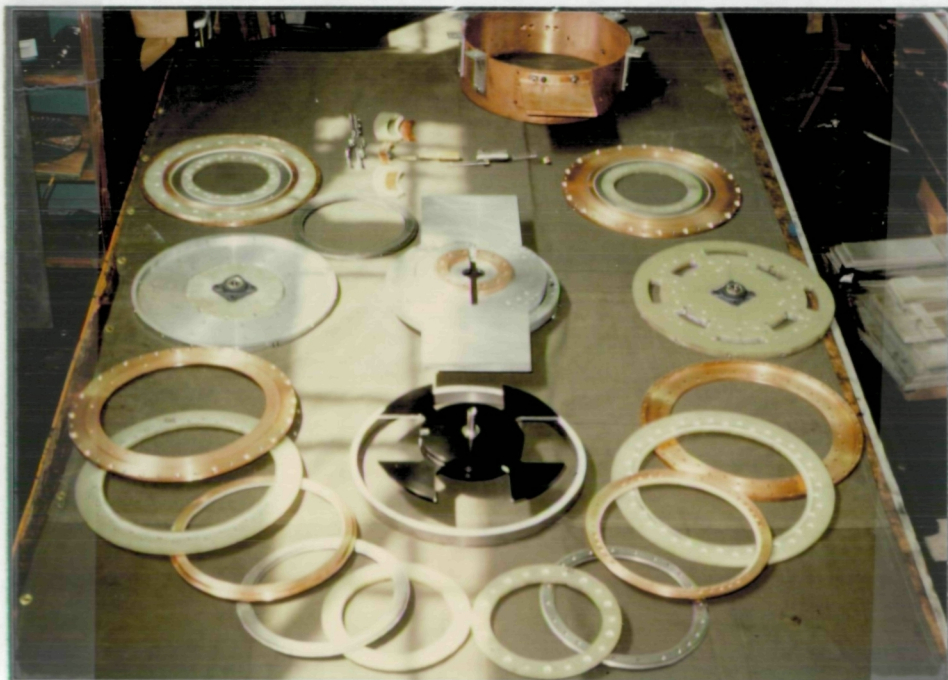


Fig. 33. Complete inventory of switch parts



### Testing of the RSOS Switch

The first series of tests of the RSOS switch was conducted with the opening switch connected to the General Dynamics railgun. During this testing, while trying to establish the static (no actuation) current rating of the switch, the shuttle became welded to the side plate. The first thought was that there had been an alignment problem, because three out of four of the current contacts in series, all seeing the same  $\int i^2 dt$ , had survived the charging duty. As was discovered in the next two series of tests, however, the current rating of the Multi-Lam had actually been exceeded. Our testing indicates that the manufacturer's data on the LAI/.15 Multi-Lam have to be derated by 40 percent. A technical note generated at CEM-UT on Multi-Lam performance is included as Appendix E.

The railgun had to be returned to General Dynamics before the next series of tests could be conducted. The railgun was replaced with a fixed-resistor load sized to approximate a slow-moving arc. Thus, the arc body drop was modeled, but no back EMF would develop. This would test the RSOS's ability to act as a single-stage switch at the front of the launcher, where the armature was the combination of a solid metal body and arcing contacts. This would model the portion of the launcher where the sliding speed would no longer permit sliding galvanic contact, but where the speed was still low enough that no appreciable back EMF was being generated.

At this point, it was still believed that the Multi-Lam contact failure was due to misalignment. To correct the presumed problem, a 0.1-mm (0.004-in.) precision-sanded spacer was installed to increase the shuttle gap. The high spots on the shuttle were marked and sanded, and all conductive surfaces except the Multi-Lam sliding interface were sprayed with insulating varnish. The Multi-Lam had previously passed static tests at 10 and 20 kA. Care was taken not to actuate the switch until its static capacity had been established. This was done so that damage associated with charging would not be confused with damage due to energy dissipation during opening. The results of the opening test at 10 and 20 kA are presented in Table 16.



Table 16. Opening of rotary shuttle switch into resistive load

Peak Charging Current (kA)	Charging Current Rise Time (ms)	Interrupted Current (kA)	Voltage Developed (V)	Current Rise Time in Load (ms)
16	300	10.5	10.3	?
24	300	15.4	15.2	1

A static charging test at 30 kA once again caused contact failure in one of the four series contacts. On disassembly, the Multi-Lam sliding contact that had not failed on charging showed roughness in the silver plating at the location indicated by the lower arrow in Fig. 34.

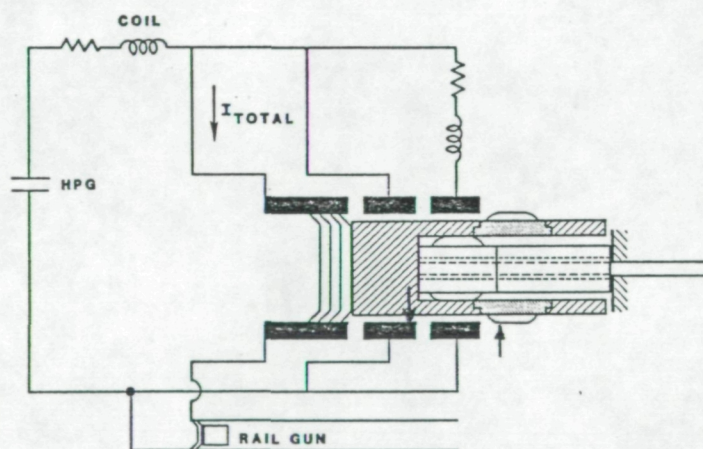
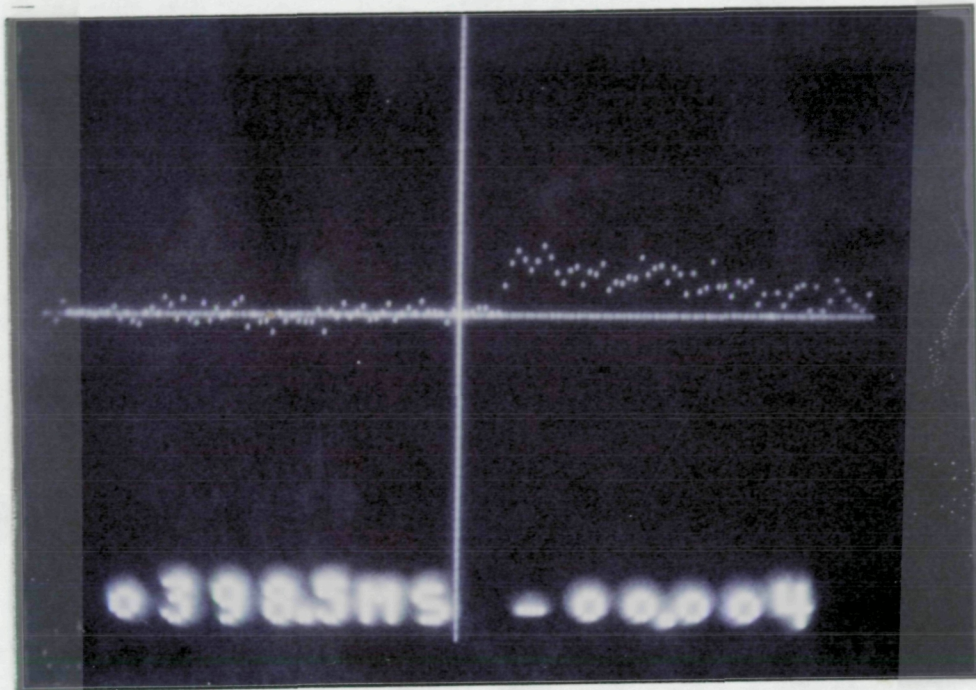


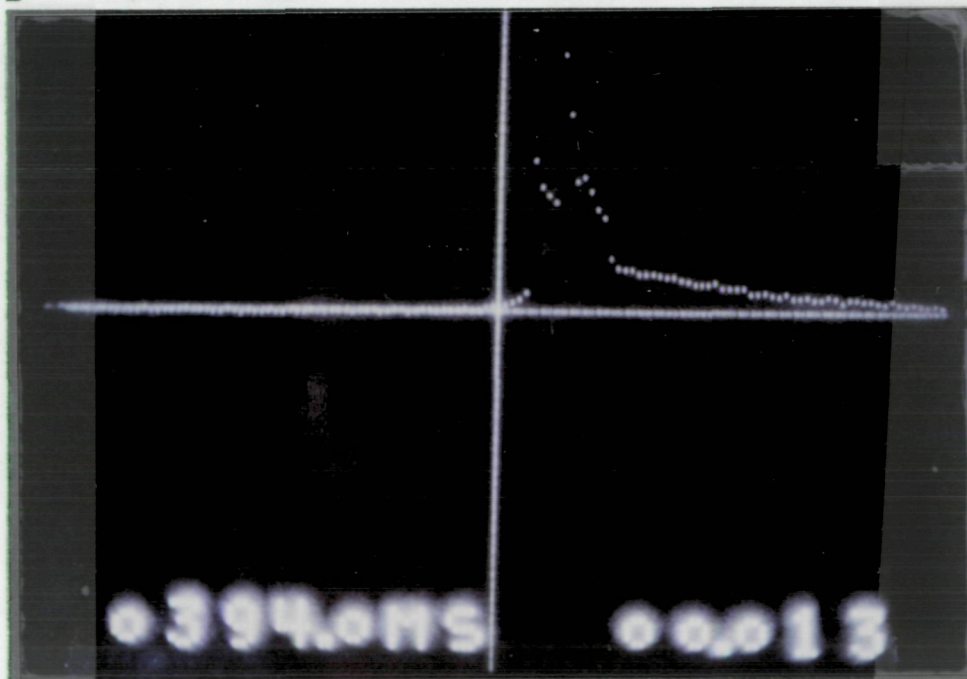
Fig. 34. Locations of damage to RSOS following testing

A slight plating of silver was seen on the fixed copper charging ring at the location indicated by the upper arrow in Fig. 34. Some arcing had occurred during transfer of the current into the resistive load. This was substantiated by examining the oscilloscope picture for the 20 kA opening test (Fig. 35). There are two voltage peaks on the voltage trace. The first voltage peak occurred when one Multi-Lam sliding joint pulled clear of the copper charging path. The second peak occurred when the other Multi-Lam joint disconnected, starting a second arc. The arc





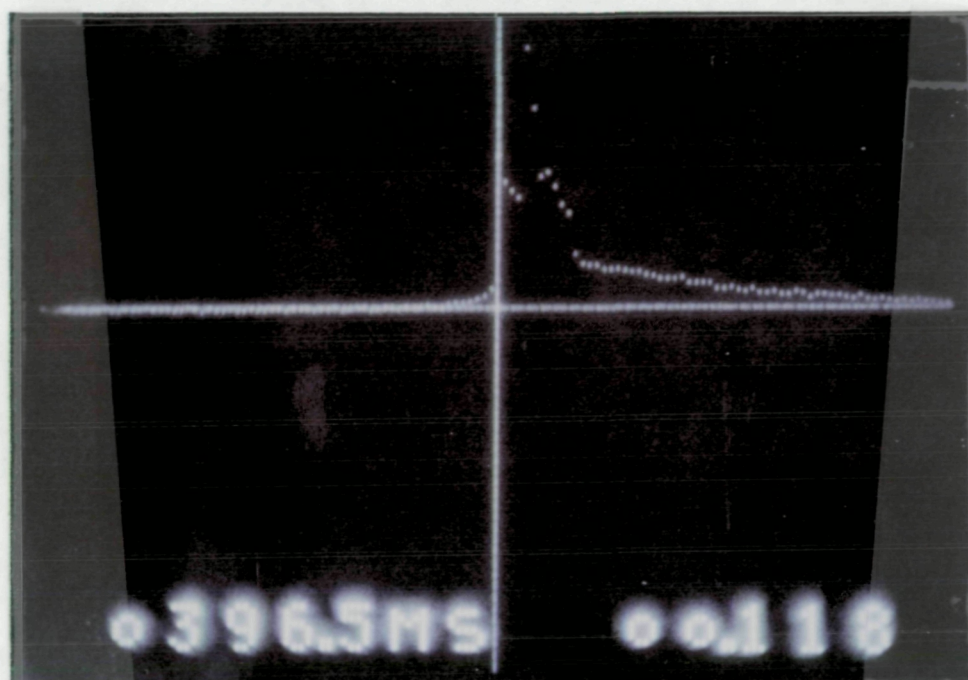
a. Load current enlarged



b. Voltage enlarged

Fig. 35. Opening test at 20 kA  
(sampling rate 1 ms/point)





c. Voltage enlarged

Fig. 35. Opening test at 20 kA  
(sampling rate 1 ms/point)



voltage then commutated current into the laminated switch resistor and the load resistor. The energy dissipation calculated by the procedure in Appendix D does not predict melting of the silver. Either the inductance of the resistive path must be higher than calculated, or there is a dominant resistive term that must be included in the switching energy considerations (Appendix B). This aspect of the switching needs further work. The calculation of the inductance of the ferromagnetic laminations is a nonlinear problem requiring a finite-element flux map. If the inductance proves to be the problem, the switch may be rebuilt with stainless steel laminations. The next series of tests performed adds further insight into the problem.

In the previous tests, the switch had failed statically at 30 kA. The Multi-Lam is so constructed that the two strips can be interleaved to double the number of contact louvers. The switch was rebuilt using this procedure. The load was changed from a stainless steel resistor that modeled an arc to a lower-resistance solid copper element that modeled a second-stage switch. The opening switch was successfully tested to 50 kA in a static mode. An opening test was then conducted at the 50-kA level. The results of that test are shown in Fig. 36. The top trace is the current trace of the HPG charging the energy storage inductor. At peak current, the HPG was crowbarred (shorted out with a heavy galvanic switch), and the current in the inductor circuit began to decay. Simultaneously, the command was given to actuate the solenoid valves that exhaust the opening switch air cylinder. In the bottom picture of Fig. 36, the top trace is the displacement of the opening switch. At the end of its travel, current is commutated into the shorting element (bottom trace of the second picture. Within the  $\pm 5$  percent resolution of the current monitors, the current in the inductor before switch opening was equal to the current in the inductor after current commutation, indicating a very efficient transfer.

Another test was performed, which was an attempt to take the double Multi-Lam to 60 kA. Once again, static Multi-Lam failure occurred. This time, two joints in series failed, and a third showed pitting. The two failed joints were on the inner shuttle.



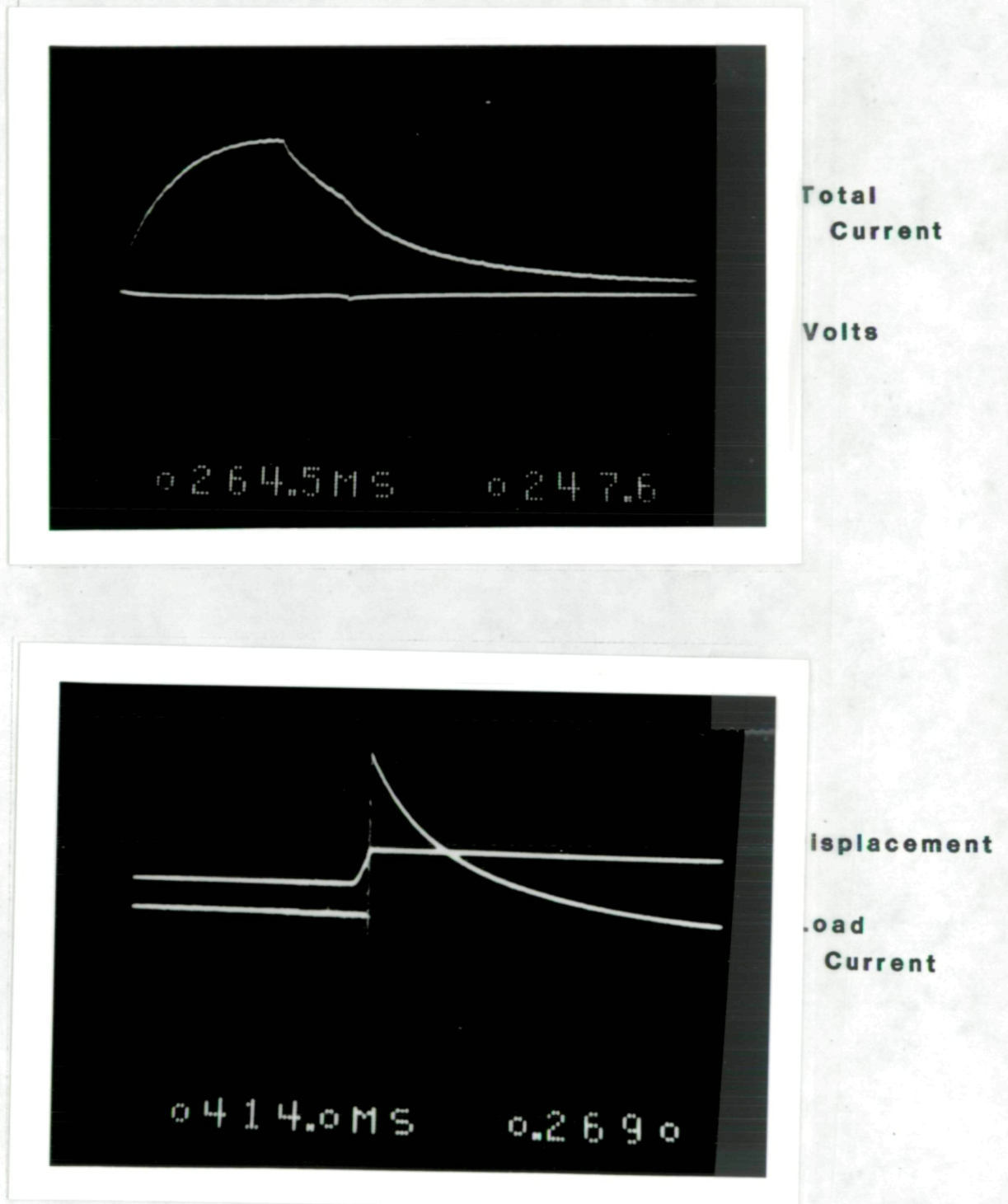


Fig. 36. Opening test at 50 kA

Failure was not due to misalignment. It was due to having exceeded the current-carrying capacity of the Multi-Lam contact strip. As mentioned earlier, this limit was 40 percent below the manufacturer's specifications. The Multi-Lam contact that was not damaged did not show scarring of the silver or silver transfer to the copper charging ring.

## SUGGESTIONS FOR FUTURE WORK

Earlier, in Task C, the switch actuation was described. That description stated that the Multi-Lam contact was designed to move from the copper charging ring to the resistive ring before the back brushes connect to the rail gun load (Fig. 20b). We now believe that the back brushes in fact seated shortly before the Multi-Lam left the copper. If this is true, the low-resistance load in parallel with the switch resistor is requiring less energy absorption than the high-resistance load in parallel with the switch resistor in the first series of tests. This is a theory that needs to be verified with further tests. The switch, though scarred, can be rebuilt.

Also, further analytical work needs to be done on the fundamental energy considerations in switching inductive stores. An electrical dissipative term needs to be included in the mathematical model.

A second shuttle needs to be added to the existing switch to look at jitter between shuttles at the time of opening. The switch should be rotated as originally designed to see whether it is possible to dissipate the switching energy more effectively. This might allow single-stage switching into a more resistive second-stage device, such as rod-array (GE RATVG) vacuum switches. [14] Increasing the speed of actuation of the first-stage switch is an issue that needs attention. To insure proper timing, armature position and velocity must be measured as close to the switching point as possible. This is equivalent to saying that the total switching time needs to be very fast. Switching time for the galvanic switch already requires milliseconds. Further penalty should not be added to this time by actuators that trigger the mechanical motion (valves, solenoids, etc.). One solution would be to have a precharged accumulator sealed with a diaphragm. The diaphragm could have an explosive detonator attached that triggers the actuation.

In conclusion, a good first pass effort has been made during this grant to identify a practical ESRL switching scheme. More work needs to be

done on galvanic switches, and a testing program is needed to develop or identify a reliable fast second-stage switch. Insulation design for the galvanic switch needs to be studied. The switch at the end of the launcher will be required to hold off the developed speed voltage.

Similar efforts are required for launcher design, experimental analysis of large-bore arc dynamics, continued power supply development, and the identification of technology that would simplify the launch scheme.

## ACKNOWLEDGMENTS

Special thanks goes to Don Holmes of of Holmes Engineering for his interest in the project and the fabrication of a cylinder that met all design specifications.

Special thanks goes to Jaime Cuadros of General Dynamics for giving us the opportunity to test with an actual railgun.

The authors would like to thank the students who worked on the project, Greg Milliken and David McFerren.

Credit for the success of the project must be shared with Jim Upshaw, for his incredible energy in the fabrication and testing effort. Thanks to him, many important tests were conducted late in the contract period that otherwise might not have been performed.

Finally, the authors would like to thank NASA/Lewis Research Center for sponsoring this grant to the Center for Electromechanics and Capt. Mike Brasher, the Project Officer. We hope that we will have an opportunity to work together again in the future.

## REFERENCES

1. Rice, J. M., et al., "Final Technical Report on Preliminary Feasibility Assessment for Earth-to-Space Electromagnetic (Railgun) Launcher", Battelle Columbus Laboratories, Final Report to National Aeronautics and Space Administration, Contract No. NAS3-22882, June 30, 1982.
2. Marshall, R. A., "Earth-to-Space Rail Launcher System", Center for Electromechanics, Univ. of Texas at Austin, Publ. No. PN-74, Feb. 1982.
3. Inall, E. K., "A Proposal for the Construction and Operation of an Inductive Store for 20 MJ", J. Phys. E: Sci. Instrum., 5, 1972, pp. 679-685.
4. Marshall, R. A., "High Energy Pulse Production and Application", Proc. Australian-U.S. Seminar on Energy Storage Compression and Switching, Australian Natl. Univ. Press (Canberra), 1978.
5. Deis, D. W., et al., "EMACK Electromagnetic Launcher Commissioning", IEEE Symposium on Electromagnetic Launch Technology, 2nd, Boston, MA, Oct. 11-14, 1983.
6. Bird, W. L., and Woodson, H. H., "Detailed Design, Fabrication, and Testing of an Engineering Prototype Compensated Pulsed Alternator", Final Rept. to Lawrence Livermore National Laboratory, Purch. Order No. 3325309, March 1980.
7. Hawke, R. S., "Results of Railgun Experiments Powered by Magnetic Flux Compression Generators", IEEE Trans. on Magnetics, MAG-18 (1), Jan. 1982, pp. 68-81.
8. Morgan, C. A., "A 10-MJ Active Rotary Flux Compressor for Driving Xenon Flashlamps", IEEE Intl. Pulsed Power Conference, Albuquerque, NM, June 6-8, 1983.
9. Zowarka, R. C., "Electromagnetic Propulsion Experiments", Final Report to General Dynamics Corp., Purch. Order No. 389564, Dec. 1982.
10. Ford, R. D., and Vitkovitsky, I. M., "Explosively Actuated 100-kA Opening Switch for High Voltage Applications", Naval Research Laboratory, Memorandum Rept. No. 3561, July 1977.
11. Delmas, A., et al., "Study of a Rapid Circuit Breaker for Intense Currents", Rev. Phys. Appliq., 10 (4), July 1975, pp. 241-245.
12. Bleys, C. A., et al., "200 kA Circuit Breaker with 10  $\mu$ s Current Transfer Time", Rev. Sci. Instrum., 46 (11), Nov. 1975, pp.1542-1545.

13. Honig, E. M., "Repetitive Opening Switches for Railguns", in Railgun White Paper, Los Alamos National Laboratory, Mar. 14, 1983.
14. Rich, J. A., et al., "High Power Triggered Vacuum Gap of Rod Array Type", General Electric Co. Rept. No. 81 CRD 321, 1981.
15. Rich, J. A., et al., "Development of a High-Power Vacuum Interrupter", Rept. to Electric Power Research Institute, EPRI Rept. No. EL-1895, June 1981.
16. Conte, D., et al., "Two stage Opening Switch Techniques for Generation of High Inductive Voltages", Proc. IEEE Symposium on Engineering Problems of Fusion Research, 7th, Cat. No. 77CH1267-4NPS (1977) p. 1066.
17. Inall, E. K., et al., "The Use of the Hall Effect in a Corbino Disk as a Circuit Breaker", Proc. IEEE Symposium on Engineering Problems of Fusion Research, 6th, Cat. No. 75CH1097-5-NPS (1975) pp. 666-668.
18. Barber, J. P., "The Acceleration of Macroparticles and a Hypervelocity Electromagnetic Accelerator", Ph.D. Dissertation, Australian National Univ., Canberra, 1972.
19. Rashleigh, S. C., and Marshall, R. A., "Electromagnetic Acceleration of Macroparticles to High Velocities", J. Appl. Phys., 49 (4), Apr. 1978, pp. 2540-2542.
20. Deis, D. W., and McNab, I. R., "A Laboratory Demonstration Electromagnetic Launcher", IEEE Trans. on Magnetics, MAG-18 (1), Jan. 1982, pp. 23-28.
21. Rylander, H. G., et al., "Investigation of the Homopolar Motor-Generator as a Power Supply for Controlled Fusion Experiments", IEEE Symposium on Engineering Problems of Fusion Research, 5th, Princeton, NJ, Nov. 1973.
22. Weldon, W. F., et al., "The Design, Fabrication, and Testing of a Five Megajoule Homopolar Motor-Generator", Intl. Conference on Energy Storage, Compression, and Switching, 1st, Torino, Italy, Nov. 5-7, 1974.
23. Driga, M. D., et al., "Fundamental Limitations and Topological Considerations for Fast Discharge Homopolar Machines", IEEE Trans. on Plasma Science, PS-3 (4), Dec. 1975, pp. 209-215.
24. Bird, W. L., et al., "Preliminary Engineering Design of a Pulsed Homopolar Generator Power Supply", IEEE Intl. Pulsed Power Conference, 1st, Lubbock, TX, Nov. 9-11, 1976.
25. Tolk, K. M., et al., "Inertial Energy Storage Research at The University of Texas at Austin", IEEE Intl. Pulsed Power Conference, 1st, Lubbock, TX, Nov. 9-11, 1976.

26. Woodson, H. H., et al., "Pulsed Power from Inertial Storage with Homopolar Machines for Generation", IEEE Intl. Pulsed Power Conference, 1st, Lubbock, TX, Nov. 9-11, 1976.
27. Gully, J. H., et al., "Design, Fabrication and Testing of a Fast Discharge Homopolar Machine (FDX)", IEEE Symposium on Engineering Problems of Fusion Research, 7th, Knoxville, TN, Oct. 25-28, 1977.
28. Weldon, W. F., et al., "Compulsator -- a High Power Compensated Pulsed Alternator", Intl. Conference on Energy Storage, Compression, and Switching, Venice, Italy, Dec. 5-8, 1978.
29. Weldon, J. M., and Weldon, W. F., "The Homopolar Generator as a Pulsed Industrial Power Supply", Conference on Industrial Energy Conservation Technology, 1st, Houston, TX, Apr. 22-25, 1979.
30. Spann, M. L., et al., "The Design, Assembly, and Testing of an Active Rotary Flux Compressor", IEEE Intl. Pulsed Power Conference, 3rd, Albuquerque, NM, June 1-3, 1981.
31. Weldon, W. F., "Rotating Machinery for Use in Pulsed Power", IEEE Intl. Pulsed Power Conference, 4th, Albuquerque, NM, June 6-8, 1983.
32. Gully, J. H., et al., "Compact Homopolar Generator Development at CEM-UT", IEEE Symposium on Electromagnetic Launch Technology, 2nd, Boston, MA, Oct. 11-14, 1983.
33. Walls, W. A., and Estes, E. G., "Continued Development of Higher Energy Density, Higher Current Rated Homopolar Generators at CEM-UT", IEEE Intl. Pulsed Power Conference, 4th, Albuquerque, NM, June 6-8, 1983.
34. Floyd, J. E., and Aanstoos, T. A., "A New High Current Laboratory and Pulsed Homopolar Generator Power Supply at the University of Texas", IEEE Symposium on Electromagnetic Launch Technology, 2nd, Boston, MA, Oct. 11-14, 1983.
35. Marshall, R. A., and Weldon, W. F., "Parameter Selection for Homopolar Generators used as Pulsed Energy Stores", Electric Machines and Electromech., 6 (2), Mar.-Apr. 1981, pp. 109-127.
36. Vitkovitsky, I. M., et al., "Homopolar Current Source for Mass Accelerators", IEEE Trans. on Magnetics, MAG-18 (1), Jan. 1982, pp. 157-159.
37. Fowler, C. M., et al., "Explosive Flux Compression Generators for Railgun Power Sources", IEEE Trans. on Magnetics, MAG-18 (1), Jan. 1982, pp. 64-67.
38. Hawke, R. S., et al., "Results of Railgun Experiments Powered by Magnetic Flux Compression Generators", IEEE Trans. on Magnetics, MAG-18 (1), Jan. 1982, pp. 82-93.



39. Fowler, C. M., et al., "Pulse Power Applications of Flux Compression Generators", IEEE Intl. Pulsed Power Conference, 3rd, Albuquerque, NM, June 1-3, 1981.
40. Marshall, R. A., "The Single Leaf Projectile in the ANU Railgun", Aeroballistic Range Association Meeting, 26th, San Leandro, CA, 1975.
41. Marshall, R. A., "Moving Contacts in Macroparticle Acceleration", in High Power High Energy Pulse Production and Application, E. K. Inall, ed., Australian Natl. Univ. Press (Canberra), 1977.
42. Fowler, C. M. et al., "An Introduction to Explosive Magnetic Flux Compression Generators", Los Alamos National Scientific Laboratory Report No. LA-5890-MS, March 1975.
43. Grover, I. W., Inductance Calculations: Working Formulas and Tables, Dover (New York), 1946, pp. 70ff.
44. Weldon, W. F., "Repetitive Galvanic Opening Switch", Invention Disclosure, Center for Electromechanics, The University of Texas at Austin, August 1982.
45. Stevens, H., David Taylor Ship Research & Development Center, Annapolis, MD, personal communication, June 16, 1983.
46. Orcella, F., Westinghouse Corp., personal communication, June 16, 1983.
47. Walkden, A. J., et al., "Liquid-metal Switch for Ultra-high Direct Currents", GEC J. Sci. and Technol., 45 (2), 1979.
48. Conte, D., "A Megavolt Pulse Generator Using Inductive Energy Storage", IEEE Intl. Pulsed Power Conference, 2nd, Lubbock, TX, Cat. No. 79CH1505-7, 1979, p. 276.

APPENDIX A

ENERGY STORES AND SWITCHES  
FOR RAIL-LAUNCHER SYSTEMS

Progress Report  
for  
March, 1983

Center for Electromechanics  
The University of Texas at Austin  
Taylor Hall 167  
Austin, TX 78712

Telephone 512/471-4496

## INTRODUCTION

This report covers work performed at the Center for Electromechanics at The University of Texas at Austin during March 1983 on NASA Research Grant NAG-3-303, "Energy Stores and Switches for Rail-launcher Systems."

### LAUNCHER PERFORMANCE

In this month's report, I would like to review the ESRL requirements presented in Case No. 4 of the Richard Marshall report to Battelle Columbus Laboratories in February 1982. Case No. 4 assessed the possibility of injecting payloads (with a  $\Delta V$  capability) into earth orbit. Battelle identified a desired payload of 6500 kg. An acceleration of 2500 g's ( $1 \text{ g} = 9.81 \text{ m/s}^2$ ) and a projectile diameter of 55 cm were chosen to limit projectile stresses.

A hollow titanium tube projectile can be examined as one example of the possible origin of these numbers. The assumptions associated with this design will be kept very simple. They are

- the tube projectile derives no strength from the payload material
- the tube wall thickness is held constant
- the candidate payload materials are packed in the tube with a packing factor of 1.0, with no attention paid to shapes.

An expression for the critical buckling load in a column is

$$P_{cr} = \frac{\pi^2 EI}{L^2}$$

where  $P_{cr}$  = critical buckling load, N

$E$  = modulus of elasticity of Ti ( $1.24 \times 10^{11} \text{ N/m}^2$ )

$I$  = moment of inertia =  $\pi r^3 t$ ,  $\text{m}^4$

$r$  = mean radius of the tube, m

$t$  = tube thickness, m

$L$  = tube length, m.

The applied load is the payload mass multiplied by the acceleration. For now, the mass of the tube will be neglected. An expression for this quantity is

$$P = \rho \pi r_i^2 L a$$

where  $\rho$  = payload density, kg/m<sup>3</sup>

$r_i$  = inner radius of the tube, m

$L$  = tube length, m

$a$  = acceleration ( $2.45 \times 10^4$  m/s<sup>2</sup>).

These two expressions may be equated and solved for  $L$ . The thickness of the tube will be set at 5.08 cm (2 in.). The mean radius is then 24.69 cm, and the inner radius of the tube is 22.42 cm. The expression for the tube length is

$$L = \sqrt{\frac{\pi E I}{\rho r_i^2 a}}$$

Table 1 presents a list of candidate payload materials and projectile length.

Table 1. Payload Characteristics

<u>Material</u>	<u>Density, kg/m<sup>3</sup></u>	<u>Mass, kg</u>	<u>Projectile Length, m</u>
Aluminum	2,685	2,781	6.56
Steel	7,834	5,678	4.59
Uranium	19,072	10,270	3.41

Table 1 shows that for the simple projectile design the payload mass will decrease for lower density materials. If 6,500 kg is maintained as the desired payload mass, then for the lower density materials the projectile must be longer, and buckling will result. Further projectile designs that strengthen the tube by joining it to the payload material or the reinforcement of the tube with internal bulkheads are alternatives that might allow standardization of projectile length and payload mass. Marshall addressed this problem in Section 12.0 of his report (p. 47). One solution is to try to distribute the driving force along the projectile.

Continuing with Case No. 4, the force on the projectile is

$$F = ma = 6,500 \text{ kg } (2.45 \times 10^4 \text{ m/s}^2) = 159 \text{ MN}$$

where  $F$  = force on the projectile, N

$m$  = projectile mass, kg

$a$  = projectile acceleration,  $\text{m/s}^2$ .

The energy that must be delivered to the projectile in one metre of length in order to realize this force is

$$E = \int_0^{1\text{m}} F \cdot dx = 159 \text{ MJ}$$

where  $E$  = delivered energy

$F$  = force on the projectile

$dx$  = a differential displacement,

or 159 MJ must be delivered per metre of launcher length.

In order to arrive at the total required stored energy, the transfer efficiencies from the HPG to the energy storage inductor and from the inductor to the gun must be known. Since Marshall looked at the problem, several optimization studies have put the HPG-to-inductor transfer efficiency at 70 percent, as opposed to his estimate of 85 percent. Also, the 85 percent transfer from the coil to the gun takes into account only the losses of energy in the rails and from the arc armature. It does not allow for any switching inefficiency or, more importantly, for flux trapping in the inductors. Within the conductors of the coil, magnetic flux density cannot change instantaneously, so when current transients occur during energy transfer to the gun, the flux density in the conductor remains zero, shielded by induced currents on the surface of the conductors. These induced currents will decay in time, and the field distribution will reach steady state. Initially, the current flows through only a fraction of the conductor cross section. While the resistance is large at first, in time it decreases to the familiar steady state value,  $\rho l/A$ . During testing of the cryogenic Brooks coil for General Dynamics, 10 percent of the energy was trapped in the coil during discharge. From the literature, it can be seen that other people are aware of this effect.

### "The efficiency of energy transfer

A cycle of operation will start . . . and the current in the inductor will increase fairly slowly . . . It will distribute uniformly over the cross section of the inner and outer conductors, and energy will be stored in the magnetic field extending from the centre to the outer surface of the outer conductor as indicated in Fig. 1.

"When the circuit is interrupted, the current will transfer to the load and decrease to a low value in a few milliseconds. The energy in the air space will be delivered to the load, but the energy associated with the field in the conductors, regions A and B in Fig. 1, will produce eddy currents within the conductors themselves, and be dissipated there. The only contribution these circulating currents can make to the external circuit is almost to compensate for the very small loss due to the resistance of the main conductors.

"Since the radius of the outer conductor will be four times the radius  $r_1$  of the inner, 15 percent of the total energy stored will be trapped in the inner conductor, and since the outer conductor will be  $r_1/2.5$  thick, 2.5 percent will be trapped in the outer conductor. Therefore, with the geometry proposed for the inductive store, 17.5 percent of the energy will be lost due to the field trapped within the thickness of the conductors."

This is an excerpt from a paper by Ken Inall of the Australian National University (J. Physics Series E, 5, 1972). The coil of which he writes is a single-turn coax.

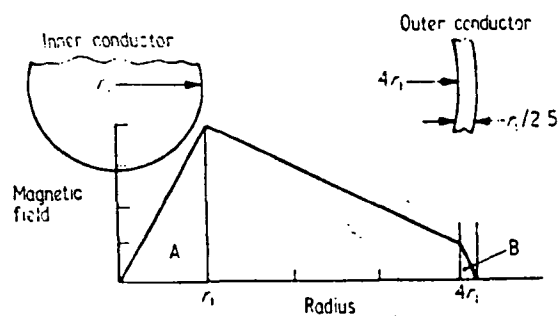


Fig. 1. The variation of magnetic field with radius in the coaxial inductor

The efficiency of transfer from the inductor will more approximately be  $0.9 \times 0.85 = 76.5$  percent. Therefore, the overall efficiency is now

$$0.765 \times 0.7 = 53.6 \text{ percent.}$$

The required energy density along the launcher is now

$$\frac{159 \text{ MJ/m}}{0.536} = 297 \text{ MJ/m}$$

Staying with the same 56-MJ machine that Marshall identified, five such machines are required per metre of gun length. The overall launcher length is

$$S = \frac{v^2}{2a} = \frac{(10,000 \text{ m/s})^2}{2 \cdot 2.45 \times 10^4 \text{ m/s}^2} = 2,040 \text{ m}$$

If 159 MJ/m must be delivered to the launcher, the energy stored per inductor is 41.6 MJ. For now, I will continue to use Marshall's 4-turn coaxial cryogenic aluminum inductor. These units were designed with an inductance of 6  $\mu\text{H}$  and a resistance of 2.7  $\mu\Omega$ . It is instructive to examine the discharge characteristic of the 56-MJ HPG discharging into the 6  $\mu\text{H}$ , 41.6-MJ inductor. The capacitance of the generator is

$$C = \frac{2E}{V^2} = \frac{2 \cdot 56 \times 10^6}{(110)^2} = 9,256 \text{ F.}$$

where C = generator equivalent capacitance

E = stored energy

V = generator open-circuit voltage.

The inductance of the circuit is

HPG machine and buswork	1 $\mu\text{H}$
Inductor	6 $\mu\text{H}$
Total	<u>7 <math>\mu\text{H}</math></u>

The resistance of the circuit is

Generator	~ 6 $\mu\Omega$
Buswork	~ 4 $\mu\Omega$
Coil	<u>2.7 <math>\mu\Omega</math></u>
Total	12.7 $\mu\Omega$

The damping factor for the circuit is

$$\zeta = R/(2\sqrt{L/C}) = 0.23$$

where R = circuit resistance  
 L = circuit inductance  
 C = circuit capacitance.

The circuit is underdamped, and the time to peak current is

$$t_{\text{peak}} = \frac{\tan^{-1} \left( \frac{2L \sqrt{\frac{1}{LC} - \frac{R^2}{4L^2}}}{R} \right)}{\sqrt{\frac{1}{LC} - \frac{R^2}{4L^2}}}$$

where  $t_{\text{peak}}$  = time to peak current = 350 ms.

The expression for the current is

$$I = \frac{V_{\text{oc}}}{L \sqrt{\frac{1}{LC} - \frac{R^2}{4L^2}}} \exp\left(\frac{-t/2L}{R}\right) \sin \sqrt{\frac{1}{LC} - \frac{R^2}{4L^2}} t$$

where  $I_{\text{peak}}$  = peak current =  $2.91 \times 10^6$  A  
 $V_{\text{oc}}$  = open-circuit voltage.

This means that 25.4 MJ of energy are stored in the coil at peak current. This is only a 45 percent transfer efficiency. The assumed generator and bus impedance must be larger than the numbers Marshall used. This will require a more detailed examination as further simulations are developed.

The time of flight in the launcher is

$$t = \sqrt{\frac{2s}{a}} = 0.408 \text{ s}$$

where t = dwell time in the launcher  
 s = launcher length  
 a = acceleration.

This indicates that at the front portion of the launcher where the acceleration is changing, position, velocity, and acceleration will all



have to be sensed. To insure that the energy stores are at peak current when the projectile passes their locations, machines further up the launcher will have to be discharged while the payload is in flight. Within a short distance along the rails, the projectile acceleration will approach a steady value. If the velocity is sensed at discrete positions, then supplies located

$$x = v_0 t + \frac{1}{2} a t^2$$

where  $x$  = predicted displacement

$v_0$  = projectile velocity at the sensor location

$t$  = time to peak current, 350 ms

$a$  = acceleration

metres up the launcher can be discharged. Also a window 20 ms before and after peak current is an appropriate error margin because the current is fairly constant near the peak value. This indicates that when the controller calculates

$$v = v_0 + at, \quad t = 350 \text{ ms},$$

and, say, 5,000 m/s is the result, then  $5,000 \text{ m/s} \times 0.020 = 100 \text{ m}$ . This means that 500 HPGs could be discharged simultaneously  $x$  metres up the launcher, and they would all be within 20 ms of their peak current when the projectile passes. Present making switch technology allows the initiation of discharge 3 ms after the discharge command is given. This actuation time is repeatable and will simply be incorporated in the 350-ms charging time.

The next event is the synchronization of the opening switches. The individual stores are in operation for approximately 4 m of projectile travel. If the switching is to occur within 1 percent of this total distance, and if the projectile is traveling 10 km/s, then the resulting switching time is

$$\frac{0.04 \text{ m}}{10,000 \text{ m/s}} = 4 \times 10^{-6} \text{ s.}$$

Some magnetically driven opening switches have operated in this domain, but with much lower inductor charging currents.

The speed voltage associated with armature motion is given by

$$\begin{aligned} V &= I \, dL/dt = I (\partial L/\partial x) (\partial x/\partial t) \\ &= (25 \times 10^6 \text{ A}) (0.5 \times 10^{-6} \text{ H/m}) (10 \times 10^3 \text{ m/s}) \\ &= 125 \text{ kV} \end{aligned}$$

where  $V$  = speed voltage

$I$  = current

$\partial L/\partial x$  = inductance per unit length of launcher

$\partial x/\partial t$  = projectile velocity.

Because this large voltage is seen by discharged stores, it is required that stores no longer in operation be removed from the launcher. From Marshall's simulations, approximately 20 stores were operational simultaneously. This corresponds to 4 m of launcher length. The timing for store removal at the end of the launcher then becomes

$$t = \frac{4 \text{ m}}{10,000 \text{ m/s}} = 400 \times 10^{-6} \text{ s.}$$

The two switching experiments that are being performed, the RSOS and the liquid metal experiment, will begin to explore switching times and efficiencies. If the times fall closer to  $6 \mu\text{s}$ , the efficiency will be very good. If they are closer to  $400 \mu\text{s}$ , this additional inefficiency will have to be considered in the launcher design. Also, the number of repetitive switching operations these devices can perform becomes a very important parameter in a system that requires such a large number of devices. Most important is that the technology is so new that these experiments will provide invaluable data for the design of second-generation devices.

APPENDIX B

ENERGY CONSIDERATIONS IN SWITCHING CURRENT FROM AN  
INDUCTIVE STORE INTO A RAILGUN

H. H. Woodson and W. F. Weldon

Presented at the  
4th IEEE International Pulsed Power Conference  
Albuquerque, New Mexico  
June 6-8, 1983

Publication No. PN-87  
Center for Electromechanics  
The University of Texas at Austin  
Taylor Hall 167  
Austin, TX 78712  
512-471-4496

H. H. Woodson and W. F. Weldon  
Center for Electromechanics  
The University of Texas at Austin  
Austin, TX 78712

Summary

A mathematical model containing no electrical or mechanical losses is analyzed to determine the energy that must be absorbed by the switching element while switching current from a storage inductance of constant value to a railgun. Results are obtained for instantaneous switching and for two different current waveforms for switching over a finite time interval. The results show that the switch must absorb the least amount of energy when switching is instantaneous, and that a linear buildup of railgun current causes more switch energy absorption than a nonlinear buildup. Numerical examples are presented to illustrate values for typical railguns of interest.

Introduction

The purpose of this paper is to examine in a fundamental way the energy flows that occur when current is switched from an inductive store of constant inductance into a railgun. In particular, we will calculate the amount of energy that must be absorbed by the switching element. The analyses will be performed neglecting electrical and mechanical losses, the rationale being that we are most interested in high-performance, high-efficiency systems. The lossless model is a good approximation that is more amenable to analysis, and the effects of losses can be evaluated as perturbations on the results obtained from the lossless model.

Lossless Model

The electrical part of the lossless model to be analyzed is shown schematically in Fig. 1. The storage inductance  $L_1$  is constant and is assumed to be charged by a separate circuit not shown. The inductance  $L_2$

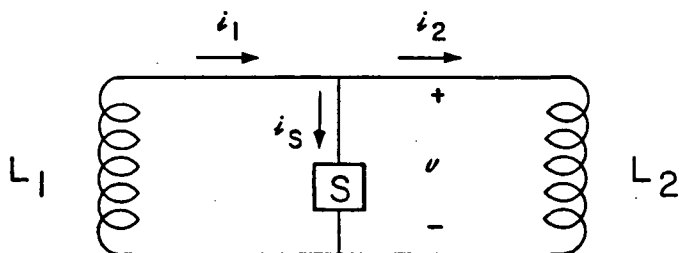


Fig. 1. Schematic diagram of electrical part of lossless model

represents a railgun and hence will change with the position of the armature. The switching element S is not specified except to require that it accept or supply energy as necessary to accomplish the required switching function. As will be illustrated later, the switching element does not need to be dissipative, although it can be.

With reference to Fig. 1, we enumerate in Table 1 a set of initial conditions and a set of final conditions that define the switching operation. By these conditions we merely say that at time  $t = 0$ , the storage inductance  $L_1$  is charged to current  $I_i$  and is short-circuited by switching element S, and that during the interval  $0 < t < t_f$  the switch current  $i_s$  goes to zero while the railgun current  $i_2$  goes from zero to  $I_f$ .

Table 1. Switching Operation Conditions

Initial Conditions	
$t = 0$	$i_1 = I_i$
$v = 0$	$i_s = I_i$
$L_2 = L_{2i}$	$i_2 = 0$
Initial magnetic energy: $W_i = \frac{1}{2}L_1 I_i^2$	
Final conditions	
$t = t_f$	$i_1 = I_f$
$L_2 = L_{2f}$	$i_s = 0$
	$i_2 = I_f$
Final magnetic energy: $W_f = \frac{1}{2}(L_1 + L_{2f})I_f^2$	

For the circuit of Fig. 1 in the time interval  $0 < t < t_f$ , Kirchhoff's voltage law requires

$$v = -\frac{d}{dt}(L_1 i_1) = \frac{d}{dt}(L_2 i_2)$$

from which

$$\frac{d}{dt}(L_1 i_1 + L_2 i_2) = 0 \quad (1)$$

Integrating this expression with respect to time gives the result

$$L_1 i_1 + L_2 i_2 = \text{const},$$

and application of initial conditions from Table 1 fixes the constant as

$$L_1 i_1 + L_2 i_2 = L_1 I_i \quad (2)$$

This equation describes the relation between  $i_1$  and  $i_2$  during switching. It can also be used to find the current in the switching element as

$$i_s = i_1 - i_2 \quad (3)$$

At the completion of switching,

$$i_1 = i_2 = I_f = \frac{L_1 I_i}{L_1 + L_{2f}} \quad (4)$$

and the final magnetic energy is

$$W_f = \frac{1}{2}(L_1 + L_{2f})I_f^2 = \frac{L_1}{L_1 + L_{2f}} W_i \quad (5)$$

For the electrically and mechanically lossless system being considered, the difference

$$W_i - W_f = \frac{L_{2f}}{L_1 + L_{2f}} W_i \quad (6)$$

between initial and final magnetic energies can appear in one or both of two places -- in the switching element S and as mechanical work done on the armature. How the energy is divided will depend on the armature movement that takes place during switching. Therefore, we treat the two cases in which armature motion does and does not occur during switching.

#### No Armature Movement During Switching

We assume either that the armature is latched during switching or that the switching is accomplished so rapidly that no appreciable armature movement occurs during switching. In this case

$$L_{2f} = L_{2i}$$

and no mechanical work is done on the armature during switching. Thus, the energy difference between initial and final conditions is all absorbed by the switching element and is given by

$$W_{s0} = W_i - W_f = \frac{L_{2i}}{L_1 + L_{2i}} W_i \quad (7)$$

Note that the energy given by Eq. 7 is absorbed by the switching element S, but that there is no fundamental requirement that it be dissipated, although it can be.

#### Armature Movement During Switching

The second case to be considered is one in which the railgun armature moves during switching, and

$$L_{2f} > L_{2i} .$$

In this case, some energy will be converted to mechanical form by the electromagnetic force acting on the armature during switching.

When we specify the energy accepted by the switching element S as  $W_s$  and the work done on the armature as  $W_a$ , the conservation of energy requires that

$$W_s + W_a = W_i - W_f = \frac{L_{2f}}{L_1 + L_{2f}} W_i \quad (8)$$

Because  $L_{2f} > L_{2i}$ , this amount of energy is clearly greater than  $W_{s0}$  given by Eq. 7. Whether or not any of this additional energy goes into the switching element, and, if so, how much, must be determined by a more complete analysis of  $W_a$ , the work done on the armature by electromagnetic forces.

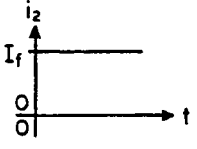
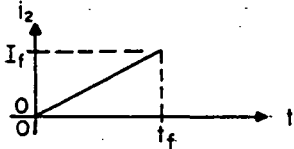
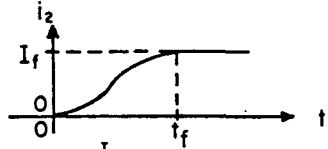
To determine how much of the energy given by Eq. 8 must be accepted by the switch S, it is necessary to calculate the mechanical work  $W_a$  done on the armature, which is assumed to move in the x direction,

$$W_a = \int_{x_i}^{x_f} \frac{1}{2} i_2^2 \frac{dL_2}{dx} dx \quad (9)$$

This quantity depends both on how  $i_2$  and  $x$  vary with time and with how  $L_2$  varies with  $x$ .

To obtain an approximate value for switching energy, assume for convenience that

Table 2. Switching in a Lossless System

Switching waveform	Instantaneous 	Linear 	Cosinusoidal 
Armature position at completion of switching	$x_f = 0$	$x_f = \frac{L_2 I_f^2 t_f^2}{24M}$	$x_f = \frac{L_2 I_f^2 t_f^2}{8M} \left( \frac{3}{4} - \frac{4}{\pi^2} \right)$
Armature velocity at completion of switching	$\left( \frac{dx}{dt} \right)_f = 0$	$\left( \frac{dx}{dt} \right)_f = \frac{L_2 I_f^2 t_f}{6M}$	$\left( \frac{dx}{dt} \right)_f = \frac{3L_2 I_f^2 t_f}{16M}$
Current at completion of switching	$I_f = \frac{L_1}{L_1 + L_{2i}} I_i$	$I_f = \frac{L_1}{L_1 + L_{2f}} I_i$	$I_f = \frac{L_1}{L_1 + L_{2f}} I_i$
Magnetic energy in system at completion of switching	$W_f = \frac{L_1}{L_1 + L_{2i}} W_i$	$W_f = \frac{L_1}{L_1 + L_{2f}} W_i$	$W_f = \frac{L_1}{L_1 + L_{2f}} W_i$
Energy accepted by switching element	$W_{s0} = \frac{L_{2i}}{L_1 + L_{2i}} W_i$	$W_s = W_{s0} + \left[ \frac{L_1 L_2^2 x_f \left( \frac{1}{3} L_1 + L_{2f} - \frac{2}{3} L_{2i} \right)}{(L_1 + L_{2f})^2 (L_1 + L_{2i})} \right] W_i$	$W_s = W_{s0} + \left[ \frac{L_1 L_2^2 x_f (0.184 L_1 + L_{2f} - 0.816 L_{2i})}{(L_1 + L_{2f})^2 (L_1 + L_{2i})} \right] W_i$

$$x_1 = 0$$

and that the inductance  $L_2$  varies with  $x$  as

$$L_2 = L_{2i} + L_2 x . \quad (10)$$

Assume further that the armature is a pure inertia of mass  $M$  and that it starts from rest ( $x = 0$ ,  $dx/dt = 0$ ) at the start of switching. In this case, the mechanical equation of motion is

$$M \frac{d^2 x}{dt^2} = 1/2 i_2^2 \frac{dL_2}{dx} = 1/2 i_2^2 L_2' . \quad (11)$$

If the current  $i_2$  is known as a function of time, Eq. 11 can be integrated twice to find both  $x$  and  $dx/dt$  as functions of time, and the energy  $W_a$  can be calculated.

To assess the sensitivity of this energy to the current waveform during switching, we will treat two cases. First, we assume that the railgun current increases linearly with time during switching,

$$i_2 = I_f \frac{t}{t_f} . \quad (12)$$

The use of this expression in Eq. 11, integration once, and use of the initial conditions yield the armature velocity

$$\frac{dx}{dt} = \frac{L_2' I_f^2}{6M t_f^2} t^3 . \quad (13)$$

Integration of this expression and use of the initial conditions yield the armature position

$$x = \frac{L_2' I_f^2}{24M t_f^2} t^4 . \quad (14)$$

The velocity and position reached at the completion of switching ( $t = t_f$ ) are

$$\left(\frac{dx}{dt}\right)_f = \frac{L_2' I_f^2 t_f}{6M} ; \quad x_f = \frac{L_2' I_f^2 t_f^2}{24M} . \quad (15)$$

From conservation of energy, the work done on the armature  $W_a$  must go into kinetic energy; thus

$$W_a = 1/2 M \left(\frac{dx}{dt}\right)_f^2 ,$$

and the use of both expressions of Eq. 15 yields the result

$$W_a = \frac{I_f^2 L_2' x_f}{3} = \frac{2L_2' x_f L_1}{3(L_1 + L_2)_f^2} W_i . \quad (16)$$

The resulting energy into the switching element is

$$W_s = W_i - W_f - W_a \\ = W_{s0} + \frac{L_1 L_2' x_f (L_1/3 + L_2' - 2L_2/3)}{(L_1 + L_2)_f^2 (L_1 + L_2)_i} W_i , \quad (17)$$

where  $W_{s0}$  is the switching energy for no armature movement given by Eq. 7. Because the coefficient of  $W_i$  in Eq. 17 is positive, the energy absorbed by the switch is greater with movement than without.

To explore how the relative current waveform during switching affects the energy the switching element must accept, we treat a second current-time relation:

$$i_2 = \frac{I_f}{2} \left(1 - \cos \pi \frac{t}{t_f}\right) . \quad (18)$$

This current begins and ends with zero slope. Substitution of this expression into Eq. 11, integration, and application of the assumed initial conditions yield the velocity

Table 3. Parameters for Railgun  
1 x 1 cm Bore

Assumptions:  $L_1 = 30 \mu\text{H}$  ;  $I_1 = 500 \text{ kA}$  ;  $W_i = 3.75 \text{ MJ}$  ;  $x_f = 1.0 \text{ M}$  ;  
 $L_{2i} = 1.0 \mu\text{H}$  ;  $L_2' = 0.5 \mu\text{H/m}$  ;  $M = 10^{-3} \text{ kgm}$

Switching waveform	Instantaneous	Linear	Cosinusoidal
Switching time $t_f$	$t_f = 0$	$t_f = 0.460 \text{ ms}$	$t_f = 0.452 \text{ ms}$
Armature velocity at completion of switching	$\left(\frac{dx}{dt}\right)_f = 0$	$\left(\frac{dx}{dt}\right)_f = 8.69 \text{ km/s}$	$\left(\frac{dx}{dt}\right)_f = 9.61 \text{ km/s}$
Current at completion of switching	$I_f = 484 \text{ kA}$	$I_f = 476 \text{ kA}$	$I_f = 476 \text{ kA}$
Magnetic energy in system at completion of switching	$W_f = 3.63 \text{ MJ}$	$W_f = 3.57 \text{ MJ}$	$W_f = 3.57 \text{ MJ}$
Energy accepted by switching element	$W_{s0} = 121 \text{ kJ}$	$W_s = 141 \text{ kJ}$	$W_s = 133 \text{ kJ}$

A comparison of Eq. 23 with Eq. 12 for a linearly varying current shows that the switch absorbs less energy with the cosinusoidal waveform.

$$\frac{dx}{dt} = \frac{L_2^{-1} I_f^2}{8M} \left[ \frac{3}{2} t - \frac{2t_f}{\pi} \sin \pi \frac{t}{t_f} + \frac{t_f}{4\pi} \sin 2\pi \frac{t}{t_f} \right] \quad (19)$$

and the position

$$x = \frac{L_2^{-1} I_f^2}{8M} \left[ \frac{3}{4} t^2 + \frac{2t_f^2}{\pi^2} \left( \cos \pi \frac{t}{t_f} - 1 \right) - \frac{t_f^2}{8\pi^2} \left( \cos 2\pi \frac{t}{t_f} - 1 \right) \right] \quad (20)$$

The velocity and position reached at the completion of switching are

$$\left( \frac{dx}{dt} \right)_f = \frac{3L_2^{-1} I_f^2 t_f}{16M}; \quad x_f = \frac{(3/4 - 4/\pi^2) L_2^{-1} I_f^2 t_f^2}{8M} \quad (21)$$

Once again, recognizing that

$$W_a = 1/2 M \left( \frac{dx}{dt} \right)_f^2,$$

the use of both expressions in Eq. 21 yields

$$W_a = \frac{9\pi^2 L_1 L_2^{-1} x_f}{8(3\pi^2 - 16)(L_1 + L_2 f)^2} W_i \quad (22)$$

In this case, the energy  $W_S$  into the switch  $S$  is

$$\begin{aligned} W_S &= W_i - W_f - W_a \\ &= W_{S_0} + \frac{L_1 L_2^{-1} x_f (0.184 L_1 + L_2 f - 0.816 L_2 i)}{(L_1 + L_2 f)^2 (L_1 + L_2 i)} W_i \end{aligned} \quad (23)$$

### Summary of Results

The results of these three analyses are summarized in Table 2. The expressions can be used to evaluate switching duty for a variety of conditions in a variety of railguns.

To give the results of Table 2 a little more concrete meaning, a numerical example has been worked, and the assumptions and results are presented in Table 3. This numerical example is typical of a railgun with a 1- x 1-cm bore and with a length of several metres.

Several features of Table 3 are worth noting. First, even though the current waveforms with armature movement are quite different, the switching times for the same switching distance are only slightly different. On the other hand, the increase in energy absorbed by the switch over that for instantaneous switching is almost twice as much for the linear waveform as that for the cosinusoidal waveform. Finally, for these conditions, the energy absorbed by the switching element is increased by only 10 to 20 percent by armature movement during switching.

### Conclusions

The analysis of energy flows during switching of current from a storage inductor to a railgun can be carried out easily for a system model with no electrical or mechanical losses. The results of such an analysis should be useful in estimating the energy a switch must absorb in a highly efficient (low-loss) system, and they should also be useful in exploring trends in other systems.

Table 4. Parameters for Railgun  
2-1/2 x 2-1/2 cm Bore

Assumptions:  $L_1 = 10 \mu\text{H}$ ;  $I_i = 750 \text{ kA}$ ;  $W_i = 2.8 \times 10^6$

$(L_2)_i = 0.5 \mu\text{H}$ ;  $L_2' = 0.45 \mu\text{H}$ ;  $M = 10^{-2} \text{ kg}$

Switching waveform	Instantaneous	Linear	Cosinusoidal
Switching time	$t_f = 0$	$t_f = 739 \mu\text{s}$	$t_f = 727 \mu\text{s}$
Armature position at completion of switching	$x_f = 0$	$x_f = 0.5 \text{ m}$	$x_f = 0.5 \text{ m}$
Armature velocity at completion of switching	$\left( \frac{dx}{dt} \right)_f = 0$	$\left( \frac{dx}{dt} \right)_f = 2.7 \text{ km/s}$	$\left( \frac{dx}{dt} \right)_f = 3.0 \text{ km/s}$
Current at completion of switching	$I_f = 714 \text{ kA}$	$I_f = 699 \text{ kA}$	$I_f = 699 \text{ kA}$
Magnetic energy in system at completion of switching	$W_f = 2.67 \text{ MJ}$	$W_f = 2.61 \text{ MJ}$	$W_f = 2.61 \text{ MJ}$
Energy accepted by switching element	$W_{S_0} = 133 \text{ kJ}$	$W_S = 156 \text{ kJ}$	$W_S = 149 \text{ kJ}$

APPENDIX C

SWITCHING FOR AN EARTH-TO-SPACE RAIL LAUNCHER

R. C. Zowarka

Presented at the  
4th IEEE International Pulsed Power Conference  
Albuquerque, New Mexico  
June 6-8, 1983

Publication No. PN-93  
Center for Electromechanics  
The University of Texas at Austin  
Taylor Hall 167  
Austin, TX 78712  
512-471-4496



R. C. Zowarka  
Center for Electromechanics  
The University of Texas at Austin  
Austin, TX 78712

### Summary

For several years, NASA Lewis Research Center has been studying methods for ballistically launching payloads from the earth's surface. Currently the Center for Electromechanics (CEM-UT) is examining possible electromagnetic railgun launcher systems. The present state of the technology suggests that the homopolar generator-charged energy storage inductor transferring the energy to the launcher via a transfer switch is the yardstick by which alternate systems must be judged. Systems of this type have powered three railguns -- the ANU railgun at Canberra, the Westinghouse railgun at Picatinny Arsenal, and the General Dynamics railgun at The University of Texas at Austin. This paper presents observations on the efficiencies of transfer switch schemes as reported by Rioux and Rioux-Damidaou and co-workers at the University of Paris, Inall at the Australian National University, Vitkovitsky and co-workers at the Naval Research Laboratory, Marshall at the Australian National University, and CEM-UT. A switch incorporating the advantages of existing switches is presented.

### Introduction

In 1981, Marshall did a study on launching payloads from the earth's surface into space with a distributed energy store (DES) railgun.<sup>1</sup> In operation the individual HPG's would discharge into an energy storage inductor. The launcher would be controlled such that at peak current in the underdamped discharge an opening switch would divert the inductive energy into the launcher to accelerate the projectile. This process would be continued at discrete locations down the launcher until the projectile reached the desired velocity. In the study very large steps in performance were extrapolated from existing data. The energy store for the launcher consisted of a 56 MJ homopolar delivering 42 MJ of energy to an inductor in a current waveform that peaked at 4 MA. The purpose of the NASA Lewis Grant at the Center for Electromechanics was to attempt the next experimental step in the realization of the opening switch technology. Present switches have operated in the 0.01 to 0.2 MA range. Their operation and performance will be discussed further. The proposed experiments would try to utilize the 0.5 MA capability of the switch test facility at CEM-UT.

### Power Supply

The intent of this paper is to explore existing opening switch technology that might successfully drive an electromagnetic launcher. The power supplies are HPGs charging energy storage inductors. This system has been used to drive three railguns: the Canberra railgun, the Westinghouse railgun, and the General Dynamics railgun at The University of Texas at Austin. The emphasis of the Marshall study was to scale existing technology. Therefore, the HPG's are iron core machines with normal excitation. These machines are inherently low voltage, tens to hundreds of volts. To achieve energy transfer efficiencies in the 50 to 60 percent range, the coils are massive and need to be cryogenically cooled. Energy transfer times are on the order of 300-600 ms.

### Switch Evaluation Criteria

In designing opening switches, several criteria need to be applied. The actuation scheme used by the device is important when judging repeatability, simplicity and the ability to synchronize several devices. The current-carrying capacity is important because it establishes the maximum energy stored in the inductor. A companion variable to the current is the  $\int i dt$ , which establishes the required cross section of the switch and ultimately the mass of the moving parts. The final characteristic examined in this review is the switching efficiency. This number influences the overall size of the facility required.

### Review of Existing Opening Switches

The switch Inall used<sup>2</sup> was operated in a homopolar-inductor circuit. His switch was a staged device. The first stage carried the inductor charging current. This current was represented as a 70-kA peak sinusoid with a quarter cycle time of 600 ms. The switch was actuated by driving the contacts apart with high pressure nitrogen and thus its name, nitrogen blast circuit breaker (Fig. 1). The parting contacts form a 20-V arc shunted by copper fuses, the second stage of the switching. This arc was cooled and extinguished by

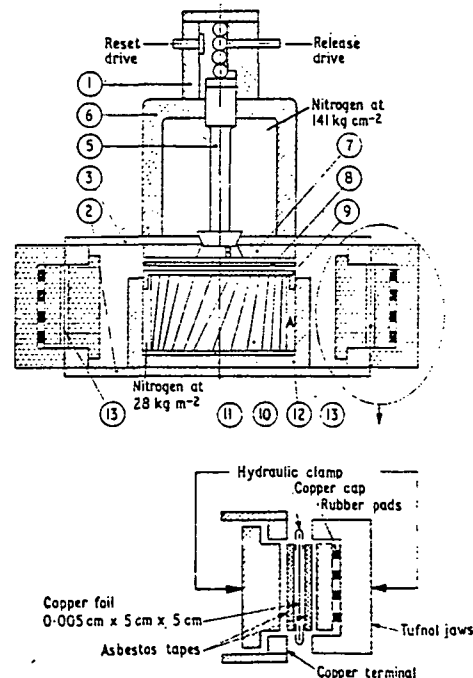


Fig. 1. Nitrogen blast circuit breaker.  
After Inall<sup>2</sup>.

the high flow rate of nitrogen. The current would dwell in the fuses for 400  $\mu$ s, a time long enough for the first stage switch to insulate and hold off 2 kV. This voltage was used to pump 16 parallel xenon flash lamps. The current transferred to the lamps was 64 kA, indicating a switching efficiency of 83.5 percent.

Chronologically, the next testing was performed by the Rioux<sup>3</sup> at the University of Paris. Their testing was directed toward a switch that would ultimately be used on a homopolar-inductor system. Their actual testing was performed on a 5-kV, 1-mf bank charging a 440-nH inductor. Their work was concerned with opening switch design, and a load was not used. The switching was staged, and when the second stage fuses ruptured the energy in the circuit was dispatched as a free-expanding arc. The first stage switch was a T-section conductor that would be ruptured at peak current. The test current was a quarter-cycle sinusoid that peaked in 40  $\mu$ s at a value of 28 kA. The T-section was ruptured with high pressure oil driven by an expanding coaxial conductor pulsed with a capacitor energy store (Fig. 2). The dielectric oil would wash the arcing conductor and increase the arc voltage. Current was then transferred to fuse elements that held in for a latent time of 20  $\mu$ s. At this time they exploded, and 9 kV was applied across the oil flowing

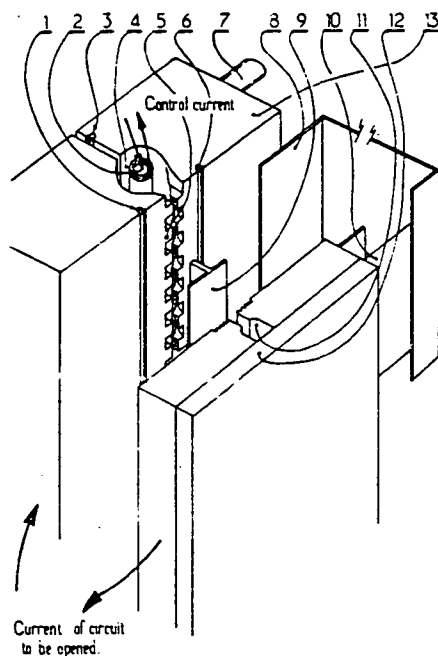


Fig. 2. Two-stage fuse-type opening switch.  
After Rioux and Rioux-Damidaou, et al.<sup>3</sup>

past the ruptured T-conductor. A load was not used in these experiments. Therefore, a transfer efficiency cannot be estimated.

Vitkovitsky and co-workers<sup>4</sup> have reported on a three-stage device. The first stage switch was a thin-wall aluminum tube. Paraffin on the inside of the tube was expanded with explosive primer cord, forcing the tube walls to be sheared by a series of ring cutters encircling the tube (Fig. 3). As a result, multiple gaps were opened along the length of the conducting tube, and paraffin flowed into the gaps to cool the arcs. From this switch current was transferred into the fuse elements.

The inductor charging pulse in these experiments was delivered by a capacitor bank. The current peaked at 54.77 kA in just under 900  $\mu$ s.

"In tests using a 60  $\mu$ H inductor storing 90 kJ, a six-section explosive switch and a 40 cm long by 1.5 in. wide by 1 mil thick aluminum fuse, generated a 30-kA, 120-kV pulse."<sup>4</sup>

The efficiency indicated by this statement is 30 percent. The explosive switch reinsulated to hold off 120 kV in 50  $\mu$ s.

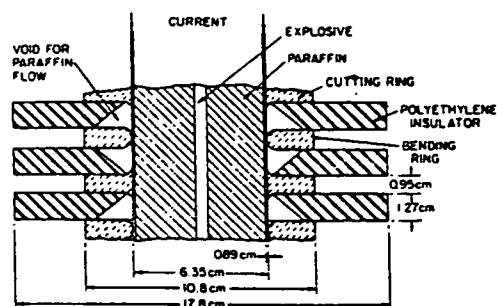


Fig. 3. Three-stage explosive opening switch.  
After Vitkovitsky, et al.<sup>4</sup>

The next switch scheme reviewed was tested by Marshall<sup>5</sup> at the Australian National University. In his work he used a homopolar inductor system to drive a railgun. His switch was actually a larger railgun that was used to switch the inductor current into the experimental gun. The projectile in the large gun was sized to carry the peak charging current in the inductor, 320 kA. At peak current, which occurred at 600 ms, the large projectile was released explosively, and it accelerated down the switching rails. At one point along the switching gun, the right hand rail was broken electrically by an insulator (Fig. 4). The length of the insulator in the direction of travel was slightly shorter than the switching projectile. The experimental railgun was brought in perpendicular to

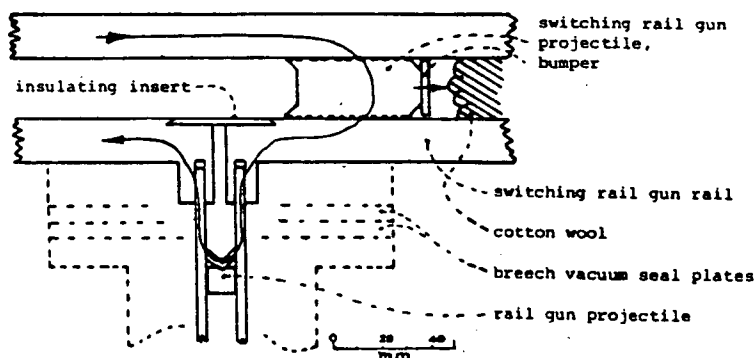


Fig. 4. Railgun-type switch.  
After Marshall<sup>5</sup>

the switching gun, and its breech was bolted across the insulator. As the switching projectile moved across the insulator, the leading conductor would connect the far rail of the experimental gun to the inductor circuit just prior to the rearmost conductor breaking this same circuit. Review of Marshall's data showed a 62 percent switching efficiency.

The final switch reviewed was a proprietary design tested by General Dynamics Corporation at the University of Texas at Austin. It was similar to the nitrogen blast circuit breaker, but instead of the high flowrate nitrogen, high flowrate dielectric fluid was used. The switch contacts were sized to carry a 500-kA sinusoid of current peaking in 350 ms. The device was therefore much heavier than any of the previously reviewed switches. This device transferred 265 kA into fuse elements in just under 2 ms. A railgun projectile was then driven by arc voltage produced by the exploding fuses. The efficiency of transfer of this two-stage device was 30 percent.

### Launcher Switch Design

The launcher design can be greatly simplified if continuous rails are used. This requires that the energy stores are charged and then connected to the rails. Further simplification can be achieved if the switches are self-synchronous. Finally, the stores need to be disconnected from the rail once their energy is delivered. A switch that satisfies two of these requirements is presented in Fig. 5. It essentially uses the Marshall shuttle design reconfigured to utilize a rotary actuation. Multi-Lam conducting strip is used to carry the charging current. The electromagnetic force trying to collapse the inner coax, the shuttle elements, is countered with pressurized air cylinders. At peak current the cylinders are exhausted and the electromagnetic force accelerates the shuttle. The shuttle then moves onto a resistive element that absorbs the switching energy and builds a voltage large enough to sustain the railgun arc. If current starts in the railgun, an additional electromagnetic force is built up, and the switching is completed as the resistive element is removed from the circuit. This switch utilizes the shuttle action and tight coupling of the Marshall design. It incorporates multiple gaps of the Vitkovitsky device to build the recovery ability. The fuse elements that absorb the switching energy of the other designs are replaced with a fixed resistor sized

to absorb the switching energy. A unit sized to operate at 500 kA and transfer 2 MJ of inductive energy is being designed and constructed at CEM-UT.

### References

1. Marshall, R. A., "Earth-to-Space Rail-Launcher System," CEM-UT Publ. No. PN-74, funded in part under NASA/Lewis Research Center Contracts NAS3-22882 to Battelle Columbus Laboratories and NAS3-22662 to the University of Pittsburgh.
2. Inall, E. K., "A Proposal for the Construction and Operation of an Inductive Store for 20 MJ," *J. Phys. E: Sci. Instrum.*, 5 (1972).
3. Bleys, C. A., Lebley, D., Rioux, C., and Rioux-Damidaou, F., "200 kA Circuit Breaker with 10  $\mu$ s Current Transfer Time," *Rev. Sci. Instrum.*, 46, 11 (Nov. 1975).
4. Conte, D., Ford, R. D., Lupton, W. H., and Vitkovitsky, I. M., "Two Stage Opening Switch Techniques for Generation of High Inductive Voltage," *Proc. IEEE Symp. on Engineering Problems of Fusion Research*, IEEE Cat. No. 77CH 1267-4-NPS (1977) p. 1066.
5. Marshall, R. A., "High Power High Energy Pulse Production and Applications," *Proc. Australian-U.S. Seminar on Energy Storage, Compression, and Switching*, Australian Natl. Univ. Press (Canberra) 1978.

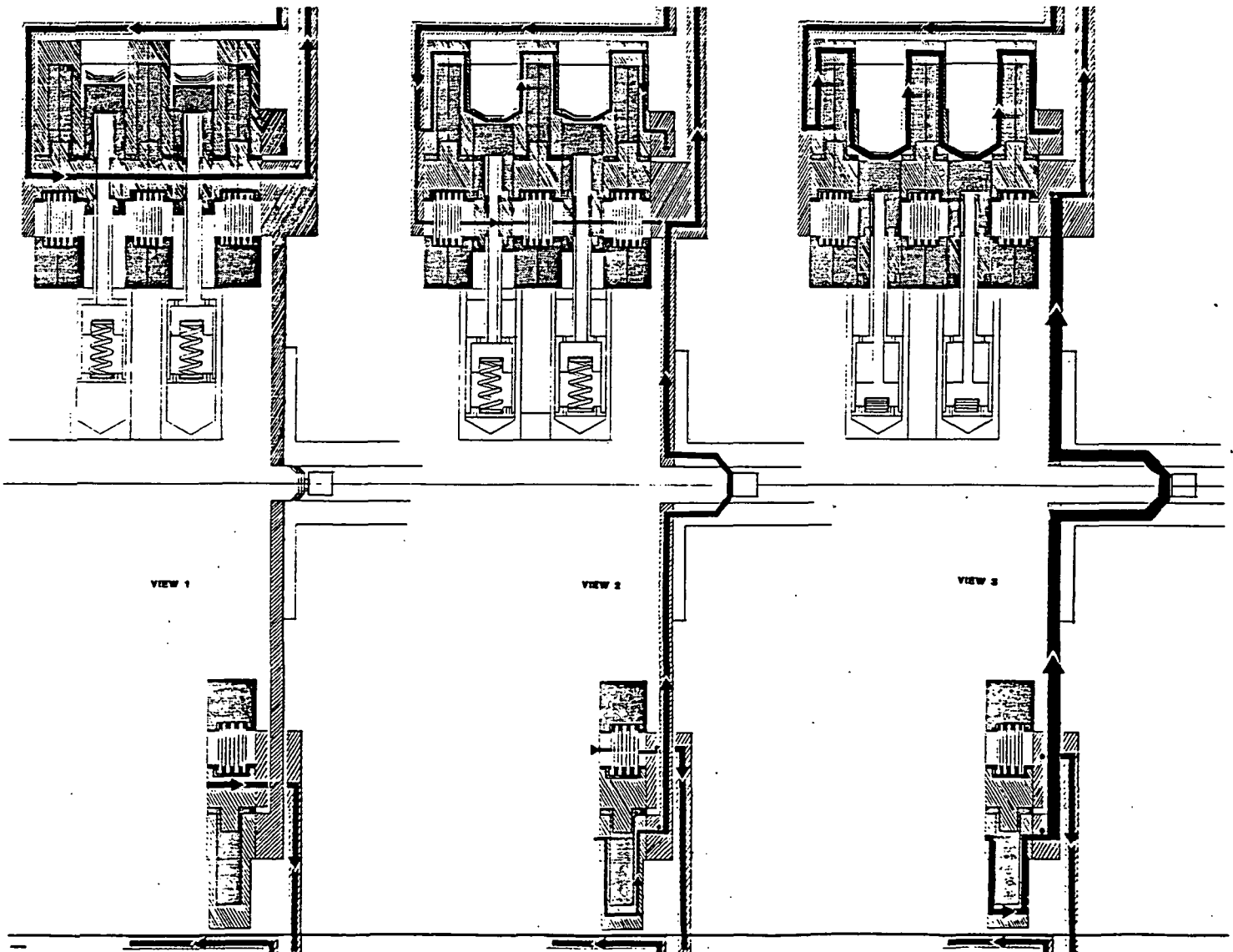


Fig. 5. Multi-gap rotary shuttle switch.

APPENDIX D

A COAXIAL RADIAL OPENING SWITCH  
FOR A DISTRIBUTED-ENERGY-STORE RAIL LAUNCHER

J. L. Upshaw and R. C. Zowarka

Presented at the  
2nd IEEE Symposium on  
Electromagnetic Launch Technology  
Boston, Massachusetts  
October 11-14, 1983

Publication No. PR-17  
Center for Electromechanics  
The University of Texas at Austin  
Taylor Hall 227  
Austin, TX 78712  
512-471-4496

## A COAXIAL RADIAL OPENING SWITCH FOR A DISTRIBUTED-ENERGY-STORE RAIL LAUNCHER

J. L. Upshaw and R. C. Zowarka  
Center for Electromechanics  
The University of Texas at Austin  
Austin, TX 78712

### Summary

The current electromagnetic launch technology base suggests that a distributed-energy-store railgun may be an attractive alternative to chemical rockets for Earth-to-space launch. If homopolar generator-charged inductors are to serve as the basic energy stores, a difficult switching problem must be overcome. Several switching schemes (arc, liquid metal, and electromagnetic) have been investigated. Studies indicate that arc opening switches would prove to be too destructive when used with continuous rail launcher systems. The most attractive alternative is an electromagnetically actuated switching scheme. The operation, calculated performance, fabrication, and initial testing of a switch based upon this scheme is presented in this paper.

### Introduction

NASA-Lewis Research Center has been studying various methods for ballistically launching payloads from Earth's surface into space. These studies, conducted over the past several years, have resulted in a ballistic launch technological base which suggests that a distributed-energy-store (DES) railgun is the most viable launcher system.

The DES rail launcher under discussion in this paper is one in which the basic energy stores are homopolar generators (HPGs). HPGs transfer energy to inductors which in turn transfer the energy to the rail launcher. This energy transfer from inductor to rail launcher presents a difficult switching problem. Several methods of accomplishing this switching were examined by the Center for Electromechanics at The University of Texas at Austin (CEM-UT) under a NASA-Lewis grant.<sup>1</sup>

An examination of several recent arc switching transfer schemes as reviewed by Zowarka,<sup>1</sup> a paper dealing with energy considerations in switching energy from an inductor into a rail launcher,<sup>2</sup> and experience gained at CEM-UT in testing an arcing opening switch at high currents (300 kA), led CEM-UT to reject arc switching schemes as too destructive in the gigawatt power ranges necessary for Earth-to-space launchers. The destructive aspects result from the fact that arcs are inherently poor methods of building the resistance (i.e., dissipating energy) necessary to develop a voltage high enough to transfer current out of the switch into the rail launcher. With an arc, most of the power dissipated occurs at the contacts and this is where the destructive effects (contact melting or pitting) occur. Attempts to cool the arc effectively have failed or do not lend themselves to a high repetition rate.

These and many other problems associated with arc switching led CEM-UT to devise a method of switching in a non-arcing manner. In this non-arcing switch, the voltage required to transfer current to the rail launcher is generated in a fixed resistor sized to absorb the energy required to accomplish the switching.

This paper presents the design, fabrication, and initial testing results of this new switching scheme.

### Design Considerations

In designing the new switch, CEM-UT worked on the

premise that a practical launcher design requires the use of continuous solid flat rails. A continuous rail launcher design requires switches capable of dissipating the heat generated without being destroyed and capable of repetitive operation with little or no maintenance between shots.

The CEM-UT design effort drew heavily on existing opening switch testing as reported in the literature by Rioux and Rioux-Damidaou,<sup>3</sup> Vitkovitsky and co-workers,<sup>4</sup> Marshall,<sup>5</sup> and Inall.<sup>6</sup> The design also drew on first-hand experience in opening switch development acquired from joint testing performed by CEM-UT and the General Dynamics Corporation.

The design effort addressed the need for synchronous switching, isolation of depleted energy stores, tight coupling, and multiple gaps for prevention of arc formation within the switch. It was decided that the switching actuation scheme should be electromagnetic to decrease the switching time. Because the electromagnetic forces are proportional to  $I^2$ , a mechanical aid was devised to assist actuation during initial testing at low current levels. It was also decided to keep the means of actuation separate from the contact area so that damage in the contact area would not ruin the actuation scheme. To assist in minimizing the switching time, the mass of the switching element must be as small as possible, which necessitated using a proven lightweight sliding contact. The minimum switching element mass size was determined from tests conducted at CEM-UT on the nondestructive current carrying capabilities of copper test samples. In the tests 6.45 cm<sup>2</sup> (1.0 in.<sup>2</sup>) copper squares were placed in series contact under approximately 6.9 MPa (1,000 psi). Testing over a charging cycle of 300 ms showed that approximately 31 kA/cm<sup>2</sup> (100 kA/in.<sup>2</sup>) could be applied before the specimens welded. These data, along with a design goal of a 200-kA switch, presented a means by which the contact surface area required could be determined. Mechanical integrity of this contact surface ultimately determined the size and mass of the moving switch parts.

Multilam contact band, a commercially available material, as shown in Fig. 1, was selected to provide the lightweight sliding contact surface. The tolerances required for proper installation of the Multilam<sup>7</sup> required that the switch parts be shapes that can be easily produced to close tolerances. A coaxial geometry consisting of concentric rings allowed flexibility in defining the conductive and resistive portions of the switch. This geometry also provided tight coupling by minimizing the inductance of the current path between the charging path and the load path to minimize the fundamental energy absorption requirements.<sup>2</sup>

The resistive portion of the switch was composed of numerous circular steel ring laminations stacked in series. The rings were chemically milled and Mylar laminated to increase the current path greatly, thereby increasing the resistance while minimizing overall size. These rings produce a fixed resistance that was designed to survive a failure to transfer the current to the load. Experimentation on the commutation phenomena could be performed knowing the switch would absorb the inductive energy in the event of projectile failure.

At lower current levels, the fixed resistance scheme suffers. This is due to the primarily mechanical and relatively slow actuation of the sliding contacts onto the steel resistor. As current levels

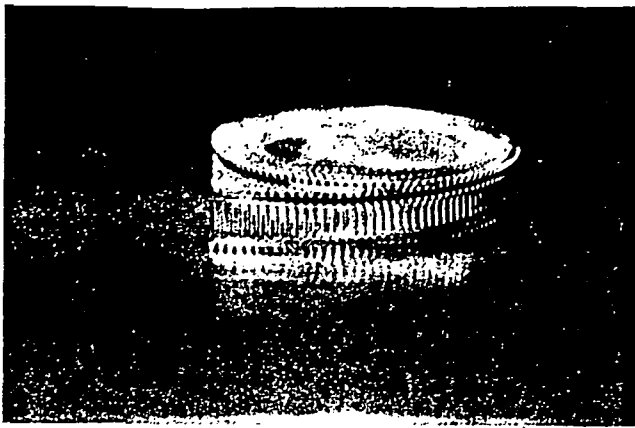


Fig. 1. Multilam band

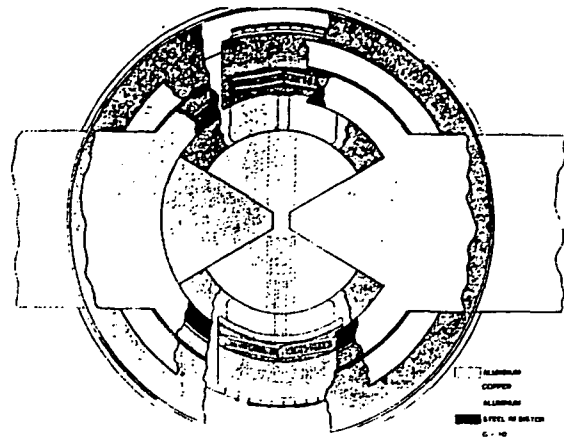


Fig. 2. Coaxial radial opening switch front cutaway

increase, the electromagnetic forces associated with the higher currents will decrease the time necessary for actuation and thereby improve the efficiency of the voltage development across the resistor. This improvement will also be seen in current transfer from the switch into the rail launcher.

Switch Design Action and Predicted Performance

A switch design that addresses the above design considerations and can be modified to disconnect the energy stores from the rails is shown in the front cutaway drawing in Fig. 2 and the cross-sectional drawings in Fig. 3. In the cross-sections, the different current paths at various stages of the switching are shown.

The launcher switch design utilizes radial actuation in which the switching is completed in three intervals. A simplified two-dimensional representation of the switch operating in the DES circuit is shown in Fig. 4. The switch position during the first interval is shown in Fig. 4a. During this time the HPG is charging the energy storage inductor through the short circuit path provided by the opening switch. Because of the coaxial geometry, a magnetic force is applied to the shuttles that form the inner conductor. The magnitude of this force in the switch as constructed is given by

$$F = \frac{1}{4} \frac{\mu_0 I^2 L}{4\pi r}$$

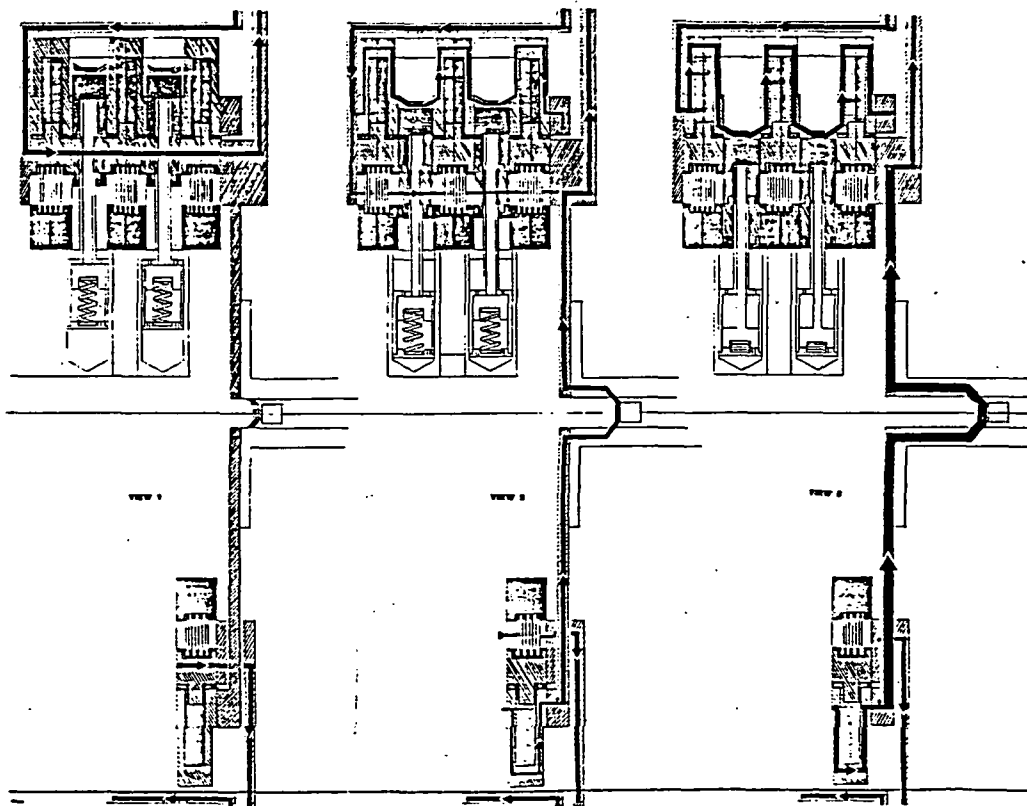


Fig. 3. Coaxial Radial Opening Switch  
Three cross-sectional views of possible current paths

$\mu_0$  = permeability of air,  $4\pi \times 10^{-7}$  Wb/A·m  
 $I$  = peak current, 47 kA  
 $l$  = length, 2.54 cm (1 in.)  
 $r$  = radius of shuttle conductor 17.2 cm (6.75 in.)

The factor of 1/4 appears because only one shuttle is under test in the four-quadrant design. The 47-kA peak current is the manufacturer's pulsed current rating for the LAI/.15 Multilam band shown in Fig. 1. The peak magnetic force during charging, 130 N (29.4 lbf) is counteracted by a telescoping air cylinder. At peak current the pressure on the back side of this cylinder is exhausted, and the pressure is redirected to the front of the cylinder. The magnetic force of 130 N (29.4 lbf) and the pneumatic force of 700 N (157 lbf) overcome the frictional force of the current-carrying Multilam louvers, 94 N (21.1 lbf), and the static friction of the air cylinder actuator, 9 N (2 lbf). The total applied force of 726 N (163.3 lbf) moves the 1.44-kg (3.173-lb<sub>m</sub>) shuttle mass to the position shown in Fig. 4b in 6.9 ms. As the trailing edge of the Multilam louvers moves onto the resistive edge path, an IR voltage is developed that commutates current into the electromagnetic launcher through the concurrently-formed conductive path B. The included inductance of the resistive path is 1.92 nH. The energy that must be absorbed as the 47-kA current transfers from the 10- $\mu$ H coil to the resistive path is

$$E = \frac{L_A}{L_{coil}} \left( \frac{1}{2} L_{coil} I^2 \right)$$

$$E = \frac{1.92 \times 10^{-9} \mu\text{H}}{10 \times 10^{-6} \mu\text{H}} \times 0.05 \times 10 \times 10^{-6} \mu\text{H} (47,000 \text{ A})^2$$

$$= 0.212 \text{ joules}$$

The current,  $I_B$ , commutating into the railgun then applies a further magnetic force to the shuttle and drives this member into the position shown in Fig. 4c. In this position, current is cut off in the resistive path A, thus establishing full current in the railgun. In DES operation, the end of this final switch path could be resistive to essentially disconnect the energy store from the launcher. Such complication was not warranted in this design because the test facility available has only one energy store.

#### Fabrication

The various parts of the rail launcher switch were machined from ETP 110 electrical tough pitch copper plate, 2000 series aluminum plate, and close-tolerance sanded G-10 glass fiber-reinforced epoxy. The switch design, which was based around the operating limits and dimensional requirements of LAI/.15 Multilam contact bands, called for a number of concentric circular parts assembled together in an interlocking manner to form insulated and discrete-resistance current pathways. The rings making up the current pathways are shown in Fig. 2.

The Multilam bands or louvers are contained in copper pieces that make up an inner and outer shuttle mechanism. This shuttle mechanism (made of copper, G-10, and Multilam) is attached to a telescoping air cylinder made of stainless steel and brass. The cylinder is contained in an insulated aluminum plate attached to a steel shaft with an interference fit. The shaft provides air passages from external air supplied to the cylinder. The shaft also serves to position the shuttle switch mechanism between the

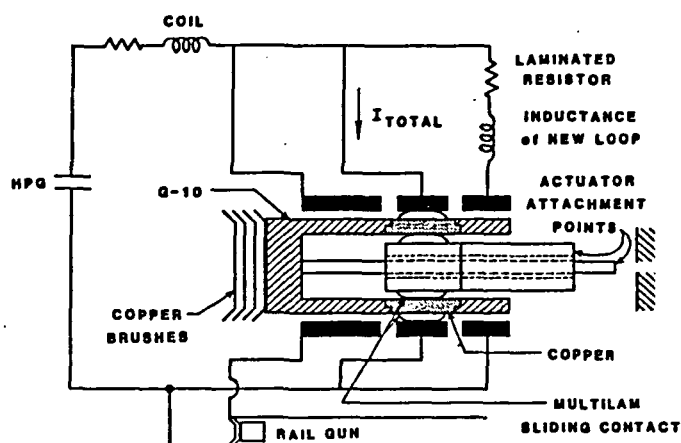


Fig. 4a. Switch in the inductor-charging position

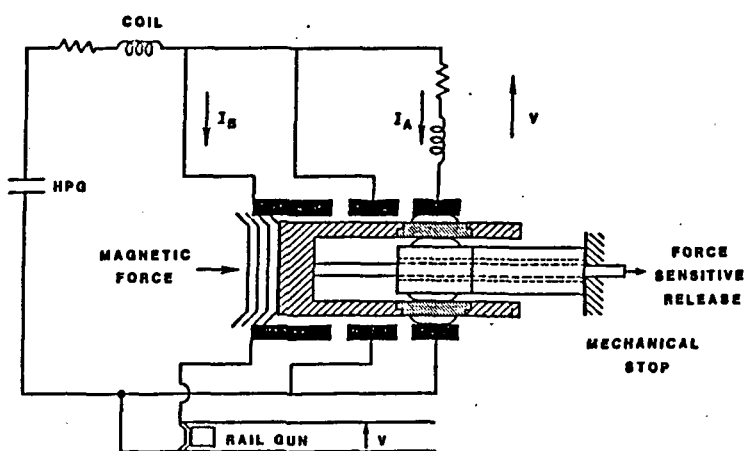


Fig. 4b. Switch building commutation voltage

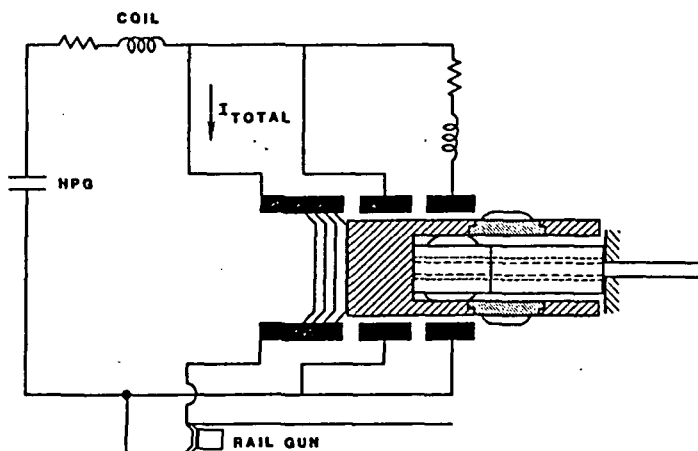


Fig. 4c. Switching complete -- total current established in railgun

Fig. 4. Action of DES circuit switch

interlocking current pathway plates that are held apart by a close-tolerance spacer ring. This spacer ring was

made of mild steel flame sprayed with aluminum oxide insulation and ground to the proper dimension required for the Multilam to make good electrical contact.

The shuttle mechanism, current pathway plates, shaft, etc., are contained in a copper housing and are secured by means of front and back plates of aluminum and G-10. The housing and back plates serve to bus current from the homopolar inductor energy store to the switch. Current that then passes through the switch is carried away by an aluminum busbar arrangement that connects the switch to the rail launcher.

#### Testing Procedure and Results

In the initial testing of the coaxial radial opening switch, it was important to separate the charging duty of the switch from the opening function. This separation was required to prevent charging damage associated with the contact dissipative losses from being confused with possible damage incurred due to excessive energy absorbed during commutation.

Two sets of tests were designed. One test would involve testing the switch up to design current without actuation. The second test would attempt to actuate the switch at design current to determine the effectiveness of the switching concept.

During the first set of tests, in which the switch was not actuated, it passed currents of 10 and 31 kA. Voltage traces at the 31-kA level showed some form of contact instability, from which it was inferred that some form of contact damage had occurred. Another test was conducted at the 30-kA level, and activation of the switch was attempted. A displacement probe indicated that no actuation had occurred. The switch was disassembled, and inspection showed a small welded spot between one of the four series contacts and one of the copper current rings. From the inspection it was felt that the damage occurred due to a possible misalignment and incorrect tolerance between the damaged parts. This conclusion was reached because the three other contacts in series, which saw the same  $\int I^2 dt$ , were undamaged. The misalignment was corrected, the damaged parts were repaired, and the switch was reassembled.

In the second series of tests, the switch was actuated at current levels of 16 and 24 kA. A calibrated displacement probe showed that actuation occurred. Data collected from these tests are shown below:

Peak Charging Current (kA)	Charging Current Rise Time (ms)	Interrupted Current (kA)	Voltage Developed (V)	Current Rise Time in Load (ms)
16	300	10.5	10.3	?
24	300	15.4	15.2	1

Switch actuation at 30 kA was attempted, but did not occur. Voltage traces showed some form of contact instability similar to that seen during the first series of tests when switch actuation was not attempted. Disassembly and inspection of the switch showed that again one of the four series contacts had failed. The 61.25 kA, 200 ms charging cycle as predicted by the Multilam Design Guide (already derated to 47 kA under the current design) now came into question. Further research into the Multilam contact performance as presented by independent researchers<sup>8</sup> predicted slight contact instability at 34 kA and pitting and slight silver transfer at 50 kA. Because these numbers approach the current at which contact failure occurred,

further design effort to increase the current-carrying capacity of the switch will focus on the sliding contact design.

#### Conclusions and Future Action

Test results at this point are inconclusive, but it has been shown that the coaxial radial switching scheme will transfer current at levels less than 20 kA. Two of the four contact series are being refurbished with double their initial Multilam contact area and future tests are planned to see whether this arrangement will allow the switching scheme to operate at higher current levels. If this change is unsuccessful, a new sliding contact system will be devised and tested.

#### References

1. Zowarka, R. C., "Switching for an Earth-to-Space Rail Launcher," IEEE Intl. Pulsed Power Conf., 4th, Albuquerque, NM, June 6-8, 1983.
2. Woodson, H. H., and Weldon, W. F., "Energy Considerations in Switching Current from an Inductive Store into a Railgun," IEEE Intl. Pulsed Power Conf., 4th, Albuquerque, NM, June 6-8, 1983.
3. Bleys, C. A., Lebley, D., Rioux, C., and Rioux-Damidau, F., "200 kA Circuit Breaker with 10  $\mu$ s Current Transfer Time," Rev. Sci. Instrum., 46, 11 (Nov. 1975), p. 1542.
4. Conte, D., Ford, R. D., Lupton, W. H., and Vitkovitsky, I. M., "Two Stage Opening Switch Techniques for Generation of High Inductive Voltage," Proc. IEEE Symp. on Engineering Problems of Fusion Research, IEEE Cat. No. 77CH 1267-4-NPS (1977) p. 1066.
5. Marshall, R. A., "High Power High Energy Pulse Production and Applications," Proc. Australian-U.S. Seminar on Energy Storage, Compression, and Switching," Australian Natl. Univ. Press (Canberra) 1978.
6. Inall, E. K., "A Proposal for the Construction and Operation of an Inductive Store for 20 MJ," J. Phys. E: Sci. Instrum., 5 (1972), pp. 679-685.
7. Multilam Corporation (now Hugin Industries, Inc., 745 Distel Dr., Los Altos, CA 94022), "Guide to Multilam Technology," revised Jan. 1978.
8. Wildi, P., "Contacts for Pulsed High Current; Design and Test," Proc. IEEE Intl. Pulsed Power Conf., 2nd, Lubbock, TX, June 12-14, 1979, pp. 195-197.



## CEM-UT

## Technical Note

Subject Information for De-rating of Multilam StripNumber 007Author Ray ZowarkaDate October 20, 1983Distribution Unlimited

In designing the NASA switch at CEM-UT, all design data were taken from the Multilam Design Guide. These data are repeated below:

MULTILAM BAND TYPE LAI

Available in 3 thicknesses, surface either unplated (is passivated) or silver-plated, 10 louvers per inch.

<u>Type</u>	<u>Thickness of Band (in.)</u>	<u>Continuous Current* Rating per Louver (A)</u>	<u>Rating per Inch (A)</u>
LAI/.15	0.006	25	250
LAI/.2	0.008	30	300
LAI/.25	0.010	35	350

3 second rating:	continuous current	x	22
12 cycle rating:	"	"	x 50
1 millisecond rating:	"	"	x 100

\* ratings based on 35 °C rise

Source: Multilam Design Guide, Multilam Corp., Jan. 1978

The cycle rating described in this guide is a 60-Hz sinusoid. This table may be regenerated using linear interpolation to fill in points between 0.2 s (12 cycles) and 3 s. In this region the curve is fairly linear.

<u>Time (s)</u>	<u>Current Rating</u>
3	continuous current x 22
1.5	" " x 37
0.3	" " x 49
0.2	" " x 50
0.001	" " x 100

In the NASA switch, 50 louvers of LAI/.15 were used, and the  $I^2t$  capacity as calculated from the Design Guide was

$$I = 25 \text{ A} \frac{\text{continuous}}{\text{louver}} \times 50 \text{ louvers} \times 49 \frac{\text{pulse}}{\text{continuous}} \sin 377 t$$

$$\int_0^{0.3} I^2 t dt = \int_0^{0.3} (61,250 \text{ A} \sin 377 t)^2 dt$$

$$= 0.562 \times 10^9 \text{ A}^2 \cdot \text{s}$$

Static failure on the NASA switch occurred between 20 and 30 kA when tested on the 10-MJ HPG charging the room temperature Brooks coil. The response is an overdamped waveform that peaks in 0.3 s.

$$(30,000)^2 \int_0^{0.3} (\sin 5.236 t)^2 dt = 0.135 \times 10^9 \text{ A}^2 \cdot \text{s}$$

In 1979 Paul Wildi tested LAI/.25 on the 10-MJ HPG (then a 5-MJ machine) using it in a welding configuration. The response was an overdamped waveform that peaked in 100 ms. He noticed contact instability at 54 kA peak current and a total  $\int I^2 dt$  of  $1.6 \times 10^9 \text{ A}^2 \cdot \text{s}$ . His pulse duration was 1.5 s. This can be checked against the Multilam Design Guide.

$$I = 35 \text{ A} \frac{\text{continuous}}{\text{louver}} \times 54 \text{ louvers} \times 37 \frac{\text{pulse}}{\text{continuous}} \sin 377 t$$

$$\int_0^{1.5} I^2 dt = (69,930)^2 \int_0^{1.5} \sin^2 377 t dt$$

$$= 3.67 \times 10^9$$

In conclusion, LAI/.15 must be de-rated by a factor of

$$1 - \sqrt{\frac{0.135}{0.562}} = 51 \text{ percent on peak current,}$$

and LAI/.25 must be de-rated by a factor of  $1 - \sqrt{\frac{1.6}{3.67}} = 34 \text{ percent.}$

We found that doubling the Multilam by interleaving louvers will double the capacity of the de-rated Multilam strip.